UNIVERSIDADE DA BEIRA INTERIOR
Engenharia

Forecasting Tools and Probabilistic Scheduling Approach Incorporating Renewables Uncertainty for the Insular Power Systems Industry

Gerardo José Osório da Silva

Tese para obtenção do grau de Doutor em

Engenharia e Gestão Industrial

(3º Ciclo de Estudos)

Orientador: Prof. Doutor João Paulo da Silva Catalão
Coorientador: Prof. Doutor João Carlos de Oliveira Matias

Covilhã, julho de 2015

This thesis was supported by FEDER funds (European Union) through COMPETE and by Portuguese funds through FCT, under Projects FCOMP-01-0124-FEDER-014887 (Ref. PTDC/EEA-EEL/110102/2009), FCOMP-01-0124-FEDER-020282 (Ref. PTDC/EEA-EEL/118519/2010) and PEst-OE/EEI/LA0021/2013. Also, the research leading to these results has received funding from the EU 7th Framework Programme FP7/2007-2013 under grant agreement no. 309048.

Dedicatory

To my closest family, who with love, dedication and effort, always believed in my capabilities and my humanity, supporting me unconditionally in the hardest times, even in their absence.

Acknowledgement

I would like to express my gratitude first to my supervisor and friend Prof. Dr. João Paulo da Silva Catalão for the excellent guidance, motivation, support and expertise he shared with me in my PhD studies, and all the friendship, sympathy, support, honesty, trust and confidence in all the steps I have taken over the past few years, as well as for all the lessons and experiences that we had together, even in those moments which were really difficult. I will be eternally grateful to the noble Professor for all the respect that we have shared in these years.

I am also grateful to my co-supervisor Prof. Dr. João Carlos de Oliveira Matias for all the support, friendship, encouragement, affection and life experiences he transmitted and shared over the years of my PhD in Industrial Engineering and Management, setting an example to follow whether in personal or professional live. Also, I would like to express my gratitude to him for giving me the opportunity to be his PhD student.

I cannot forget the shared affection, enrichment and professional experience of the international researchers belonging to the Sustainable Energy Systems laboratory (SES), in the University of Beira Interior, associated with *“Instituto de Engenharia de Sistemas e Computadores – Investigação e Desenvolvimento”* (INESC-ID), because without the resources available in the SES laboratory it would not have been possible to carry out this work. In particular, I would like to thank Dr. Juan Miguel Lujano Rojas, colleague and friend, for all the friendship, help, lessons and support that he offered me in the last few years.

Also, I want to thank the University of Beira Interior for all the support, care and resources made available in these years, such that I consider it as my second home. My respectful thanks to all personnel of the University of Beira Interior, especially those in the Electromechanical Engineering Department.

Finally, to all my colleagues and friends who are also an integral part of my life, who shared with me the good and bad times in their lives too, I want to express my gratitude for all the support, especially those who helped me, supported me and gave their precious time to help me, especially in my hardest times. Also, my kindest and respectful thanks to Prof. Cláudio Domingos Martins Monteiro, of the Engineering Faculty of the University of Oporto (FEUP), whose active participation and shared ideas in the FP7-SiNGULAR project in which I collaborated, having been really enriching for me in the past few years.

Resumo

Hoje em dia, a mudança de paradigma do setor elétrico e o desenvolvimento da rede elétrica inteligente, em paralelo com as crescentes exigências para uma redução gradual das emissões de gases com efeito de estufa, apresentam inúmeros desafios relacionados com a gestão sustentável dos sistemas de energia elétrica.

A indústria de energia elétrica nos sistemas insulares é profundamente dependente da importação de energia primária, nomeadamente de combustíveis fósseis, e também do comportamento do turismo sazonal, o qual influencia significativamente a economia local. Comparativamente ao sistema elétrico continental, o comportamento dos sistemas elétricos insulares é profundamente influenciado pela natureza estocástica dos recursos energéticos renováveis disponíveis.

A rede elétrica insular é particularmente sensível aos parâmetros de qualidade do sistema elétrico, principalmente aos desvios de frequência e tensão, e a integração massiva do potencial renovável endógeno no sistema elétrico poderá afetar a fiabilidade e segurança do fornecimento de energia, pelo que deve ser dada peculiar atenção aos procedimentos de previsão e operação do sistema.

Os objetivos da presente Tese incidem na criação de novas ferramentas de apoio à decisão, para a previsão fiável dos preços de mercado e da potência eólica, para o despacho económico e afetação ótima de unidades considerando a geração renovável, e para o controlo inteligente de sistemas de armazenamento de energia. As novas metodologias desenvolvidas são testadas em casos de estudo reais, demonstrando a sua proficiência computacional comparativamente ao atual estado da arte.

Palavras-Chave

Indústria de energia elétrica; Gestão sustentável; Despacho económico; Energias renováveis; Armazenamento de energia.

Abstract

Nowadays, the paradigm shift in the electricity sector and the advent of the smart grid, along with the growing impositions of a gradual reduction of greenhouse gas emissions, pose numerous challenges related with the sustainable management of power systems.

The insular power systems industry is heavily dependent on imported energy, namely fossil fuels, and also on seasonal tourism behavior, which strongly influences the local economy. In comparison with the mainland power system, the behavior of insular power systems is highly influenced by the stochastic nature of the renewable energy sources available.

The insular electricity grid is particularly sensitive to power quality parameters, mainly to frequency and voltage deviations, and a greater integration of endogenous renewables potential in the power system may affect the overall reliability and security of energy supply, so singular care should be placed in all forecasting and system operation procedures.

The goals of this thesis are focused on the development of new decision support tools, for the reliable forecasting of market prices and wind power, for the optimal economic dispatch and unit commitment considering renewable generation, and for the smart control of energy storage systems. The new methodologies developed are tested in real case studies, demonstrating their computational proficiency comparatively to the current state-of-the-art.

Keywords

Power systems industry; Sustainable management; Economic dispatch; Renewable energies; Energy storage.

Table of Contents

Dedicatory ... iii
Acknowledgement ... iv
Resumo ... v
Palavras-Chave ... v
Abstract ... vi
Keywords ... vi
Figures List ... x
Tables List ... xii
Acronyms ... xiii
Nomenclature ... xvi
Introduction ... 1
1.1. Framework ... 1
1.2. Motivation ... 10
1.3. Thesis Structure ... 15
1.4. Notation ... 16
State-of-the-Art ... 17
2.1. Electricity Market Prices and Forecasting Tools ... 17
2.2. Wind Power Forecasting Tools ... 22
2.3. Economic Dispatch and Unit Commitment Tools ... 26
2.4. Energy Storage System Tools Management ... 29
2.5. Stochastic Programming ... 33
Hybrid Forecasting Tool ... 35
3.1. Mutual Information ... 35
3.2. Wavelet Transform ... 37
3.3. Evolutionary Particle Swarm Optimization ... 39
3.4. Adaptive Neuro-Fuzzy Inference System ... 42
3.5. Proposed Forecasting Tool ... 44
3.6. Case Studies and Results ... 47
3.6.1. Forecasting Accuracy Evaluation ... 48
3.6.2. Short-Term Electricity Market Prices Results ... 49
3.6.3. Short-Term Wind Power Forecasting Results ... 59
Economic Dispatch Problem ... 64
4.1. Probabilistic Economic Dispatch Problem and Proposed Approach ... 64
4.1.1. Discretization of the PDF of Forecasted Wind Power Generation ... 65
4.1.2. Simplification of PDF of Initial Power Production ... 66
4.1.3. Incorporation of Wind Power Forecasting Error ... 67
4.1.4. Incorporation of Generators Reliability ... 69

4.2. Case Studies and Results 71
4.2.1. Analysis of 5-Unit Power System 72
4.2.2. Analysis of 10-Unit Power System 75
Unit Commitment Problem 81
5.1. Scenario Generation Process 81
5.2. Problem Description 84
5.2.1. Objective Function 84
5.2.2. Generation Limit Constraints 85
5.2.3. Operating Ramp rate Constraints 85
5.2.4. Startup and Shutdown Ramp Rate Constraints 85
5.2.5. Reserve Requirements Constraint 85
5.2.6. Power Balance 86
5.2.7. Minimum Up/Down Time Constraint 86
5.3. Priority List Method to the Unit Scheduling 86
5.3.1. Primary Unit Scheduling 87
5.3.2. Minimum Up/Down Time Repairing 87
5.3.3. Spinning Reserve Repairing 88
5.3.4. Shutdown Repairing Process 89
5.3.5. Unit Substitution Process 89
5.3.6. Shutdown Excess of Generation 90
5.4. Proposed Approach 91
5.5. Case Study and Results 92
Control Strategy with Energy Storage System 97
6.1. Power System under Analysis 97
6.1.1. Thermal and Renewable Generation Units 98
6.1.2. Power Converter 99
6.1.3. Vanadium Redox Battery and Charge Controller Model 100
6.2. Unit Commitment Problem Incorporating Energy Storage System 101
6.2.1. Proposed Methodology 101
6.2.2. Solving the Unit Commitment Problem by Priority List Method 104
6.3. Case Study and Results 107
Conclusions 111
7.1. Main Conclusions 111
7.2. Guidelines for Future Contributions 113
7.3. Research Contributions Resulting from this Work 113
7.3.1. Articles in Journals 113
7.3.2. Book Chapters 114
7.3.3. Papers in Conference Proceedings 114
References 116

Figures List

Figure 1.1 —	Power capacity in EU28 from 2008 till 2013 in MW and shared renewable power capacity.	6
Figure 1.2 —	Wind power capacity evolution in Europe between 2001 till 2013 in MW in onshore and offshore installation.	6
Figure 1.3 —	Overall renewable energy capacity installed in Portugal from January 2005 till July 2014.	7
Figure 1.4 —	Wind power profile showing intermittency and volatility.	8
Figure 1.5 —	Distribution of Portuguese electrical mix production in 2013.	8
Figure 2.1 —	Brief characterization of electricity market.	18
Figure 2.2 —	Daily electricity market procedure.	18
Figure 2.3 —	Activity sequence in electricity intraday market.	19
Figure 2.4 —	Variability and foreseeability of renewable energy sources.	24
Figure 2.5 —	General block diagram for wind power forecasting from physical models.	24
Figure 2.6 —	Stochastic programming problems classification.	34
Figure 3.1 —	General mutual information representation.	37
Figure 3.2 —	Three-level decomposition model of WT.	39
Figure 3.3 —	EPSO movement rule of a particle.	41
Figure 3.4 —	Most used ANFIS membership functions.	42
Figure 3.5 —	Inference system architecture.	43
Figure 3.6 —	General ANFIS architecture.	43
Figure 3.7 —	Flowchart of proposed HEA tool.	46
Figure 3.8 —	Winter week 2002 results for the Spanish market.	50
Figure 3.9 —	Spring week 2002 results for the Spanish market.	51
Figure 3.10 -	Summer week 2002 results for the Spanish market.	51
Figure 3.11 -	Fall week 2002 results for the Spanish market.	52
Figure 3.12 -	May 8, 2006, results for the Spanish market.	52
Figure 3.13 -	Daily error comparative results between NN, NNWT, WPA and HEA methodologies.	53
Figure 3.14 -	January 20, 2006, results for the PJM market.	55
Figure 3.15 -	February 10, 2006, results for the PJM market.	55
Figure 3.16 -	March 5, 2006, results for the PJM market.	56
Figure 3.17 -	April 7, 2006, results for the PJM market.	56
Figure 3.18 -	May 13, 2006, results for the PJM market.	57
Figure 3.19 -	February 1–7, 2006, results for the PJM market.	57
Figure 3.20 -	February 22–28, 2006, results for the PJM market.	58
Figure 3.21 -	Measured and forecasted results for the Winter season.	60
Figure 3.22 -	Measured and forecasted results for the Spring season.	60

Figure 3.23 -	Measured and forecasted results the Summer season.	61
Figure 3.24 -	Measured and forecasted results for the Fall season.	61
Figure 4.1 —	Power system under study.	65
Figure 4.2 —	Characteristics of the discretized beta PDF.	66
Figure 4.3 —	PDF of P_n^{t-1} and CDF of P_n^{t-1}.	68
Figure 4.4 —	Selected cases of power production at time $t-1$.	68
Figure 4.5 —	Allocation of power generation $\left(P_{n,i_s}^t\right)$ in the PDF of P_n^t.	69
Figure 4.6 —	Illustration of the join PDF of failure events and power production.	71
Figure 4.7 —	CDF of power generation loss and PDF of power loss due to failure events.	71
Figure 4.8 —	PDF of wind power generation (5-Unit system).	73
Figure 4.9 —	PDF of power generation of unit 1.	73
Figure 4.10 -	PDF of generation cost.	73
Figure 4.11 -	PDF of CO_2 emissions of unit 1.	75
Figure 4.12 -	PDF of power generator of unit 4.	76
Figure 4.13 -	PDF of power generator of unit 6.	76
Figure 4.14 -	PDF of generation cost related with fuel consumption.	77
Figure 4.15 -	PDF of energy not supplied.	78
Figure 4.16 -	PDF of wind power generation.	78
Figure 4.17 -	PDF of power generation of unit 6.	79
Figure 4.18 -	PDF of generation cost.	79
Figure 4.19 -	Behavior of computational time.	79
Figure 5.1 —	Probability transformation.	83
Figure 5.2 —	Repairing process of minimum up-time constraints.	87
Figure 5.3 —	Repairing process of minimum down-time constraints.	87
Figure 5.4 —	Selection of generators in unit substitution process.	90
Figure 5.5 —	Results from scenario generation and reduction process.	94
Figure 5.6 —	CDF of supply reserve requirements for $t = 1$ and $t = 17$.	94
Figure 5.7 —	CDF of supply reserve requirements for $t = 12$ and $t = 20$.	94
Figure 6.1 —	Architecture CDF of the power system under analysis.	98
Figure 6.2 —	SOC and charging power simulation.	101
Figure 6.3 —	Charge and discharge periods according to the wind power curtailed.	102
Figure 6.4 —	Charge and discharge periods according to the load profile.	103
Figure 6.5 —	Reference power of ESS.	103
Figure 6.6 —	Hourly aggregated wind power generation.	109
Figure 6.7 —	Power from/to ESS under study.	109
Figure 6.8 —	State of charge behavior of ESS under study.	109
Figure 6.9 —	Load to be supplied by thermal and wind units.	109

Tables List

Table 1.1 —	Total wind power capacity installed in some countries in EU28.	5
Table 2.1 —	Most widespread wind power forecasting tools used around the world.	25
Table 3.1 —	Parameters of MI, EPSO and ANFIS.	47
Table 3.2 —	MAPE criterion: Comparative results for Spanish market.	53
Table 3.3 —	Weakly error variance criterion: Comparative results for Spanish market.	54
Table 3.4 —	MAPE criterion: comparative results for PJM market.	58
Table 3.5 —	Error variance criterion: comparative results for PJM market.	58
Table 3.6 —	MAPE outcomes for all methodologies.	62
Table 3.7 —	Error variance outcomes for all methodologies.	62
Table 3.8 —	Comparative NMAE results.	62
Table 3.9 —	NRMSE results.	62
Table 3.10 -	Comparative MAPE outcomes for 2009.	63
Table 3.11-	Comparative NMAE outcomes for 2009.	63
Table 4.1 —	Description of 5-Unit system.	72
Table 4.2 —	Expected value comparison between MCS and proposed approach.	74
Table 4.3 —	CO_2 emission model.	74
Table 4.4 —	Expected value of CO_2 emissions.	74
Table 4.5 —	Description of 10-Unit system.	76
Table 4.6 —	Expected value comparison between MCS and proposed approach.	77
Table 4.7 —	Expected value comparison between MCS and proposed approach incorporating generator reliability.	80
Table 5.1 —	Description of the power system under analysis (part 1).	93
Table 5.2 —	Description of the power system under analysis (part 2).	93
Table 5.3 —	Load demand and wind power forecasting.	93
Table 5.4 —	PDF of unit scheduling.	95
Table 5.5 —	Average power production results (MW).	96
Table 5.6 —	Probability of supply the required reserve.	96
Table 6.1 —	Characteristic of thermal units.	108
Table 6.2 —	Unit scheduling of day 2 without incorporating ESS (MW).	110
Table 6.3 —	Unit scheduling of day 2 incorporating ESS (MW).	110

Acronyms

AC	Alternating current
AHL	Augmented Hopfield Lagrange
ANEM	Australian electricity market
ANFIS	Adaptive neuro-fuzzy inference system
ARIMA	Auto regressive integrated moving average
ARMA	Autoregressive moving average
ARTMAP	Adaptive resonance theory mapping
AWNN	Adaptive wavelet neural network
AWPPS	Armines wind power prediction system
AWPT	Advanced wind power prediction tool
BESS	Battery energy storage systems
CAES	Compressed air energy storage system
CDF	Continuous distribution function
CLSSVM	Chaotic least squares support vector machine
CNEA	Cascaded neuro-evolutionary algorithm
CNN	Cascaded neural network
COP	Conference of parties
CSP	Concentrated solar power plant
CWT	Continuous wavelet transform
Db4	Daubechies mother-wavelet function of fourth order
DC	Direct current
DR	Demand response
DWT	Discrete wavelet transform
ED	Economic dispatch
EGARCH	Exponential generalized autoregressive conditional heteroskedastic
ENS	Energy not supplied
EPL	Enhanced priority list
EPSO	Evolutionary particle swarm optimization
ESS	Energy storage system
EU28	Europe Union 28 States Members
FA	Firefly algorithm
FF	Fuzzy algorithm
FNN	Fuzzy neural network
FOR	Forced outages rates
GHE	Greenhouse emissions
HFO	Heavy fuel oil
HIS	Hybrid intelligent system

HNES	Hybrid neuro-evolutionary system
ILR	Improved Lagrangian relaxation
IPPD	Improved pre-prepared power demand
ISO	Independent system operator
KPCA+IVM	Kernel principal component analysis with informative vector machine
ktoe	Kilo tons of oil equivalent (10^3)
LCOE	Levelized cost of energy
LFO	Light fuel oil
LHS	Latin hypercube sampling
LHS-CD	Latin hypercube sampling with Cholesky decomposition
MCS	Monte Carlo simulation
MI	Mutual information
MIBEL	Iberian electricity market
MILP	Mixed-integer linear programming
MIP	Mixed-integer programming
MO	Market operator
Mton	Mega tons (10^6)
MW	Megawatt
NF	Neuro-fuzzy
NN	Neural network
NNWT	Neural network combined with wavelet transform
NRM	New reference model
NWP	Numerical weather prediction
NYISO	New York Independent System Operator's
OMEL	Futures contracts market operator in Spain
OMIP	Daily and intraday market operator in Portugal
PDF	Probability distribution function
PHES	Pumped hydro energy storage
PJM	Regional transmission organization in USA that coordinates the movement of wholesale electricity (PJM market)
PL	Priority list
PNAEE	National Action Plan for Energy Efficiency (from Portuguese abbreviation)
PNAER	National Action Plan for Renewable Energy (from Portuguese abbreviation)
PSF	Pattern sequence-based forecasting
PSO	Particle swarm optimization
PV	Photovoltaic power plants
RAL	Research applications laboratory (wind energy predictions)
RBF	Radial basis function
RBFN	Radial basis function neural network
RDFA+KF	Fuzzy ARTMAP recursive dynamic factor analysis combined with Kalman filter
REN	*Redes Energéticas Nacionais*

SCADA	Supervisory control and data acquisition system
SDNN	Similar days neural network model
SEN	National Electrical System (from Portuguese abbreviation)
SOC	State of charge
SRN	Elman network or simple recurrent network
SUW	Solid urban waste plants (waste)
SVM	Support vector machine
TNF	Time numerical forecasting
TSO	Transmission system operator
UC	Unit commitment
UK	United Kingdom
VOLL	Value of lost load
VRB	Vanadium Redox batteries
WNF	Wavelet neuro-fuzzy
WNN	Weighted nearest neighbors
WPA	Wavelet transform combined with particle swarm optimization and adaptive neuro-fuzzy inference system
WPPT	Wind power prediction tool
WT	Wavelet transform
WT+FF+FA	Combination technique based on wavelet transform, fuzzy, firefly algorithm

Nomenclature

A_i	ANFIS linguistic label.
a_i	ANFIS contribution parameter set.
α_{pdf}	Parameter of continuous beta PDF.
α	Significance level value.
A_n	Approximation coefficient in wavelet transform.
a_n	Parameter of fuel consumption of generator/unit n.
av_0	Auxiliary variable.
av_1	Auxiliary variable.
av_2	Auxiliary variable.
av_3	Auxiliary variable.
A_w	Continuous distribution function of time series W^t.
awp_j^t	Value of available wind power generation in discrete state j at time t.
AWP^t	Discrete PDF of available wind power generation at time t.
a_{wt}	Continuous scale parameter of wavelet propagation.
A	Continuous distribution function.
β_{pdf}	Parameter of continuous beta PDF.
β	Significance level limit index of l_m.
BFE	Increment in spinning reserve due to uncertainty in the power to be discharged from ESS.
b_g^*	EPSO best global position of a particle.
B_h	Number of elements of spinning reserve in ESS.
B_i	ANFIS linguistic label.
b_i	ANFIS contribution parameter set.
b_n	Parameter of fuel consumption of generator/unit n.
BS_{shape}^t	Binary vector of battery state of ESS due to load profile shape at time t.
BS_{WC}^t	Binary vector of battery state due to wind power curtailment at time t.
b_{wt}	Continuous translation parameter of wavelet position.
B	Total number of bins of discrete PDF of power production.
b	Discrete state of power production $\in \{1, B\}$.
$CH_{n,m}^t$	Generators/units to be substituted matrix.
c_i	ANFIS contribution parameter set.
c_n	Parameter of fuel consumption of generator/unit n.
CP^t	Available charge power at time t for ESS.
$CST_{n,m}^t$	Cold start-up time of generator/unit n, at time t, in scenario m.
$CSU_{n,m}^t$	Cold start-up cost of generator/unit n, at time t, in scenario m.
CWT_{ab}	Continuous wavelet transform set.
C_ω	Objective decision at scenario ω.
C	Random set of scenario.

D_{avg}	Average value of the hourly load.
ΔP	Discretization step of the power values P_b.
$\Delta\theta$	Sampling increment of interval $\{\gamma, 1-\gamma\}$.
Δt	Time-step of the simulation in ESS.
DL_i^t	Value of the power consumed by dump load at time t in sampling point i.
DL^t	Dump load at time t.
D_n	Detail coefficient in wavelet transform.
$D_{n,m}^t$	Binary matrix of generator/unit to be substituted.
DR_n	Operating ramp-down rate of generator/unit n.
D^t	Load demand at time t.
$DWT(m_{wt}, n_{wt})$	Discrete wavelet transform set.
E_0	Energy stored in ESS to be discharge.
$E_{(l,n)}$	Discrete PDF of power production when generators/units reliability is considered.
E_{max}	Maximum energy to be stored on VRB of ESS.
$ENS_{i_s}^t$	Energy not supplied at time t in sampling point i_s.
ϵ	Gaussian white noise
η_b	Efficiency of VRB of ESS.
η_v	Efficiency of the power converter in ESS.
ETG^t	Excess of thermal power generation at time t.
F_b^e	CDF of power loss as consequence of failure in generator/unit system.
F_c	Control factor in charge process of ESS.
F_h^n	Discrete PDF of lack of power of generator/unit n as a consequence of a failure event.
$\emptyset$	One-lag autocorrelation parameter.
F_n	Vector of binary elements of generator/unit n.
f_n^t	Fuel consumption of generator/unit n at time t.
FOR_n	Forced outage rate of generator/unit n.
f	Expected value of total operating cost.
γ	Significance level.
GHE_n	CO_2 emissions of generator/unit n.
G_n	Average production cost of generator/unit n.
g_n	Average power production of generator/unit n.
G^t	Power to be supplied by thermal and wind units at time t.
HF_n^t	Histogram frequency of generator/unit n, at time t.
h	Discrete state of power production.
h_n^t	Intermediate time series variable.
$HSU_{n,m}^t$	Hot start-up cost of generator/unit n, at time t, in scenario m.
$H(X,Y)$	Conditional entropy.
$H(X)$	Entropy of random discrete variable X.
H	Last state of t.
i_e	EPSO actual iteration.

$\mathrm{x}i_{mx}$	EPSO maximum number iteration.
i_s	Index of sampling point $\theta_i, i_s \in \{1, I\}$.
i_{th}	ANFIS output node.
I	Total number of sampling points of interval $\{\gamma, 1-\gamma\}$.
i	Data index with N dimension.
J_h	Number of elements with excess of spinning reserve in ESS.
j_h	Position of the element with excess of spinning reserve in ESS.
J	Last state of $(L = (H+1)^2 = B^2)$.
j	Data index with M dimension.
k	EPSO generation step.
l_m	Degree index at which a scenario under analysis fulfills the hourly forecasting error
Ln_i	ANFIS layer.
L^t	Value of load demand at time t.
l	Discrete state of power production when generators reliability is considered.
m_1	Battery parameter determined by experimental information.
m_2	Parameter of charge process of ESS.
m_3	Parameter of charge process of ESS.
M_{avg}	Defuzzification maximum average.
M_{cen}	Defuzzification centroid.
MDT_n	Minimum down-time of generator/unit n.
$MI(X,Y)$	Mutual information.
m_0	Battery parameter determined by experimental information.
MUT_n	Minimum up-time of generator/unit n.
μ	Gaussian mean deviation value.
m_{wt}	Integer scaling parameter of wavelet transform.
M	Scenario maximum number.
m	Scenario generated index.
NP_r	Normalized probability of occurrence of a determined event.
n_{wt}	Integer translation parameter of wavelet transform.
n	Number of generator/unit index.
$OFF_{n,m}^t$	Integer variable of cumulative account of the number of hours that generator n has been de-comitted.
Ω	Total scenario universe.
ω	Scenario index.
$ON_{n,m}^t$	Integer variable of cumulative account of the number of hours that generator n has been committed.
P_b	Power value that corresponds to the discrete state b.
P_{bt}^t	Power to charge/discharge VRB of ESS.
P_d	Discharged Power of ESS.
PDF_n^t	Probability density function of generator/unit n, at time t.
$P_{d,max}^f$	New power to be discharge from ESS.
$P_{d,max}^0$	Maximum power to be discharge from ESS.

P_{ESS}^{t}	Power exchange between ESS and electrical framework at time t.
P_h	Power value in discrete state h.
φ_{mn}	Father-wavelet function.
p_i	ANFIS parameter set of membership function.
π_{ω}	Probability of scenario ω.
P^{max}	Maximum power to be considered.
P^{min}	Minimum power to be considered.
P_{n,i_s}^{t-1}	Power production of generator/unit n at time $t-1$ in sampling point i_s.
P_n^{max}	Maximum power production of generator/unit n.
P_n^{min}	Minimum power production of generator/unit n.
P_n^t	Discrete PDF of power production of generator/unit n at time t.
$P_r(m)$	Probability of occurrence of a determined scenario m.
ψ_{ab}	Mother-wavelet function.
$P_{n\,,m}^{t}$	Power production of generator/unit n, at time t, in scenario m.
$p(t_{wt})$	Signal input of wavelet function.
$PUS_{n,m}^{t}$	Primary unit scheduling of generator/unit n, at time t, in scenario m.
P_v	Power through the inverter in EES.
P_v^{rated}	Rated power of the inverter in ESS.
$P(X)$	Distribution probability of random variable X.
q_i	ANFIS parameter set of membership function.
r_i	ANFIS parameter set of membership function.
RP^t	Reference power of ESS at time t.
R	Last discrete state of beta PDF.
r	Discrete state of beta PDF in interval $\{0,1\}, r \in \{0,R\}$
SDR_n	Shutdown ramp rate of generator/unit n.
σ_p	Parameter of discretization process.
σ	Gaussian standard deviation value.
SOC_{max}	Maximum state of charge allowed to be reached by VRB of ESS.
SOC_{min}	Minimum state of charge allowed to be reached by VRB of ESS.
SOC_t	State of charge at time t.
s_r	Value that corresponds to the discrete state r.
SR	Spinning reserve variable.
$SUC_{n,m}^{t}$	Starting-up cost of generator/unit n, at time t, in scenario m.
SUR_n	Startup ramp rate of generator/unit n.
τ'	EPSO mutated learning parameter.
τ	EPSO learning parameter.
θ_{i_s}	Sampling point I of the interval $\{\gamma, 1-\gamma\}$.
t_f	Ending time of charge of ESS.
t_i	Starting time of charge of ESS.
t_0	Bound time between the periods of charge/discharge ESS.
t_{wt}	Time-step used in wavelet function.

t	Scheduling time index.
U_n	Parameter of the CO_2 emission curve of generator/unit n.
$U_{n,m}^t$	Binary variable of (de)-committed generator/unit n, at time t, scenario m.
UR_n	Operating ramp-up rate of generator/unit n.
V_{i_e}	EPSO actual particle velocity.
$V_{i_e}^{new}$	EPSO new particle velocity.
V_n	Parameter of the CO_2 emission curve of generator/unit n.
$VOLL$	Value of lost load.
$VOWE$	Value of wasted energy.
WFE	Increment in spinning reserve due to wind power forecasting error .
w_i	ANFIS firing strength.
$w_{i_e}^*$	EPSO weight parameter.
w_{IN}	EPSO inertia weight.
w_j^t	Value of wind power generation of discrete state j at time t.
W_{max}^t	Maximum value of available wind power generation at time t.
W_{min}^t	Minimum value of available wind power generation at time t.
w_{mn}	EPSO minimum inertia weight.
w_{mx}	EPSO maximum inertia weight.
W_n^t	Total wind power generation at time t generator/unit n.
W^t	Time series of the total wind power generation at time t.
$w(t_{wt})$	Computed mother-wavelet function.
X_{i_e}	EPSO actual particle position.
$X_{i_e}^{new}$	EPSO new particle position.
X_n	Parameter of the CO_2 emission curve of generator/unit n.
x_n^t	Scenario time series of wind power nature.
X	Random discrete variable.
y^t	Normalized wind power profile at time t.
Y	Random discrete variable.
z_b	Generation cost incorporating ESS.
$z_{i_s,j}$	Total generation cost in sampling point i_s at discrete state of available wind power generation j.
z_n^t	Normalized total wind power generation at time t generator/unit n.

Chapter 1

Introduction

This chapter describes the framework of the electricity industry sector and the new paradigm related to renewable energy sources and their integration in the electricity framework, in particular, wind power capacity. This chapter also describes the motivations that support the proposed work and gives an overview of the organization of the thesis and the notation used.

1.1. Framework

The conversion of energy and its use, since the days when humans first learned to exploit its potential for their own benefit, has been the utmost factor in the growth of the economy and society and their sustainable development. In this way, the energy sector plays an important role in the national economy, since it is the propellant of greater stimulus and dynamism in creating new business and employment opportunities.

Historically, the electricity sector worldwide, before the 1980s, was characterized by a vertical structure of integrated companies (generation, transmission and distribution), which allowed the natural expansion and growth of the electricity infrastructure as a scale economy whose imperative ideology was to minimize production costs. Consequently it came to be regarded as a natural monopoly structure. Nonetheless, during the 1980s the idea of natural monopoly began to be questioned with the advent of new independent electricity producers, since the companies concerned with the transport and distribution of electricity were obliged to acquire the electricity produced by the new electricity producers [1]. Since the 1980s, the worldwide electricity sector has been subject to a constant process of restructuring, which allowed the creation of liberalized electricity markets and a competitive environment among different players, and consequently it allowed the necessary conditions for consumers to be able to participate in the electricity market, i.e., offering their proposed purchase of electricity to different suppliers [2].

The planning, management and exploitation of the electricity system are three important concepts for the electricity companies, which must operate in accordance with the global liberalization of the electricity sector, i.e., manage their operations with a concern to guarantee the rationality, sustainability and robustness of the complex energy mix that makes up the electricity system [3]. Thus, the mechanisms and tools that allow the proper participation in the electricity market should include a number of factors whose objectives are intrinsically related to profit maximization via optimizing the use of electricity system production, i.e., providing adequate support strategies for participation in liberalized electricity markets [4].

This new paradigm has not been ignored in Portugal. The initiative of electricity market liberalization happened in the 1990s with Directive 1996/92/CE of the European Parliament and of the Council (published December 19, 1996), whereby the rules for the creation of an internal electricity market were established, and allowing liberalization of the electricity sector. The same liberalization also took into account improvement of the efficiency of the electricity system and increased economic competitiveness [5]. On June 26, 2003, Directive 2003/54/CE of the European Parliament and of the Council was published, which triggered the liberalization of the electricity sector throughout the Iberian Peninsula, allowing the creation of the Iberian electricity market (MIBEL). Such restructuring of the electricity sector had a strong impact on the production and transmission of electricity [6].

In July 2007 MIBEL started its activity, with the expected competitive environment among players in the Iberian market mediated by the futures contracts market operator (OMEL) on the Spanish side, and by the daily and intraday market operator (OMIP) on the Portuguese side. However, it was only in April 2010, with Portuguese Resolution of the Council of Ministers no. 29/2010, that a harmonized MIBEL market was created in which some mechanisms have been defined, notably [7]:

- Definition of dominant operators;
- Harmonized mechanism of power guarantee;
- Definition of an interruptibility mechanism which harmonized the service system.

Resulting from the liberalization of the electricity sector with its competitive environment, there are currently two ways of transacting the supply of electricity:

- The bilateral contracts market, which is responsible for the agreements made between buyers and sellers of electricity, relative to the price and the quantity of electricity to be traded, which will later be implemented by the independent system operator (ISO).
- The spot market, where the purchases and sale of electricity are made, held by the market operator (MO). The MO determines the quantity of electricity to be produced and the market price of electricity, according to the offers of purchase and sale made by the market players.
- After the technical feasibility resulting from the agreements between the ISO and MO operators, related to the technical program of electricity production, a complementary service is also required to ensure the safety, robustness, and quality of the electricity supply.

Nowadays, the activity of electricity production with a liberalized and organized electricity market is associated with a wholesale market, where the producers' agents present their production and ensure the placement of that production, and agents seek to purchase electricity for two main reasons: one, to satisfy the demand of end customers; and two, for their own consumption. The trading activity is associated with a retail market where the trading agents compete to ensure the provision of electricity for end customers.

Monitoring the proper operation of the electricity market in the current liberalized environment is necessary because it is required to follow some characteristics and behavior of others organized electricity markets, as well as the developments in other markets, whose transactions can influence the determination of electricity prices (e.g., fossil fuel trading, carbon dioxide emissions trading, and financial markets, among others) [7]. Therefore an organized electricity market is composed of the following architecture:

- The wholesale electricity market, composed of the daily market (where electricity is purchased for the next day); the futures market (where electricity for long-term periods is purchased); and other mechanisms such as bilateral contracts or other specific legal mechanisms [8], [9]:
  - The daily market works through the intersection of offers (of buying and selling) by the various agents registered to operate in that market. Each offer indicates the day and time to which it relates with the price and amount of corresponding electricity. Furthermore, it follows its own operating rules;
  - The intraday market is where the electricity transacted in the daily market is corrected, in six sessions starting at 20h00 of the previous day (1st session), and ending at 16h00 of the current day (6th session). The electricity price is corrected with the corresponding electricity transaction;
  - The futures market which involves instruments of risk management for buying and selling electricity in the future (from one week to one year) between agents. These instruments are agreed under contracts, which can be divided into:
    - Future contract, which is a standardized contract to buy and sell electricity for a determined horizon time; where the players (producer and buyer) agree with each other to buy and sell electricity at a determined price;
    - Forward contract, which is similar to the future contract but differs on the final price of the electricity at the time of acquisition of the electricity;
    - Swap contract, which is a standardized contract where a positional variable price is exchanged for a fixed price, or vice versa, depending on the direction of exchange between the parties. This type of contract is applied to manage or take a financial risk, and it is not for the exchange of any subjacent product.
  - Bilateral contract, which can be divided into:
    - Forward contracting market, where future commitments for the production and purchase of electricity are established;
    - Daily contracting market, which is divided into daily contracting and intraday-adjustment, and where the programs of production and selling electricity are established for the next day of negotiation;
    - Service market, where the adjustment between production and consumption of electricity is performed in real time;
    - Bilateral contract, where the parties contract for the production and purchase of electricity for all different horizon times.

- The retail electricity market, where any customer can freely choose their electricity supplier. It is also helpful to guarantee the competition between the different operators in a balanced way and to minimize the information asymmetries between consumers and other market agents.

Since the ratification of the Kyoto Protocol in 1999, enhanced by the Climate Conference in Copenhagen in 2009, and the continuous conferences of parties (COP), the last one held in Lima, Peru, in December 2014, campaigners are trying to assess, warn, and encourage all nations to create a set of measures and targets to meet the emerging need for the continued mitigation of anthropogenic greenhouse gas emissions (GHE) around the world [10] to reduce rising seawater levels and mediate global warming.

In Portugal, the challenge of anthropogenic GHE mitigation is addressed through a series of encouraging targets. These satisfy Directive 2001/77/CE of the European Parliament and of the Council of Ministers, published in September 2001, which defined the incentives and motivations for production of electricity by renewable energy sources in order to maintain the standards of equity and sustainability in the whole economy [11]. The targets for the mitigation of GHE include a substantial increase in the share of electricity production from renewable sources (higher incidence of wind energy) through the encouragement of the private sector and consequently reducing the production of electricity from fossil fuels [12].

The endogenous use of renewable energy has a substantial level of social acceptance, it actively contributes to a sustainable economy and reduces dependence on importation of foreign energy. Beyond the inherent ecological advantages, the implementation costs are decreasing [13]. In the renewable energy field, wind power stands out as the most promising, since it is considered a very evolved and mature technology worldwide, with a good relationship between the implementation cost and profitability throughout its lifetime. Therefore, many European governments, despite the epidemic of economic crises which have struck Europe in recent years, have taken great efforts to continue their incentive programs for installing more wind farms or enhancing existing ones, as well as other incentives, and reforming laws to sustain further plans to decarbonize the global electricity system [14].

Such measures to decarbonize the electricity industry are supported by the policy adopted in 2007 by the European Council, i.e., the binding obligation on Member-States to increase by 20% the share of renewable energy by 2020, commonly referred to as the “20-20-20 program”. The policy imposes the following targets [15], [16]:

- Reducing the anthropogenic emissions of GHE in 20% relative to 1990 emissions;
- Increase the amount of renewable energy by 20% in the final energy consumption;
- Reduce in 20% the total primary energy consumption by increasing the energy efficiency.

At the end of 2013, and despite the economic crisis, more than 11,159 wind-power units were installed in the 28 Member States of the European Union (EU28), but with a decrease in installations of 8% compared with 2012.

This decrease had a negative impact on regulatory markets, the consequence of political uncertainties throughout Europe, which causes disturbances in legislative frameworks and future investments. Nevertheless, wind power capacity represents 32% of total power capacity installed in Europe, i.e., 5% more than in 2012. Furthermore, since 2000 more than 28% of the total renewable power capacity is derived from wind power.

Table 1.1 shows the total wind power capacity installed in EU28 (onshore capacity), where some countries such as Germany, Spain, United Kingdom, Italy, France, Denmark and Portugal stand out. Other countries show a noticeable increment of wind power capacity installed between 2012 and 2013. Figure 1.1 shows the total power capacity from 2008 to 2013 in MW and shared renewable power capacity in the EU28 (light green area), representing 72% at the end of 2013. The high contribution of wind power capacity over the years, which is briefly described in [17] is also shown in Figure 1.2.

In the case of Portugal, and despite the deep economic crisis that has affected other areas in this country, the harnessing of endogenous renewable energies and the decarbonization of the electricity sector has not been set aside. The constant demands to face new challenges are faced with new strategies such as the Resolution of the EU Council of Ministers no. 20/2013, which reinforces the ambitious Portuguese strategy for 2020, for a sustainable and progressive decarbonization of the electricity sector, through the "National Action Plan for Energy Efficiency" (PNAEE) and the "National Action Plan for Renewable Energy" (PNAER).

As shown in Figure 1.3, the integration and penetration of renewable energies into the electricity framework in Portugal from 2005 to July 2014 has deeply modified the dynamic behavior of the electricity generation mix [18], which requires appropriate studies to maximize the use of the available renewable potential. It also shows the relevance of renewable energy, which reached 4808MW at the end of July 2014.

Table 1.1. Total wind power capacity installed in some countries in EU28 [17].

Country	Total Capacity in 2012 (MW)	Capacity Installed in 2012 (MW)	Total Capacity in 2013 (MW)	Capacity Installed in 2013 (MW)	Increment (%)	Variation (%)
Denmark	4162	220	4772	657	12.78	14.66
France	7623	814	8254	631	7.64	8.28
Germany	30989	2297	33730	3238	8.13	8.85
Greece	1749	117	1865	116	6.22	6.63
Ireland	1749	121	2037	288	14.14	16.47
Italy	8118	1239	8551	444	5.06	5.33
Netherlands	2391	119	2693	303	11.21	12.63
Poland	2496	880	3390	894	26.37	35.82
Portugal	4529	155	4724	196	4.13	4.31
Spain	22784	1110	22959	175	0.76	0.77
UK	8649	2064	10531	1883	17.87	21.76

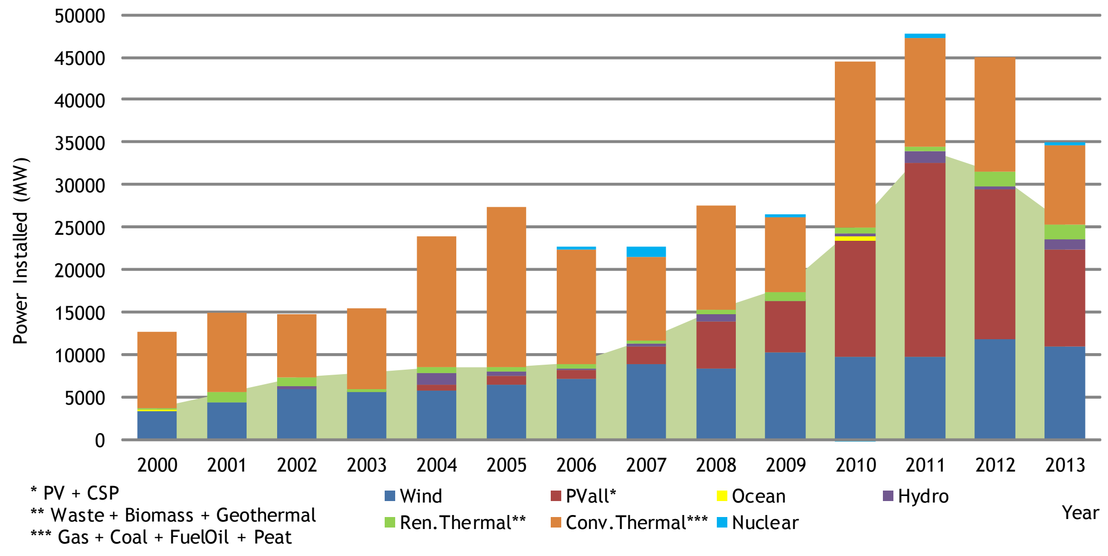

Figure 1.1. Power capacity in EU28 from 2008 till 2013 in MW and shared renewable power capacity [17].

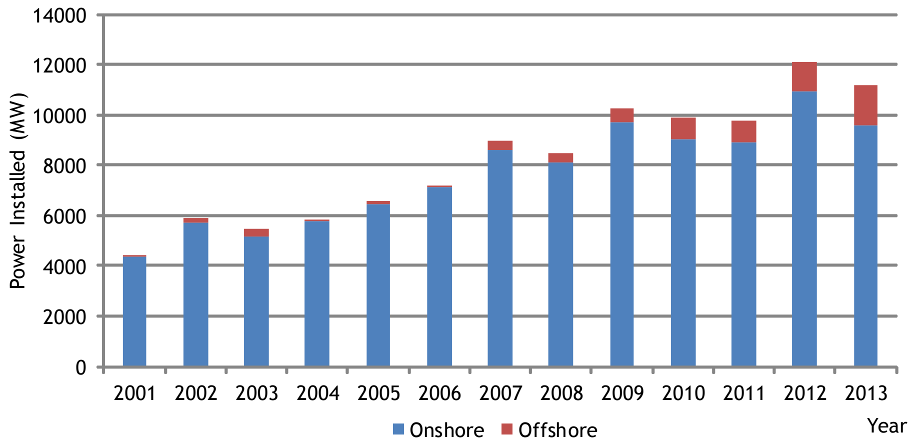

Figure 1.2. Wind power capacity evolution in Europe between 2001 till 2013 in MW in onshore and offshore installation [17].

Meanwhile, from January 2005 to July 2014, renewable thermal generation (biomass, biogas, solid urban waste plants (SUW), and geothermal) increased from 447MW to 752MW, overall hydro power plants from 4816MW to 5535MW, and photovoltaic power plants (PV) from 3MW to 332MW. In the final results, the total renewable capacity represents 24% of total primary energy consumed in Portugal at the end of 2012, of which 21% was related to wind power, and also a substantial reduction of 4618ktoe of conventional equivalent thermal energy with equivalent GHE reduction [19]. Wind energy is a mature and viable technology economically, in comparison with other renewable endogenous energies. It contributes to a significant reduction of GHE and also encourages competition in today's liberalized electricity markets due to its intermittency and volatility. In other words, the electricity frameworks face the need for greater flexibility and adaptability in terms of fluctuations and also demand variation because, in comparison with other renewables integration, wind energy is itself a non-dispatchable energy, in comparison with classical generation units (thermal or hydro power plants) [20].

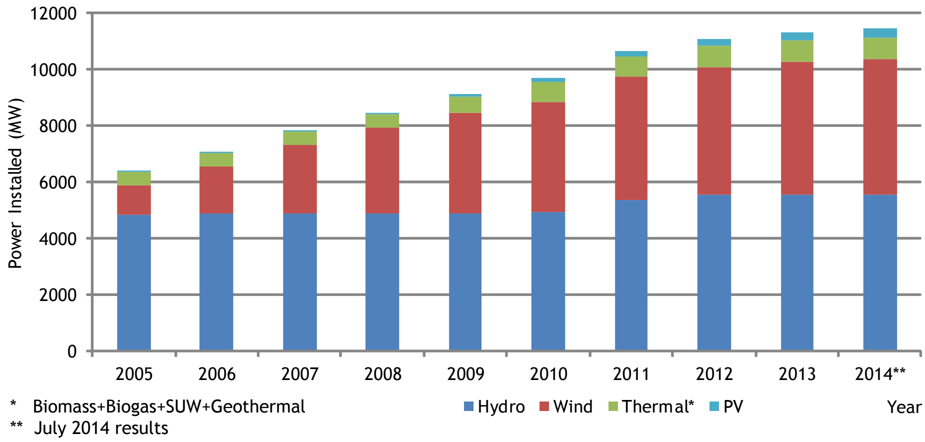

Figure 1.3. Overall renewable energy capacity installed in Portugal from January 2005 till July 2014 [19].

Therefore, it is necessary to differentiate the concepts of intermittency and volatility. Intermittency is an event that starts but abruptly culminates, whereas volatility is related to fluctuating variation around the trend line [21]. To represent these characteristics, Figure 1.4 shows the profile of wind power during one week of January 2014 in Portugal, in which it is possible to observe the difference between intermittency and volatility along a hypothetical trend shape of the wind power profile [22].

Regarding the consumption of fossil fuels and their use in the Portuguese electricity sector, it should be noted that there are ambitious plans for a gradual decommissioning of the biggest thermal power plants (mostly coal) between 2017 and 2030. However, despite the importance of gas for the robustness and quality of service of the electricity sector, Portugal will be dependent on natural gas supplies from Algeria and Nigeria, which requires a future improvement of infrastructure for its storage. Notwithstanding, there are some interesting plans for the reinforcement/replacement of 10% of the power generated by these conventional plants by biomass and natural gas power plants. These measures are planned in order to guarantee the energy mix of electricity production, the robustness and quality of service, and also to help in attenuating as much as possible the marginal costs of electricity, and finally to maintain competitiveness with other electricity markets [9].

Moreover, there are some studies that show a reduction of competitiveness in the Portuguese electricity market in the coming years, mainly because of the increment of the marginal cost of electricity. However, it will be easier in the coming years to export surplus electricity due to the strengthening of electricity connections between Spain and France, which will allow an increased flow of electricity produced in the Iberian Peninsula [23]. It should also be noted that, in order to minimize the impact of decommissioning the conventional thermal power plants in Portugal in the coming years, the necessary conditions are being created to increase the harnessing of hydro energy, i.e., by the construction of hydro power plants, either by strengthening existing plants or the construction of new hydro reversible plants (which allow more energy storage by converting the electricity surplus into potential surplus energy).

In the final calculation, the previously stated contributions will allow a reduction of Portugal's GHE to about 8Mton in the coming years, compared with the current emissions of 14.4Mton, which is significant. Finally, it is also important to note that there are more details that could be analyzed from the Portuguese national electricity system (SEN) report for the period 2013-2030 [24], but which are outside the scope of this work. Figure 1.5 shows the actual mix of electricity production in Portugal. Note the importance of wind energy as a slice of overall electricity production and the weight of thermal units (including biomass, natural gas and SUW plants) [23].

The energy storage system (ESS) is one of the answers for the new paradigm shift in renewable grid integration and the advent of smart grids, which helps to increase the flexibility of the generation mix, mitigating the stochastic nature of the impact of renewable electricity production in the electricity framework. Hydro storage or pumped hydro is the oldest and cheapest solution for this purpose, but it needs a favorable chain and adequate physical conditions, among others.

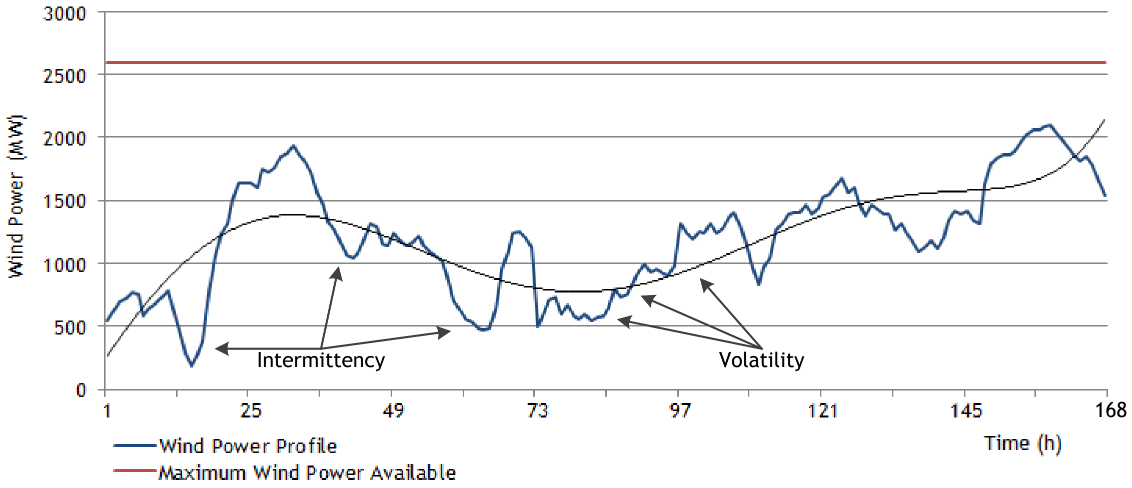

Figure 1.4. Wind power profile showing intermittency and volatility.

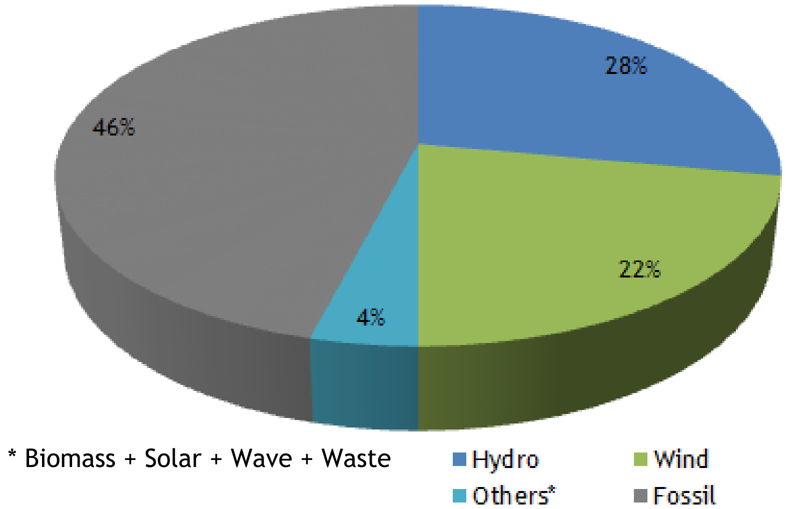

Figure 1.5. Distribution of Portuguese electrical mix production in 2013 [23].

Some pilot projects related to battery technologies are based on small-scale storage units, for self-consumption (in small industries), residential purposes or in locations highly dependent on fossil energy with high retail prices, such as islands, other isolated locations or those with less profitable hydro resources. Meanwhile, the same study concludes that, with adequate innovative policies and regulation, the final cost of the available technologies in ESS will be reduced in the following years making such options profitable.

The work that has been developed in this thesis is intended to produce new contributions by formulating mathematical models to be inserted in computational applications for decision and management support.

The aim is to combine the stochastic and volatility behavior of electricity market price forecasting, the volatility and intermittency of wind power behavior, the uncertainty related to wind power forecasting when wind power and conventional thermal electricity production are combined, applying also the possibility of small energy storage systems, usually found as pilots in island systems, which will be taken as examples for real application.

From the analysis of the literature review carried out during the research work, there are several challenges that the power systems industry and the scientific community have been facing in last years, namely:

- Reduction of fossil fuel dependency and mitigation of GHE;
- Development of computational tools for decision support with higher accuracy and improved proficiency;
- Harmonization between conventional and renewable power production, helping to increase the overall flexibility of the system;
- Reduction of generation costs in a sustainable and reliable manner;
- Development of algorithms for managing ESS based on batteries.

In summary, it is important in the context of Industrial Engineering and Management to develop innovative computational tools for the sustainable management of power systems, with a special focus in this thesis on the insular power systems industry. The following research topics are addressed in the forthcoming chapters:

- Electricity market prices and wind power forecasting, combining advances techniques such as mutual information (MI), wavelet transform (WT), evolutionary particle swarm optimization (EPSO) and adaptive neuro-fuzzy inference system (ANFIS), in real applications;
- Solving the economic dispatch (ED) problem using heuristic and stochastic approaches, in order to incorporate wind power forecasting error, system reliability and net load uncertainty. A probabilistic point of view using different configurations of conventional generation will be applied to an insular electricity framework;

- Solving the unit commitment (UC) problem using a stochastic approach under high wind power penetration, with several case studies using different configurations of conventional generation and scalability;
- Devising a strategic way to manage an ESS via battery configuration, combining conventional thermal generation and renewable generation in an insular electricity framework.

The approach developed for forecasting electricity prices and wind power has a stochastic feature. Uncertainty is the utmost important factor to be considered in rational decision making, since the omission of its influence can radically stimulate the correct benefits associated with wind energy exploitation. Most of the decisions are based on forecast profiles which lead to increasing difficulty, since the usual lack of information in datasets collected to create a forecast profile may make the decision-making processes more difficult. Furthermore, the scalability problem of the electricity framework, associated with the increased uncertainty of wind power forecasting, the increasing integration of renewable potential with its stochastic nature in the electricity framework, the storage cost (new strategies, or conventional strategies – hydro resources), and even the strategies and decisions may lead to increased costs of electricity production by conventional thermal power plants, which can translate to a waste of resources, increased GHE, and the diversion of government decarbonizing objectives in the electricity system.

Thus, treating the aforementioned topics in their different stages could provide major contributions to help the different players in the electricity system, enabling a rational and effective decision-making. It may ensure the correct co-existence of a robust and high quality energy production mix, contributing also to future lines of research to create efficient computational tools on the topic of sustainable management of power systems, given the advent of smart grids.

1.2. Motivation

An insular power systems industry is one where the entire electricity power grid infrastructure is physically located in an isolated geographical area surrounded by water. Typically, these have several limitations, including among others and [25]:

- Limited range of natural resources;
- Limited economies of scale;
- Seasonal population;
- Higher infrastructure costs;
- Distance from the mainland prevents interconnection of electricity supply;
- Different climatic conditions and microclimates from the mainland.

These limitations lead to negative outcomes such as dependency on overseas trade, economic weakness reducing the possibilities to play in conventional markets, the oversizing of infrastructures including the electricity industry, and vulnerability to climate change. Moreover, islands are heavily dependent on imported fossil fuels, and lack availability of fresh water and capacity for proper management of SUW, among other factors that directly affect the insular economy.

Such island economies have as their main revenue the inflows generated by seasonal tourism, which also creates indirect challenges to be overcome, such as the seasonal increment of population, resources management, and cost per tourist during their stay, among others. Natural resources such as fresh water may be compromised, making it necessary to resort to desalination processes or import fresh water, which undermines the local economy even more and the energy requirements [26]. In this sense, the oversizing of infrastructure, including the electricity framework, is a reality which makes its exploitation more expensive.

The mitigation of dependence on imported fossil fuels, especially for electricity production, is an important parameter for the economic sustainability of insular areas. Electricity production from fossil fuels is costly, especially due to transportation costs. Thus, the utilization of local and endogenous resources, mainly renewable energy systems, is of the utmost importance in many energy policies especially during the last decade, and the structures of electric power grids have started to change significantly with the recently increasing interest in renewable energy systems.

Compared with mainland electricity industries, the insular electricity grid structures are more sensitive to power quality issues, such as frequency and voltage deviations, especially if the level of penetration of renewable energy resources is high. Insular electricity grids have lower inertia due to the lower number of generating units connected to the framework. This makes them more vulnerable to large range frequency and voltage deviations, rendering the system reliability and security constraints more fragile. Moreover, the policies that allow the penetration of renewable energy resources in the electricity industry are limited.

In this sense, the insular power systems industry in general is considered as a good starting point for research and improvement and also for testing the impacts of new technologies and strategies for future technological advancements, ultimately including the advent of smart grids [25], [26].

Electricity frameworks in insular systems, can be classified according to their daily peak power demand (in MW) and annual energy consumption (in GWh) [27]:

- Very small islands: Less than 1MW per day and 2GWh per annum;
- Small islands: Within a range of 1-5MW and 2-15GWh;
- Medium islands: Within a range of 5-35MW and 15-100GWh;
- Big islands: Greater than 35MW and 100GWh.

Usually, the insular power systems industry is composed of a few conventional thermal units, especially in the case of very small and small islands. As stated previously, the inertia of the total system is significantly lower and the current status of insular power systems can be considered unreliable due to possible outages and fuel shortages, having such a small number of generating options that may reduce reliability and economic sustainability. In other words, the technical and nontechnical losses in insular areas are proportionately higher compared with the mainland, inciting the increase of fuel utilization and increasing the unit cost of electricity. Moreover the overall efficiency in the operation of insular power systems is significantly lower, which adds further economic burdens on energy companies and end-user customers [28]. Despite there being some successful examples of liberalization of electricity markets in the world, there are still constraints to be overcome in islands due to several barriers, [25] such as :

- In contrast with a continental electricity industry, an electrical unit in an island cannot have significant capacity due to system security reasons;
- The island electricity framework needs more reserve capacity than a continental electricity framework due to isolation and consequently the incapacity of interconnections with other electricity frameworks;
- Electricity production in islands is more costly (usually 2 to 5 times more) for the reasons given above, related to fuel provision and consumption;
- The geographical and local factor limitations of islands do not allow investment in conventional power plants, due also to social and seasonal factors;
- Renewable energy resources are the best candidates for the improvement of electricity production; however, the security issues of the electricity network and its stochastic nature limit their integration.

The aforementioned concerns may affect the economical sustainability of insular areas. As a real example, the electricity energy prices for end-users in insular areas varied between 25 and 34 cents per kWh, while the same cost was in the range of 10 to 14 cents per kWh in the mainland for the United States in 2005 [26]. The cost of electricity for residential and commercial end-users was approximately 31 cents per kWh in September 2010, 40 cents per kWh in December 2012, and 42 cents per kWh in the third quarter of 2013 in American Samoa [29]. It is clear that the price was significantly volatile in a short time period for Samoa, an insular area, largely due to the higher cost of fuel. Another reason for this cost difference is the increasing percentage of maintenance events, due to the aging of the electricity infrastructure [25].

Another example of these issues is located in Sicily, Italy, where the Ministry of Industry gives support [30] to improve and renew the electricity system. However, this is not common to all the cases and is also an additional burden on the economy of the country. As stated before, most islands do not have any exploitable fossil fuel sources [25].

An example of this is the case of the Canary Islands, Spain, where 94% of the electricity generation depended on imported fuels in 2010 [31]. Similarly, the island of Cyprus uses exclusively heavy fuel oil and diesel for electricity generation [32]. However, at present, there are some interesting cases of opportunities and challenges for insular power systems industries, showing valuable results in islands around the world. Some of these cases involve a high level of integration of renewable and endogenous resources; they are listed in brief below according to [25]:

- In 2010, PV farms generating 112MW were installed on the Canary Islands. Furthermore, the Canary Islands Energy Plan aims to have 30% of the electricity produced by RES, mainly solar (160MW) and wind (1025MW) [31];
- Due to the commitment of Cyprus to comply with the EU 2020 obligations, the country developed a program (National Renewable Energy Action Plan of Cyprus) that, among other targets, aims to install 192MW of PV farms and 75MW of concentrated solar power (CSP) by 2020 [32];
- In Rhodes, Greece, approximately 6% of the energy production comes from the 11.7 MW of installed wind power farms [33]. The biggest Greek island, Crete, has an installed wind capacity of 105MW, which accounts for 12.5% of the total capacity; however, the total licensed capacity exceeds 200MW; Furthermore, Crete is expected to have installed 140MW of solar energy by 2030 [34];
- In 1998 Samso Island was chosen by the Danish government as a pilot island to achieve 100% of electricity production from renewable resources, with more than 23MW of offshore and 11MW of onshore wind capacity, sufficient to satisfy the demand. The Spanish island of El Hierro is also subject to an ambitious target of becoming a 100% renewable energy island and currently wind power penetration has reached 30% [35];
- In Pantelleria, Italy, studies have shown that it is possible to install a plant generating 2.5MW of geothermal power. It may be possible to achieve a production of 20,000MWh per year, representing about 46% of the island's consumption [36];
- The government of the Azores has launched an ambitious plan to achieve 75% of renewable electricity production by 2018. Reflecting this ambition is the additional investment in geothermal plants in the major island (São Miguel) [37];
- Furthermore, other endogenous and renewable energy resources such as biomass, urban waste and wave or tidal energies are being studied in some pilot islands around the world.

Hence, this thesis has the objective to respond to the impact of the inherent challenges of electricity supply to islands. In detail, it focuses on the lines of research designed to support the decisions and management of the electricity companies which are the owners of conventional electricity conversion systems, renewable energy systems, or a combination of both for electricity conversion. In addition, this thesis also aims to analyze the different methodologies currently used, with a critical appreciation, and also to introduce several new contributions that address the uncertainties in the sustainable management of existing resources, seeking to provide viable solutions for the electricity industry.

The power systems of islands are characterized by their isolated and remote geographical location, which makes their interconnection with other power systems unworkable and makes it a challenging task to maintain a properly robust and quality service. One of the main consequences of this situation is the high generation cost related to the type of fuel consumed and its transportation.

However, in many cases these types of systems are located in places with important renewable and endogenous resources that could allow generation costs and GHE to be reduced. Yet, the stochastic nature of the behavior of such renewable energy sources is one of the most important technical barriers to be overcome.

ESS has been applied to face and mitigate this problem, because it can improve the flexibility of the system and allow the penetration of renewable energies more easily. Nonetheless, several factors, such as capacity tariffs, the renewable potential and investment costs, can affect the economic viability of the integration of such a mix in the electricity framework by the electricity industry.

The requirements of the electricity framework provide a line of research that uses not only the knowledge of the interface between scientific areas already established, but also the creation of self-knowledge with appropriate interfaces. New hybrid forecasting approaches can potentially reveal major levels of support decisions, allowing the electricity producer to proceed and manage its resources with higher levels of rationality, mitigating the problems associated with the inherent uncertainty of forecasting electricity market prices and wind power, or even other sources of uncertainty.

Accurate forecasting of electricity market prices and wind power are of the utmost importance for the success and profits in energy policy, since the accuracy of these forecasts allows a better management of the associated risks in the electricity framework. The present work focuses on the problems of operational planning in the short-term horizon, considering the uncertainty associated with the variables required for this propose, which should be investigated in order to obtain a set of solutions stochastic in nature, combining the use of methodologies to forecast and optimize the operation of conventional thermal power units and/or wind farms. A stochastic approach usually requires major computing resources due to the substantial increment of variables involved, the restrictions and the several scenarios considered; however, it provides more beneficial outcomes.

The growing integration of wind power capacity in the electricity industry has increasingly motivated the need to redefine the operational planning of the electricity sector in order to mitigate its natural variability and uncertainty. These factors increase the need for new computational tools and new strategies to integrate, manage and operate the daily electricity generation in an optimal way, without jeopardizing safety, robustness and reliability of the electricity framework. The randomness associated with wind power implies a considerable increase of reserves required to mitigate the fluctuations created by the wind potential.

The viability of renewable potential capacities is a current topic of great importance across the globe, and therefore the scientific literature on this subject is extensive. Due to the broad diffusion that has occurred in recent years, this thesis focuses on conventional thermal power units and wind farms in order to contribute with new computational tools for their proper management with a focus in the electricity industry located in islands, which have more difficulties with the reliable energy management.

1.3. Thesis Structure

This thesis is organized in seven chapters, briefly described hereafter. Chapter 2 presents a literature review concerning forecasting tools for electricity market prices and wind power, the methodologies used for optimal ED and UC, and also the ESS management methods. Chapter 3 presents the novel hybrid forecasting tool proposed to forecast electricity market prices and wind power in the short-term applied in real cases studies. Chapter 4 presents the new ED tool proposed for different scalabilities of conventional thermal power plants. Chapter 5 presents the new UC tool considering wind power uncertainty. Section 6 discusses the ESS problem and the new management tool. Chapters 4, 5 and 6 also take into account real cases studies located in islands to empirically proof the capabilities of the proposed tools Finally, Chapter 7 concludes the thesis.

In more detail, Chapter 2 presents the general framework of the electricity market structure in the Iberian Peninsula and the state-of-the-art related to the innovative contributions made by the scientific community with new forecasting tools in the short-term horizon for electricity market prices. Also, it presents the state-of-the-art wind-power forecasting tools available in the short-term horizon. It presents the state-of-the-art techniques found in the scientific literature for the ED and UC problems related to the management of conventional thermal power plants combined with renewable power generation. Moreover, it presents the most recent contributions related to ESS tools reported in the scientific literature as applied in the electricity framework combining conventional and renewable power generation. Finally, this chapter presents a brief characterization of stochastic programming.

Chapter 3 presents the new hybrid methodology/tool based on the successful combination of advanced techniques, namely on the combination of mutual information, wavelet transform, evolutionary particle swarm optimization and adaptive neuro-fuzzy inference system, to forecast the electricity market prices and wind power in the short-term (for 24h to 168h ahead). This chapter also presents the proposed hybrid evolutionary approach and the case studies analyzed for each topic (electricity market price forecasting or wind power forecasting) and the reported results, which were compared with other tools previously reported in the recent scientific literature.

Chapter 4 presents the new ED problem from a probabilistic point of view, i.e., the representation of wind power forecasting error and the power production at previous time-steps as a discretized beta probability distribution function, incorporating also the generator reliability by means of the discretized joint probability distribution function and failure events. Afterwards, a convolution process is carried out taking into account the wind power forecasting error and the discretized probability distribution function of the energy not supplied. The new methodology will be tested with two case studies and the chapter will conclude with a report of the results obtained.

Chapter 5 presents the new UC problem methodology used in this work with a case study considering an electricity framework combining renewable energy resources, mainly wind power. The proposed approach was based on a probabilistic point of view, being redesigned into a stochastic tool with accurate results. This chapter presents the mathematical formulation used, the case study analyzed and the reported results.

Chapter 6 presents a new management methodology for ESS. The ESS considered is based on batteries in an electricity framework which integrates conventional and renewable electricity production. Furthermore, this chapter describes the main mathematical formulation used to support the proposed management methodology, the case study under analysis and the reported results.

Finally, chapter 7 presents the main conclusions of this work related to forecasting, optimization and management methodologies in the short-term horizon, used to improve the combination of renewable energy resources, conventional power sources and the ESS system, used in real case studies from the electricity industry. Guidelines for future research and contributive works in these fields of research are provided. Moreover, this chapter reports the scientific contributions that resulted from this research work and that were published in journals, as book chapters or in conference proceedings.

1.4. Notation

The present thesis uses the notation commonly used in the scientific literature, harmonizing the common aspects in all sections whenever possible. However, whenever necessary, in each section a suitable notation may be used. The mathematical formulas will be identified with reference to the subsection in which they appear and not in a sequential manner throughout the thesis, restarting them whenever a new section or subsection is created. Moreover, figures and tables will be identified with reference to the section in which they are inserted and not in a sequential manner throughout the thesis. Mathematical formulas are identified by parentheses (x.x.x) and called "Equation (x.x.x)" and references are identified by square brackets [xx]. The acronyms used in this thesis are structured under synthesis of names and technical information coming from both the Portuguese or English languages, as accepted in the technical and scientific community.

Chapter 2

State-of-the-Art

This chapter starts by describing the organization of the electricity market and the evolution of the tools developed for forecasting electricity market prices and wind power in the short-term horizon. This chapter also provides an overview of the most recent published works related to the ED, UC and ESS management problems, aiming for sustainability.

2.1. Electricity Market Prices and Forecasting Tools

The restructuring of the electricity sector was motivated by the abolition of what was considered a natural monopoly, where the premise was the minimization of costs with vertical production integration. Nowadays, with the evolutionary course of the electricity market, the paradigm is based on organized competition between electricity market players and consumers (also market players), where the latter have the ability to choose their electricity supplier, creating the new premise for reduction of electricity prices.

In this new paradigm the electricity can be traded in two main ways. The first is by bilateral contracts, which are freely established between electricity producers and consumers, under defined conditions such as duration of contract, quantity of electricity and its price. The second is the pool market, which is an organized electricity market, such as stock exchanges, i.e., where the necessary articulations between buying and selling are carried out, and also where the quantities of electricity and its respective market prices are determined [38]. This structure is briefly presented in Figure 2.1. The pool market has three different sessions where all market players can proceed with electricity transactions in the following ways:

- The daily or spot market, where the electricity transactions occur one day before the time of the physical delivery of electricity, i.e., the offers should be sent before its opening, depending also on the subdivision of time horizon in which the market was created [39]. This procedure can be more easily explained by referring to Figure 2.2.
- The intraday market or adjustment market, which is a complementary market to the spot market, where the quantities of adjustment electricity transacted in the spot/daily market are traded.

This market is divided into several sessions, as shown in Figure 2.3. In this figure, the market is subdivided into six sessions [8], [40]:

- 1st Session establishes the electricity market price for the last 4 hours of trading on the negotiation day and for the next 24 hours ahead.
- 2nd Session establishes the electricity market price for the 24 hours ahead of the day of negotiation.
- 3rd Session establishes the electricity market prices for the next 20 hours ahead, between hour 5 and hour 24 of the next day of negotiation.
- 4th Session establishes the electricity market prices for the next 17 hours ahead, between hour 8 and hour 24 of the next day of negotiation.
- 5th Session establishes the electricity market prices for the next 13 hours ahead, between hour 12 and hour 24 of the next day of negotiation.
- 6th Session establishes the electricity market prices for the next 9 hours ahead, between hour 16 and hour 24 of the next day of negotiation.

It is important to note that, analogously to the daily/spot market, the intraday market runs at all times of day with its specific session. In a similar way to the daily/spot market, in the intraday market the authorized players can buy and sell electricity, stating the bidding session, the day and time, the price and the quantities of electricity to be traded.

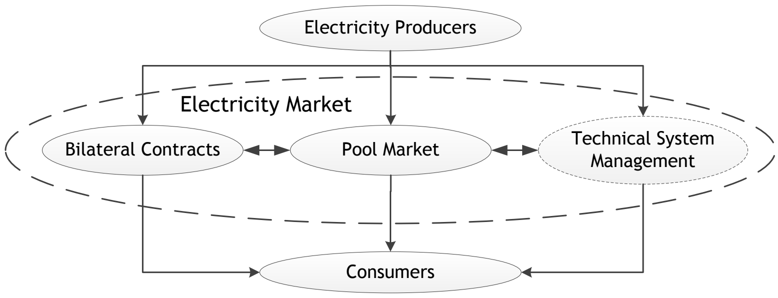

Figure 2.1. Brief characterization of electricity market.

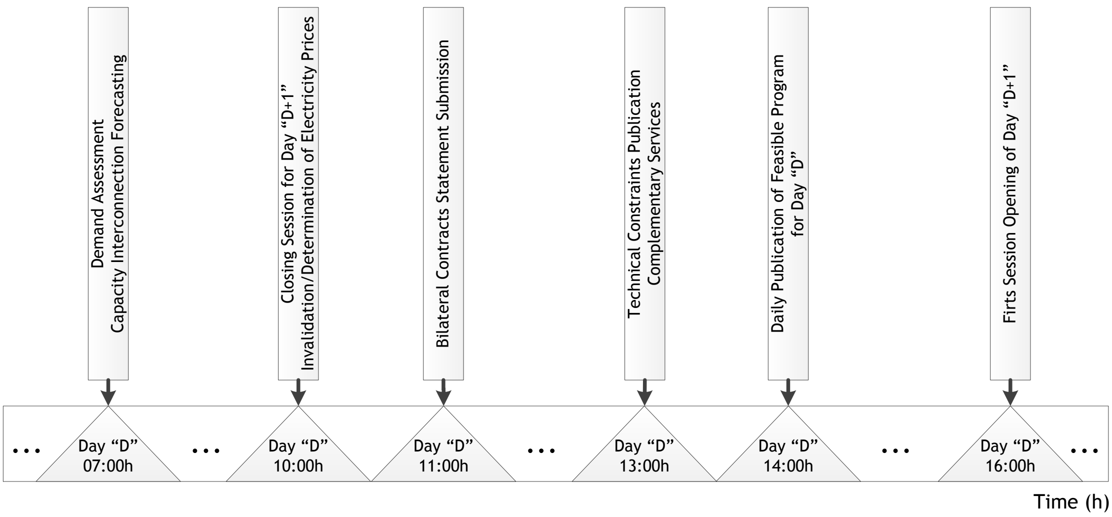

Figure 2.2. Daily electricity market procedure.

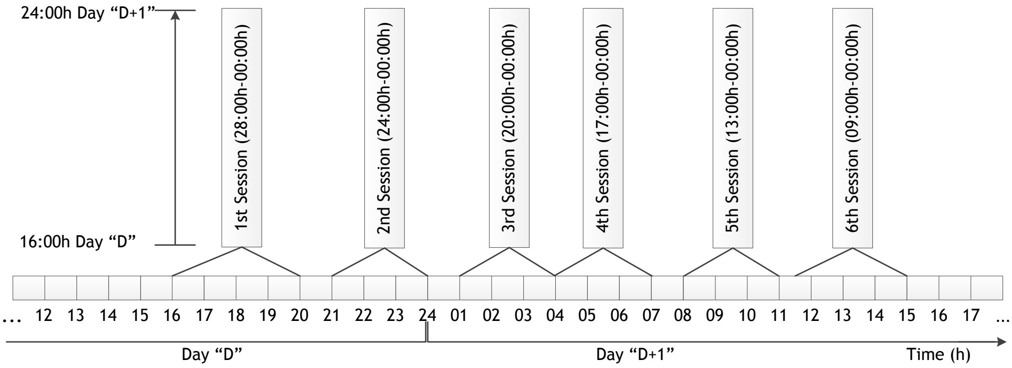

Figure 2.3. Activity sequence in electricity intraday market.

- The balance market is where the quality and robustness of the electricity supply are guaranteed through permanent monitoring of the relation between production and demand.

Moreover, in the MIBEL structure there are two entities responsible for the coordination of the different activities carried out in the electricity market [8]:

- The market operator (MO), which is responsible for the economic system management of electricity market. It is also responsible to receive, accept or reject the bidding for electricity, determine the closing electricity prices sessions every day, and all the activities that guarantee the quality, balance, and sustainability of the electricity market with all the players involved.
- The independent system operator (ISO), which is responsible for guaranteeing the quality condition of the transmission system, and also carries out the transit and electricity flow forecasting and solves the eventual bottleneck effects. More details regarding the ISO can be found in [41] where some aspects of the actual Portuguese electricity framework and electricity market are defined.

Nevertheless, to ensure the benefits for all market players it is mandatory to have accurate decision support tools, which include: the mathematical formulation of problems, the objective function and all restrictions involved, and tools for optimizing processes, such as the forecasting of electricity market prices, wind power and demand. For instance, whereas an electricity producer is interested to launch its electricity bids to maximize its profits, a consumer is interested to find and satisfy their electricity needs while minimizing the final cost. In a deregulated electricity market, the most important signal for all market players corresponds to the price [42]. Several characteristics of electricity market prices series make them harder to forecast than demand series, such as non-stationary behavior, high volatility and frequency, seasonality and the calendar effect [43]. As stated above, an accurate tool for forecasting short-term electricity market prices is needed to assist producers in designing their offering strategies to the electricity market to achieve maximum profits [44], [45], on the one hand, and to assist consumers in protecting themselves against elevated prices and for planning purposes, on the other [46], [47].

Furthermore, forecasting electricity market prices has grown to be one of the main research areas in power engineering [48], [49], [50], but the corresponding tools or techniques have not yet reached maturity [51]. Forecasting electricity market prices is indeed a crucial task for all market players [52] in their decision making, especially with the advent of smart grids [53]. In recent years, several forecasting methodologies have been described in the specialized literature. These can be divided into two groups: hard and soft computing methodologies [54]. In hard computing, some known methodologies can be found, such as auto regressive integrated moving average (ARIMA) [55], WT with ARIMA [56], and transfer function models [57]. This family of methodologies usually needs a large amount of physical data, requiring also the exact modelling of the system and resulting in high computational burden.

The present work will demonstrate the techniques of so-called soft computing, which use an auto-learning process from historical sets to identify future patterns. Starting from 2006, these so-called hybrid techniques started to be published more intensively in the scientific community. Such techniques, combining fuzzy neural network (NN) [58] and hybrid intelligent system (HIS) [59] are applied to forecast in the short-term (from 24h to one week ahead) the electricity market prices of some liberalized electricity markets.

In 2007 a technique was proposed based on NN with the Levenberg-Marquardt algorithm to forecast the electricity market prices in mainland Spain with historical data for the year 2002 for all four seasons of year, and also to forecast the electricity market prices in the Californian market in 2000 for 168h-ahead, reporting a lower computation time in comparison with the ARIMA technique [60]. Also, in the same markets and with similar historical data related to electricity market prices, there are some published studies applying a similar days algorithm [61] and weighted nearest neighbors (WNN) [62], which reported interesting results in short-term forecasting.

In 2008, a hybrid method was proposed corresponding to the combination of WT and cascaded NN (CNN) with evolutionary algorithms to forecast the electricity market prices in the Californian market with historical data of 2006, for 168h-ahead [63]. Also in 2008, a non-parametric technique of dimensional reduction was reported [64], integrating a locally linear embedding to forecast the electricity market prices in the New York Independent System Operator's (NYISO) with historical data from 2005 and 2006. In [65], a technique based on NN was reported to forecast the electricity market prices in the Spanish market for 24h-ahead, considering historical data of years 2002 and 2003. The adaptive wavelet NN (AWNN) technique has been reported to forecast electricity market prices in the Spanish and PJM markets (PJM is a regional transmission organization in the USA that coordinates the movement of wholesale electricity in all thirteen states between Pennsylvania and New Jersey), for 168h-ahead, considering historical data for years 2002 and 2004, respectively [66]. Still in 2008, another technique based on NN was proposed to forecast the electricity market prices in the PJM market for the next 168h, considering historical data of year 2002 [67].

In 2009, a hybrid technique based on a modified relief algorithm, MI and CNN was proposed to forecast the electricity market prices for 168h-ahead on the PJM and Spanish markets considering historical data of years 2006 and 2002, respectively [68]. Moreover, in [69], the cascaded neuro-evolutionary algorithm (CNEA) technique was also proposed for the PJM and Spanish markets, while in [70] a hybrid technique based on modified relief and CNN algorithm with correlation analyses was proposed to forecast electricity market prices in the Spanish and Australian (ANEM) electricity markets. In [71], a technique based on a mixed model with iterative NN and MI was proposed to forecast electricity market prices in NYISO and the Spanish market. Still in 2009, a technique based on self-adaptive radial basis NN with fuzzy inference was proposed to forecast the next 24h of electricity market prices of the ANEM market, considering historical data of 2006 [72]. Further, in [73], a technique based on sensitive analysis and NN algorithm was proposed to forecast the next 24h of electricity market prices in the PJM market, considering historical data from 2006.

In 2010, a hybrid technique based on NN with evolutionary algorithms was proposed to forecast the 168h-ahead electricity market prices of the PJM and Spanish markets, considering historical data of years 2006 and 2002, respectively, called the hybrid neuro-evolutionary system (HNES) [74]. In the same field, [75] presented a combination of NN and WT to forecast in the short-term the electricity market prices in liberalized markets. In [76] a technique based on ARIMA and NN was proposed to forecast electricity market prices 168h-ahead in the ANEM market, considering historical data of 2006. In [77], a technique based on recursive model combined with NN was proposed to forecast 24h-ahead electricity market prices in the PJM market, considering historical data of 2006. Still in 2010, a technique based on NN with an enhanced radial basis function network algorithm was proposed to forecast the electricity market prices for 24h and 168h-ahead of PJM market [78], and in the same field with relevant results, a hybrid model proposed in [79] and the modified relief technique in [80].

In 2011, a hybrid technique based on a combination of WT, particle swarm optimization (PSO) and fuzzy algorithm was proposed to forecast electricity market prices in the Spanish market for 168h-ahead, considering the historical data of 2002 [49]. In [81], EPSO and ANFIS were combined to forecast the 168h-ahead electricity market prices in the Spanish market. Also, in the same year a technique was published applying the pattern sequence-based forecasting algorithm [82] to forecast electricity market prices in the liberalized markets that are usually used in the scientific community to compare and testing their proposed techniques.

In 2012, a technique called “extreme learning machine” was proposed to forecast the electricity market prices in the ANEM market for 168h-ahead, considering historical data of 2006 and 2007 [83]. Besides, in [84], a technique that combined MI and composite NN algorithms in two stages was proposed to forecast the electricity market prices of the PJM and Spanish markets 168h-ahead with historical data of 2006 and 2002.

In [85], a technique that combined WT, inference system and NN algorithm was proposed to forecast electricity market prices in the Ontario market for 24h and 168h-ahead, considering historical data of year 2010. Still in 2012, a grey model based on PSO algorithm was proposed to forecast the electricity market prices in the Nord Pool, Californian and Ontario markets for 24h-ahead, considering historical data of 2007, 2000-2003 and 2006, respectively [86]. In [87], PSO and ANFIS algorithms were combined to forecast 168h-ahead electricity market prices of the Spanish market, considering historical data of 2002. In 2013, a hybrid technique called panel co-integration and particle filter was proposed to forecast 168h-ahead electricity market prices of the PJM market, considering historical data from 2008 [88] Furthermore, there are some interesting methodologies/techniques reporting results in the aforementioned markets in different short-term horizons, such as WT combined with chaotic least squares support vector machine (CLSSVM) and exponential generalized autoregressive conditional heteroskedastic (EGARCH) model, designed as (WT+CLSSVM+EGARCH) [89], singular spectrum analysis (SSA) method [90], a combination technique based on wavelet transform fuzzy, firefly algorithm and fuzzy adaptive resonance mapping theory (ARTMAP) designed as (WT+FF+FA) structure [91], a recursive dynamic factor analysis combined with Kalman filter (RDFA+KF) structure tool [92], and a derived methodology integrating the kernel principal component analysis, combined with the local informative vector machine, derived from a local regression method (KPCA+IVM) [93] technique.

2.2. Wind Power Forecasting Tools

The integration of wind power in the electricity framework has seen faster growth in the EU28 in comparison with conventional electricity units such as thermal or hydro power plants in recent years. Wind power presents a volatile and intermittent behavior that requires accurate tools for its convenient use. In [94] it is reported that this source should be forecasted in the short-term to achieve the best results, due to the lower influence of the uncertainty associated with this resource influencing the final forecasting results. The wind power integration in conventional electricity systems is responsible for the introduction of more variability, volatility, and uncertainty into system operation, which complicates the proper management of all production sources [95], [96].

Moreover, at present there is no consensus in the scientific community regarding the bounds of the time horizon to be adopted in wind power forecasting, due to the means of application and markets where it can be inserted or used. However, the following divisions are accepted within the scientific community: — very short-term horizon, which can be from a few minutes to a few hours, short-term horizon, which can be from a few hours to a few days, and the long-term horizon which can be from a few days to more than one week [97]. Hence, wind power forecasting tools represent a very important field of research for system operators, helping to reduce power fluctuations and to optimize the installed wind power resources, mitigating GHE [98].

Moreover, the short-term forecasting tools are really useful in supporting decisions in the spot, day and intraday markets, for wind power producers and for electricity ISO, helping to manage the balance between load and demand and the flexibility and robustness of the electricity system [99]. As referred to in [100], wind energy has more uncertainty and more volatility in comparison with other renewable sources, as shown in Figure 2.4.

Several wind power forecasting tools have been developed and described in the technical literature in recent years; these can be divided into physical and statistical methodologies [101]. Physical methodologies need an extensive number of physical specifications, and their inputs are also physical variables, such as orography, pressure, and temperature, presenting advantages in long-term forecasting [102]. Statistical methodologies try to establish inherent relationships within the measured data, which can have advantages in short-term forecasting [103], [104].

Figure 2.5 presents a general block diagram of physical models used in wind power forecasting. It is shown that the time numerical forecasting (TNF), i.e., the physical data, can be divided into specific models or power models, which use the physical data, and can also be combined with statistical forecasting tools [105]. In [106] it is stated that physical models use only physical considerations to reach the best estimations of wind speed in a specific site and eventually, in a second stage, a statistical model can be used to mitigate the remaining errors. In this way, the persistence model has proved be useful to establish a first approximation to forecast the behavior of wind power in the short-term, and also helps as a comparative reference for alternative tools [105].

Generally, the statistical tools are based on auto regressive techniques, i.e., ARIMA [107] or new reference model (NRM) [108], which are also time-series models that can provide a valuable first approximation, and inclusively are all able to beat numerical weather prediction (NWP) models for very short-term horizons. Soft computing models have become very widespread and accepted in the scientific community in recent years, mainly due to the reduced computational burden required, by using an auto learning process from historical sets to identify future patterns. Such models include: NN techniques [109], [110], hybrid models combining some techniques such as NN with WT (NNWT) [111], adaptive WT with NN (AWNN) [112], neuro-fuzzy (NF) algorithms [113], [114], evolutionary algorithms [115], wavelet-neuro-fuzzy (WNF) algorithm or a combination of WT, PSO and ANFIS (WPA) [116]. Table 2.1 presents the most widespread forecasting tools in the short-term and their classification model [106].

In the last few years the state-of-the-art in this field of knowledge has become extensive and varied. The literature review presented here will attempt to focus on the most interesting tools found and reported in the scientific community in recent years related to soft-computing techniques applied in short-term wind power forecasting. For instance, in [102] a tool was proposed to forecast wind power in the short-term based on the application of an evolutionary algorithm optimization for the automated specification of NN and nearest neighbor search.

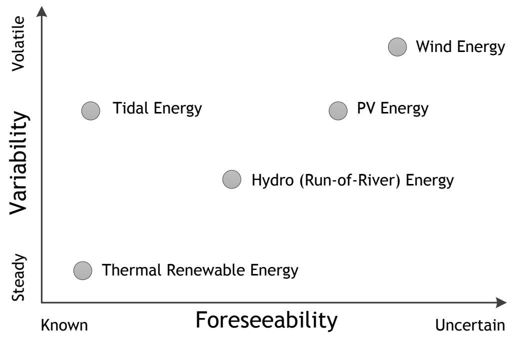

Figure 2.4. Variability and foreseeability of renewable energy sources [100].

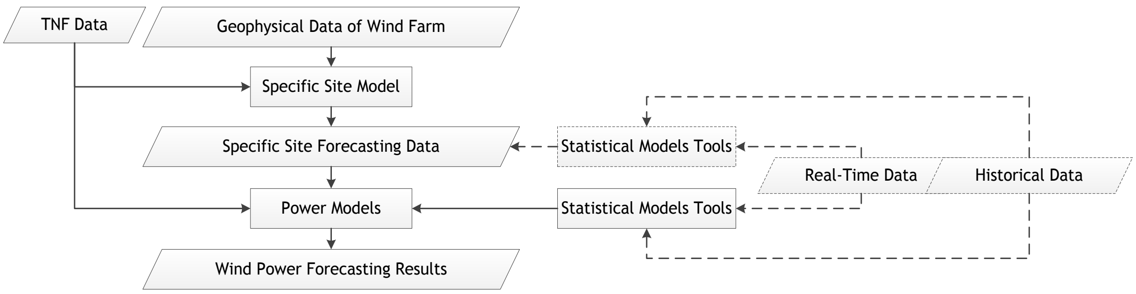

Figure 2.5. General block diagram for wind power forecasting from physical models.

In the same work, the forecast results were compared with two other algorithms based on PSO and differential evolution. The proposed method used weather data combined with historical wind power data from several wind farms located in Germany. The system was also tested with data from 2004 to 2007 with a time-step of 1h. In [117] a forecasting tool is presented to forecast the wind power in two wind farms in Portugal for the subsequent 72h-ahead, combining feed forward NN with entropy and correntropy theories in other to achieve a reduced forecast error distribution. The proposed tool was tested in online and offline frameworks for the years 2005 and 2006. In [107], a forecasting tool was proposed to forecast the wind speed for the next 24h and 48h-ahead using a fractional ARIMA model. The presented results were collected from four wind farms in North Dakota, USA. After the wind speed forecasting, the obtained results were combined with the mechanical characteristics of wind-driven data to determine the wind power output. Furthermore, the final results were compared with a persistence model.

In [118] a forecasting tool was proposed for the very short-term horizon, combining an exponential sweetening method and data mining. The proposed tool combined the collected data with a supervisory control and data acquisition system (SCADA) with weather, physical and mechanical wind-driven data. In addition, the forecasting system was compared with other systems such as NN and support vector machine (SVM). The tool forecast, with different time-steps, results for more than 168h-ahead. In summary, the system is divided into three models, where model 1 forecasts wind-driven function coefficients, model 2 uses mechanical wind-driven data and wind speed to forecast the wind power output, and model 3 uses data mining parameters combined with previous models to forecast the wind power data.

Table 2.1. Most widespread wind power forecasting tools used around the world [106].

Forecasting Tools	Model
AWPPS (More-Care)	Statistical, NF
AWPT	Statistical, NN
Prediktor	Physical
Previento	Physical
RAL (More-Care)	Statistical
Sipreólico	Statistical
WPPT	Statistical

In [119] a forecasting tool was proposed using a differential evolutionary algorithm with a new crossover operator and selection mechanism to train the Ridgelet NN and WT for the next 24h-ahead without exogenous variables. The case studies reported used historical wind power data from a wind farm located in Ireland in 2010, forecasting its wind speed, and the wind power in Spain with historical data from 2010. In [101] a wind power forecasting tool was proposed to forecast 24h and 48h-ahead, composed of feature selection components which perform irrelevance and redundancy filtering of historical data. This tool also used a forecasting engine based on cascaded NN structure with enhanced PSO. The system was tested at two wind farms located in Alberta, Canada, and Oklahoma, USA, respectively.

In [111], a wind power forecasting tool was proposed based on WT and NN to forecast the next 3h-ahead up to 24h-ahead with a time-step of 15 minutes. The system used historical data of wind power provided by the SCADA system in Portugal between 2006 and 2007 without exogenous or weather variables. Similarly in [113] a forecasting tool was proposed based on ANFIS technique to forecast the next 3h-ahead up to 24h-ahead with a time-step of 15 minutes. The system used the previous data from Portuguese wind farms connected to the SCADA system between 2006 and 2007 and also without exogenous variables. The proposed system was compared with ARIMA and NN forecasting tools. Finally, [120] reported a hybrid forecasting tool based on ANFIS and PSO, without exogenous or weather variables, to forecast the wind power behavior in Portugal with the aforementioned data.

In [121] a new hybrid and evolutionary forecasting tool is presented, based on a combination of EPSO and ANFIS algorithms to forecast the next 24h-ahead, with a time-step of 15 minutes for wind power production in Portugal, without exogenous or weather variables. The proposed forecasting system was compared with other forecasting tools, such as ARIMA, NN, data mining, and others. In [122] a forecasting model was proposed based on multi-observation points divided into two stages, to forecast the speed and direction of wind (stage 1). Stage 2 uses the data obtained from stage 1 to forecast the wind power output of the wind farm using dependent power curves. The study was performed with physical data from a wind farm on an Australian island. The proposed tool was also compared with a grey model and a persistence model.

In [95] a forecasting model is presented with a switching regime based on artificial intelligence to forecast wind power, specifically the extreme events associated with the uncertainty of NWP data. The NN algorithm used was based on resonance theory and probabilistic methods, and was tested at two different wind farms, namely, one in Denmark with historical data from 2000 to 2002, and one in Crete, Greece, with historical data from 2006 to 2008. In [123] the problem regarding the large penetration of new wind farms in the electricity framework was tackled, reviewing the advantages, disadvantages, and the advances in wind power forecasting tools. In this work a NN algorithm was also proposed to forecast the active and reactive power in the electricity grid using the case study of a wind farm in Germany. The time-step of this approach is 1h to forecast from 24h to 48h-ahead. As stated in [9], the forecast results can help in wind farm management and also in controlling the power transmission system.

In [124] a probabilistic model forecasting tool for wind power was proposed, which uses forecast points and uncertainty data from deterministic models. These results come from the quality of NWP data, daily wind power forecasting, and weather stability (speed and direction of wind). This forecasting approach also used a combination of a multiple NN with PSO algorithm. The historical data used comes from wind farms located in Denmark and Greece, as stated in [95]. Furthermore, this method forecasts the wind power for the next 60h-ahead. In [125] a wind power forecasting tool was proposed based on three models of WT and SVM to forecast, with a time-step of 1h to 3h-ahead, forecasting the wind power output of a wind farm located in Texas, USA. Model 1 is assembled accordingly with the wind-driven characteristics and WT principles. Model 2 combines the wind-driven characteristics with the substitution of Kernel radial basis function (RBF). Model 3 is a combination of the two previous models and the output is the wind power forecast.

In [112] a wind speed and wind power forecasting tool was proposed for the next 30h-ahead using in the first stage a combination of WT and NN to forecast the wind speed, and in the second stage a feed-forward NN to create a non-linear mapping between the wind speed and wind power results. These results were obtained without weather variables and performed for a wind farm located in Denver, USA. Reference [126] presents an overview of the wind power forecasting tools published in recent years using probabilistic methodologies, and other proposed tools used for wind power forecasting involving probabilistic techniques are reported in [127] and [128], showing an increasing interest among the scientific community in this methodology.

2.3. Economic Dispatch and Unit Commitment Tools

The most important technical barriers in the electricity framework that have to be overcome are related to the variability and uncertainty of wind power and other renewables.

In this context, ESS has been widely suggested as a way to overcome the aforementioned problems, due to its potential to improve the flexibility of the system and allow the penetration of renewable energies to be maximized. Nonetheless, several factors such as capacity tariffs, wind potential, governmental and social policies, and investment costs, can affect the economic viability of the project [129]. The implementation of demand response (DR) programs is another way to increase system flexibility and the accommodation of renewable energy sources by manipulation of a system load curve. However, DR response programs have to deal with the uncertainty in human behavior also, when electricity prices change dynamically, which is reflected in the estimation of electricity price elasticity, which is frequently used to decide the optimal use of DR resources [130]. In this way, the incorporation of stochastic tools in power system management has been thoroughly analyzed in the literature. As a result, several tools have been presented in the scientific community, such as stochastic programming, chance constrained programming, stochastic dynamic programming, robust optimization, and probabilistic approaches. Note that stochastic programming approaches consist of carrying out the optimal management, taking into account some possible situations or scenarios randomly generated. Specifically, these scenarios can be represented from the stochastic behavior of load demand, wind power generation and failure events. For instance, in [131] it is stated that a robust and flexible DR program, capable of dealing with high renewable integration in the electricity framework, could save more than 30% of generation costs, as well as helping to increase the system flexibility in facing sudden variations of wind power production. Nevertheless, the complete success of DR programs is strongly dependent on the awareness and knowledge of electricity users about the generation costs and the automation of household electric appliances. Notwithstanding, another valid option is to introduce the uncertainty of renewable power forecasting in ED problems. For several years now, representing wind power forecasting error by scenario generation has been widely adopted, as this is a flexible approach that enables a fast representation of the cross-temporal characteristics of wind power time series, which influences the determination of spinning reserve [132]. In this context, in [133], a scheduling model based on scenario generation was proposed. In this tool, several scenarios of wind power production, load demand and forced unit outages are randomly generated considering the auto-correlated nature of each time series. The optimal scheduling is then determined using a mixed integer stochastic optimization algorithm where the main objective is the minimization of the expected cost generation. In this tool, temporary displacement of the rolling time window was also introduced in order to improve the quality of the solution obtained by incorporation of the possible changes of wind power generation, load demand, and system reliability.

In [134], a scenario-generation method was employed to solve multi-objective dynamic economic emission dispatch problems where scenarios are generated using a roulette wheel mechanism using the probability distribution function (PDF) of the interest variables, while the optimization problem, including the nonlinear, non-smooth and non-differentiable characteristics, has been solved using an enhanced PSO algorithm.

In [135], a NWP technique was integrated into a stochastic unit scheduling model based on scenario generation in order to analyze the capabilities of NWP models from an operational point of view. The results show that the benefit obtained from updating the forecasts in intra-day operations is not significant. Scenario generation is a time-consuming method in which the analysis of a large amount of cases must be carried out, which requires intensive computational effort. To overcome this disadvantage, in [136] a tool that combines the advantages of stochastic and robust unit commitment methods is presented. This combination is carried out by incorporating weights that could be adjusted by the system operator, while scenarios are solved using Benders' decomposition. However, evaluating a randomly generated determined amount of cases could be a source of error. To deal with this problem, in [137] the incorporation of reserve specifications was proposed. In other words, a stochastic optimization is carried out considering the same spinning reserve specifications for all scenarios considered. In consequence, an improved solution to the unit scheduling is achieved by compensation of all scenarios that have not been taken into account.

In [138] and [139] some models were proposed introducing wind power generation into the ED problem as restriction in the optimization problem. Based on the probabilistic infeasibility and using the Lagrange multiplier method, the influence of wind power behavior and penetration level on total generation cost was analyzed. In [140] the effects of wind power generation on the ED problem and oxides of nitrogen (NO_x) emissions were modelled using the incomplete gamma function. In [141] a scheduling problem is presented as a dynamic programming problem, while wind power behavior was represented as a first-order Markov process. Based on the fact that aggregation of wind power generation reduces its forecasting error, in [142] an ED model valid for a short interval (validity interval) was proposed; this approach allows the stochastic relations in the optimization problem to be avoided. In [143], a methodology using a combination of a 2^m point estimated method and modified teaching-learning algorithm was proposed for solving multi-objective probabilistic ED taking into account GHE. In [144], a tool was proposed that incorporates wind power uncertainty by means of several states related to each other through a Markov process. The unit scheduling problem is then stochastically formulated in terms of these states.

Power system reliability and spinning reserve allocation are two other important topics from an operational point of view, due to serious difficulties in the management of the remaining generation capacity of the system when most of the units fail [145]. The incorporation of failure events has been analyzed in the literature. In [146] a tool was proposed that, as well as load forecasting error, it incorporates forced outages of generation units and transmission systems by means of a Monte Carlo simulation (MCS). This tool enables an estimation of the optimal reserve required in the solution of unit scheduling problems, taking into account a determined reliability level. In [147] a scheduling tool based on mixed-integer linear programming (MILP) was proposed to determine the optimal frequency-regulating reserve, while [148] presented another model based on mixed-integer programming (MIP) and MCS considering $N - 1$ contingencies.

In [149] a short-run ED tool was proposed, in which the different states that take place during the contingency event are analyzed and represented as a linear programming problem. Meanwhile, in [150] a methodology was proposed in which scenarios are randomly generated by using a roulette wheel technique that uses the corresponding PDF of load demand and wind power generation. The stochastic optimization problem is solved by means of an improved multi-objective PSO algorithm. Another optimization theory widely used is chance constrained programming, in which the stochastic variables of the optimization problem are represented by using equivalent deterministic constraints. In this context, in [151] a tool was developed in which stochastic variables such as load demand, forced outage rates, energy prices, and wind power generation are modeled, while the optimization problem is solved by implementing a standard branch and bound algorithm. As in the development of forecasting tools, hybrid techniques that combine stochastic programming with other optimization techniques have recently been proposed and reported in the scientific community in this field of knowledge. For instance, in [152] introduced a combined sample average approximation algorithm that combines a stochastic programming approach and chance-constrained programming in order to ensure using the wind power production at each time-step. Furthermore, probabilistic approaches based on modeling stochastic variables as a Markov process have recently been introduced, as well.

In [153] a general purpose ED tool was developed in which stochastic wind speed is represented as a Weibull PDF. Additionally, factors to represent the overestimation and underestimation of the available wind power generation are incorporated in the objective function of the ED problem. On the one hand, the factor related to the overestimation represents the purchasing of power generation from a determined source (spinning reserve) to supply the required capacity. On the other hand, the factor related to the underestimation represents the cost of consuming the excess power generated. Furthermore, the results obtained in [154] from the implementation of a hybrid methodology based on the combination of an auto regressive moving average (ARMA) model, artificial NN, and ANFIS suggest a Gaussian PDF. In [155] the analysis of a measured time series of one year was suggested using beta PDF, in order to model those PDFs similar to a Gaussian PDF, and those particular PDFs with a tail. To represent accurately those situations in which power production and consequently forecasting error are zero due to wind speed being too low or too high to produce electricity from the wind farm, in [156] a mixed PDF was proposed. Alternatively, [157] suggested employing the versatile PDF due to its analytical properties that facilitate the incorporation of wind power forecasting error in the ED problem. Other tools based on copula theory [158] and Lévy alpha-stable PDF [159] have also been suggested.

2.4. Energy Storage System Tools Management

The high penetration of renewable energy sources in the electricity framework can introduce problems for their optimal management, owing to the fact that these sources have a stochastic nature that introduces uncertainty into the scheduling process.

To deal with this problem, the incorporation of stochastic relations in the UC, the integration of ESS, and DR tools have been suggested in the literature. Battery energy storage systems (BESS) have received special attention for several years. From a global perspective, the potential for the installation of BESS in isolated power systems is estimated at 5300MWh. The greatest advantage of the incorporation of BESS is related to the reduction of levelized cost of energy (LCOE) by 6%, and increasing the penetration of renewable energies by approximately 50% to 70% where BESS are installed. In the case of regions with ample solar resources, BESS improves the correlation between solar radiation and load profile, and allows using the power generated during the day to supply peak demand, which usually occurs during the evening. However, the integration of BESS with wind energy could be affected negatively by the variability of this resource, as there could be long time periods without any wind generation. This lack of wind power requires an increment in the size of BESS, which increases the cost of the project [160].

Pumped hydro energy storage (PHES) has become a popular method for improving the flexibility of the power system. For instance [33] described the installation of PHES to be operated jointly with a wind farm, in order to supply energy demand in the Karpathos and Kasos islands of Greece. To manage PHES, the water required to be stored in the upper reservoir will be supplied by wind generation whenever it is available and by thermal generators during the night, when energy demand is low and a shortage of stored water occurs. In [161] it was suggested that this storage technology should be integrated into the power system of nearby Lesvos, where a detailed economic analysis has been carried out, concluding that, from the perspective of an investor, the optimum size is sensitive to the applicable energy and capacity tariffs, as well as wind potential and capital cost. Moreover, from the perspective of the power system, in those systems powered by liquid fossil fuels their consumption could be reduced and renewable power penetration could be increased, by integrating a small-capacity PHES. Thus, when the system is powered by liquid fossil fuels, a PHES with larger capacity is required since the power generation from renewable sources is increased. Nowadays, management and optimal control of an ESS is an important topic that has been widely analyzed in the technical literature, with several approaches proposed.

In this context, in [162] a tool was developed for the scheduling of power systems with thermal generators and an ESS. In this approach, an ESS is used to reduce the peak load and total generation cost. The scheduling process is carried out in three steps: in the first step, the scheduling of thermal units is done by applying an enhanced priority list (EPL) method, in order to reduce the computational time; in the second and third steps, an algorithm is applied to incorporate ESS into the scheduling process. A BESS is modeled by using linear expressions for charging and discharging processes, while the power inverter has an ideal behavior. The charge of the BESS is done by using the excess of electricity from the committed generators. However, if this is not enough, more units could be committed, in order to charge the batteries up to a determined state-of-charge level. The discharge is done during the peak load, in order to avoid the necessity of using the most expensive generators.

In [163] an optimization tool was developed to design ESS to be integrated into microgrids. The developed method was based on the solution to the stochastic UC problem, using the scenario-generation/reduction method in order to consider the different sources of uncertainty in a horizon-schedule of 24h, with a time-step of 15 minutes. The optimization is formulated as a mixed-integer problem, and is solved by using an improved version of the Cuckoo optimization algorithm. This problem is subject to several constraints related to the energy balance of the electricity and thermal loads, the operation of the boiler, BESS, and the power grid. Several technologies for the ESS are considered, such as hydrogen, thermal and BESS. Three management strategies are analyzed: two of them to design and manage BESS, and another to manage the thermal energy storage. The effects of incorporating ESS into the microgrid were analyzed in several case studies, obtaining an important reduction in generation costs.

In [164] a tool was proposed to design an ESS to be integrated into a microgrid. The methodology is based on determining the peak-shaving and excess of electricity according to the operating conditions, in order to determine the minimum energy to be supplied by the storage system, and to be charged into it. In addition, two mathematical models have been proposed: one to the insular system, and the other to the grid-connected systems. For the islanded microgrid, the UC problem incorporating renewable generation and ESS is solved, while for the grid-connected system, the economic benefits are considered to be the objective of the optimization process.

In [165] a methodology is presented to control a compressed air energy storage system (CAES) in order to provide ancillary services. The proposed method was based on the solution of the security constrained UC problem. The effects of the integration of CAES on locational pricing, peak-load shaving, power flows on the transmission grid, wind curtailment, and GHE were analyzed.

In [166] a method was proposed that incorporates PHES in the UC of thermal generators, taking into account environmental constraints. The methodology presented in this work consisted of two stages: in the first stage, the scheduling of PHES is determined, in order to modify the shape of the load profile, improving the operation of thermal units; in the second stage, the scheduling of thermal generators is determined, considering the changes introduced by the PHES in the first stage. Results obtained from the analysis of a case study revealed a reduction of 1.2% in the generation cost.

In [167] a tool was proposed for the integration of wind power and PHES in the UC problem, using a binary PSO (BPSO), which is an algorithm with several adjustments in order to achieve a feasible solution. These adjustments were related to the minimum up/down time constraint, limits on power generation and ramp constraints, power balance, and PHES operation. The economic benefits of the implementation of PHES were observed in the reduction of peak load.

In [168] a model was developed based on a robust optimization approach whereby the random variables are set, taking into account the worst situation, instead of establishing assumptions based on the probability distributions. The model was formulated as a two-stage robust optimization problem, where wind power production was assumed to be within a determined interval that could be obtained by using quantiles. Moreover, the conservatism of the solution obtained was controlled by introducing an integer variable that represents the number of hours that units are allowed for sudden changes in the wind power production. The incorporation of PHES allows the reduction of generating costs, while the robust optimization guarantees a reliable solution owing to the consideration of the worst-case scenario.

In [169] an optimization tool was proposed for the integration of wind power generation and PHES, in order to reduce variability, and improve its ability to be dispatched. This approach was based on the solution of the stochastic security constrained UC problem, through the scenario-generation approach, in order to incorporate several sources of uncertainty, such as error of forecasting load demand and wind generation, as well as system reliability. The optimization has been formulated as a mixed-integer programming problem, which was solved by using Benders' decomposition technique.

In [170] an optimization tool was developed integrating the ESS into the electricity market. The optimization model uses a two-stage stochastic UC formulation that aims to maximize the economic benefits; specifically, the integration of ESS was evaluated for providing primary reserve, energy arbitrage, and secondary reserve, considering different storage capacities. According to the results obtained from the analysis of a case study, the incorporation of an ESS reduces the participation of expensive generation units, such as those based on diesel and fuel-oil, in the power balance, and allows the supply of the secondary reserve in a cheap manner, using energy generated from those units with low operating costs, such as coal units. When an ESS is used for energy arbitrage, the operating efficiency of the system is improved, and the generation cost was reduced by approximately 0.5%, Moreover, when an ESS is used for energy arbitrage and secondary reserve, generation costs are reduced by approximately 1.1%. In short, using ESS to provide different services improves the accommodation of renewable energies, reducing the participation of the most expensive generators in the power balance, and reducing the operating costs of the power system.

In [171] a tool was introduced to find the optimal size and location of an ESS, improving the operation of distribution systems by reducing the risk related to the electricity price volatility, and the maximization of the economic profit. In this approach, the size of the ESS depends on the forecasting error of the load demand, and the power production of the distributed sources. This characteristic allows a reduction in the required capacity of the storage system, which consequently improves the economic performance of the project. Moreover, information about power exchange between the substation and the grid is used to optimize power purchasing, in order to maximize the benefits.

In [172] a tool is presented to design an ESS for the general purpose of mitigating the effects of variability and the uncertainty of renewable generation in the power system. The main advantage of the proposed model was the incorporation of regular deterministic and stochastic mixed-integer optimization formulations, which are frequently implemented in large-scale systems. A sensitivity analysis of the most important parameters of the storage system, such as the storage and power production efficiencies and costs, was carried out. The results obtained showed how the operating costs increase as the storage costs increase. Moreover, the generating costs decrease as efficiency increases.

Recently, in [173] a detailed review of the state-of-the-art of ESS technologies nowadays available around the world was provided, reporting the most advanced work in this field of knowledge and its applications in some isolated locations, the advantages and disadvantages of each technology, and some case studies carried out as pilot projects. Moreover [174] contains an ESS roadmap which shows how some countries can benefit from using ESS technologies in their electricity grid and the expected advances up to 2030.

2.5. Stochastic Programming

Stochastic programming is accepted in the scientific community as the most suitable solution and the closest to a real-world case approach, which is able to describe by restriction variables a considerable number of random phenomena with a proper mathematical formulation and an efficient computational burden. A particular case where the stochasticity is present in all moments is in the organized and liberalized electricity markets, where uncertainty of varied order is a determining factor in players' decision making, in which all phenomena, or at least a large set of these phenomena, should be considered [38]. In other words, for all problems involving data uncertainty it is necessary to apply stochastic programming, instead of deterministic programming where it is assumed that the nature of the data are known without uncertainty. To model a problem of stochastic programming, whose uncertainty is represented by a scenario tree, the future objectives of all the random variables used in the system to be solved should be known, or in an optional strategy it requires creating a systematically set of scenarios solution [136].

In stochastic programming formulation [40], each uncertainty set is a random variable, which will evolve over the time period and therefore it is considered as a stochastic process. The evolution of the load profile, wind power, or electricity market prices over a period time are excellent examples of stochastic processes. In stochastic programming the random sets are generally expressed by a finite set of objectives or scenarios. In this way, the random set scenarios C can be expressed by the following series: C_ω, $\omega = 1, 2, \dots, \Omega$, where ω is the scenario index of the total considered scenarios universe Ω. Moreover, C also represents the set of possible objectives of random variable: $C = \{C_1,\ C_2, \dots, C_\Omega\}$.

From the previous notation of C it is possible to describe a set of random variables, i.e., if C represents a wind power profile for a defined period of time ahead, C_ω is a set with the same length of period time of coordinates, showing the possible objectives of wind power on the period time considered. Meanwhile, each objective C_ω is related with a probability π_ω, which can be formulated as [38]: $\pi_\omega = P(\omega | C = C_\omega)$, where $\sum_{\omega=1}^{\Omega} \pi_\omega = 1$.

Stochastic programming deals with a probabilistic distribution of random variables that belong to the developed model. In this sense, stochastic programming is capable of finding matching solutions in all possible objectives, i.e., stochastic programming considers all the scenarios and their probabilities. However, the number of scenarios should be considered in a manner capable of yielding a satisfactory and timely solution.

As stated in [175], stochastic programming can be classified according to the way uncertainty is expressed and how the mathematical problem is adapted in the optimization tool, which is briefly expressed in Figure 2.6.

The most common approaches used in stochastic programming correspond with resource problems, normally having two stages:

- First stage, where the decisions are carried out before the uncertain parameter objectives are achieved. Normally, this stage is known as here-and-now decisions and does not depend on the objectives of random parameters;
- Second stage, where the decisions are carried out after the actual values of uncertain parameters objectives are found. This stage is also known as wait-and-see or resource decisions, which is dependent on each plausible value of random parameters. In other words, it is in this stage where the player can adapt the previous decisions for the actual outcomes of the random event.

Normally, stochastic problems are formulated by a linear programming problem of large dimension with a structure that models the randomness of the problem [38]. Resources problems are stochastic programs where resources actions are carried out after the uncertainty related to the problem is found. Besides, these problems are classified according to the number of their stages, due to the fact that each stage represents the moment when the decision is carried out, i.e., if the decision process is repeated more than once the problem is considered as a multistage stochastic programming problem [40].

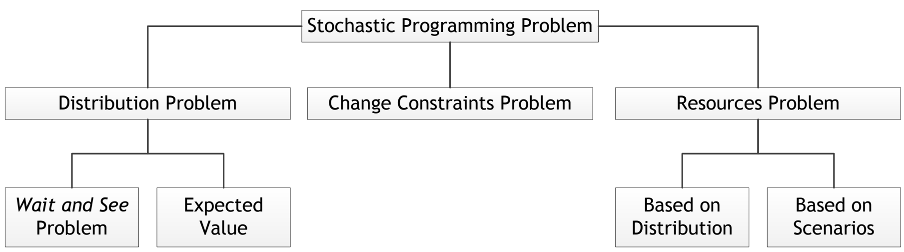

Figure 2.6. Stochastic programming problems classification.

Chapter 3

Hybrid Forecasting Tool

This section describes in detail the techniques used to create the proposed hybrid forecasting tool composed of the innovative combination of MI, WT, EPSO and ANFIS, advanced techniques applied in forecasting electricity market prices and wind power in the short-term. A comprehensive comparison with other methodologies previously published in the literature is also provided to demonstrate the enhanced forecasting accuracy and reduced computational burden, from testing on real case studies. In the hybrid evolutionary-adaptive (HEA) tool the MI is used to eliminate the randomness in the selection data series (electricity market prices or wind power) as inputs, increasing the robustness of the tool and helping to decrease the final forecasting error [176]. MI is a nonlinear feature selection technique that is more adequate for the aforementioned time series than a correlation analysis [101], [68]. For instance, the MI-based technique in [101] outperformed correlation analysis, which is a linear feature selection method, while electricity market prices or wind power are nonlinear mapping functions of their input variables. The WT is employed to decompose the sets of aforementioned data series into new constitutive sets with better behavior (smoothing effect). The forthcoming values of those constitutive sets are then forecasted with the ANFIS. EPSO brings on augmented ANFIS performance by tuning their membership functions to attain a lesser error. Compared with a classical PSO, the evolutionary concepts behind EPSO can make a real difference in terms of convergence properties. EPSO is self-adaptive, more robust and less sensitive to parameter initialization, compared with classical PSO. The evolutionary characteristics of EPSO and the adaptive characteristics of ANFIS complement each other perfectly. Finally, the inverse WT is used to reconstruct the signal, thus obtaining the final forecasting results.

3.1. Mutual Information

The MI technique is based on the concept of entropy. The concept of entropy shows that random processes may have a complexity of such order that the signal cannot be compressed or reduced. Moreover, entropy concepts are derived from statistical physics, and are used as a measure of the disorder state of a system. Entropy $H(X)$ is mathematically described as [69]:

$$H(X) = -\int P(X) \log_2\big(P(X)\big)\, dX \tag{3.1.1}$$

where X is a random continuous variable with distribution probability $P(X)$. In the case where variable X is a random discrete variable, i.e., $(X_1, X_2, \dots, X_n)$, with distribution probabilities $P(X_n)$ the entropy $H(X)$ is given by:

$$H(X) = -\sum_{i=1}^{N} P(X_i) \log_2\big(P(X_i)\big) \tag{3.1.2}$$

Hence, in entropy study the following examples should be considered:

- "A given event is equal to 0", when this event does not occur;
- "A given event is equal to 1 ", when this event does occurs;
- Consider the events: $X_1 = 0 \wedge X_2 = 1$, the individual entropy is equal to 0, i.e., $H(X_n) = 0$, if:

$$\big(P(X_1) = 0 \wedge P(X_2) = 1\big) \vee \big(P(X_1) = 1 \wedge P(X_2) = 0\big) \tag{3.1.3}$$

and the individual entropy is equal to 1, i.e., $H(X_n) = 1$, if:

$$P(X_1) = 0.5 \wedge P(X_2) = 0.5 \tag{3.1.4}$$

By extending the concepts of entropy for the case of joint distributions of random variables, where the value of a random continuous variable X is known, if the entropy of a random continuous variable Y is assumed to be known, then Equation (3.1.1) takes a new form [68]:

$$H(X,Y) = -\iint P(X_n, Y_m) \log_2\big(P(X_n, Y_m)\big) \tag{3.1.5}$$

In the case where variables X and Y are random discrete variables, the joint entropy $H(X,Y)$ is given by:

$$H(X,Y) = -\sum_{i=1}^{N}\sum_{j=1}^{M} P(X_i, Y_j) \log_2\left(P(X_i, Y_j)\right) \tag{3.1.6}$$

However, it is not possible to compute Equation (3.1.6) directly, so a new concept is necessary, which measures the level of uncertainty of the random discrete variable Y after having observed the value of random discrete variable X (or vice versa) called conditional entropy. The conditional entropy is defined as:

$$H(Y/X) = -\sum_{i=1}^{N}\sum_{j=1}^{M} P(X_i, Y_j) \log_2\left(P(Y_i/X_j)\right) \tag{3.1.7}$$

The conditional entropy $H(Y/X)$ quantifies the remaining uncertainty of Y when X is known, (or vice versa, i.e., the conditional entropy $H(X/Y)$ quantifies the remaining uncertainty of X when Y is known). Thus, the joint and conditional entropies are related by:

$$H(X,Y) = H(X) + H(Y/X) = H(Y) + H(X/Y) \tag{3.1.8}$$

Entropy theory and MI are closely related. Besides, the MI measures the level of information within a set of information data. This is described in Figure 3.1. The discrete mathematical expression is defined as:

$$MI(X,Y) = \sum_{i=1}^{N}\sum_{j=1}^{M} P(X_i, Y_j) \log_2\left(\frac{P(X_i, Y_j)}{P(X_i)P(Y_j)}\right) \tag{3.1.9}$$

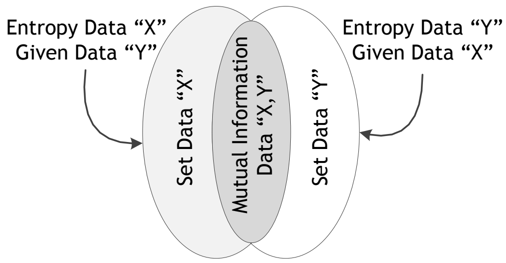

Figure 3.1. General mutual information representation.

The MI technique can be described by the following points:

- If $MI(X,Y) \approx 1$, then the sets are completed correlated (i.e., the information contained in each set is similar to each other).
- If $MI(X,Y) \approx 0$, then the sets are not related (i.e., the information contained in each set is not similar to each other).
- If $MI(X,Y) = 0$, then the sets are completely independent (i.e., no information is contained between the sets).

MI has a strong connection with the individual entropy described in Equation (3.1.2), with the conditional entropy described in Equation (3.1.7), as well as with Equation (3.1.8), so the MI in Equation(3.1.9) can be expressed as Equation (3.1.10) and Equation (3.1.11), i.e.:

$$MI(X,Y) = H(X) - H(X/Y) \tag{3.1.10}$$

$$MI(X,Y) = MI(Y,X) \tag{3.1.11}$$

To ensure the convergence of the HEA tool, the bounds of MI are very important to guarantee the best performance of the ANFIS. The MI helps to determine the best sets of candidates that will be inputs for training the ANFIS architecture [177]. These bounds differ between electricity prices forecasting results and wind power forecasting results, and were found through numerous attempts to find the best outcome for feeding the ANFIS architecture of the HEA tool.

3.2. Wavelet Transform

Nowadays, the application of the WT technique in forecasting tools is of utmost importance due to the need to overcome the limitations of non-stationary time series such as electricity market prices or wind power. It is a mathematical method applied in different engineering fields, which allows the analysis of time series in their natural state. In this way, the WT is normally used in pre-processing for understanding the non-stationary or time varying data [178], with sensibility to the irregularities of input data. WT is capable of showing the different aspects that constitute the data without losing the real signal content [179].

WT is able to reduce noise of the input data (smoothing effect) without visible degradation. It is important to note that time series data associated with random variables consist of ordered time observations and registered in the same period with the same time-step. Time series data is stationary when the mean and variance are constant and, frequently, it is considered hypothetically to impose stationary in a time series data for its analysis, i.e., the time series develop randomness over the time around a constant mean, reflecting a stable behavior [180]. The analytical processing which allows the time series representation in frequency domain and time is reached by continuous WT (CWT) and discrete WT (DWT). The CWT_{ab} of associated signal $p(t_{wt})$ of a mother-wavelet function ψ_{ab} is given by [179]:

$$CWT_{ab} = \int_{-\infty}^{+\infty} p(t_{wt})\, \psi_{ab}(t_{wt})\, dt_{wt} \tag{3.2.1}$$

where the scale parameter a is responsible for controlling the propagation of WT and the translation parameter b determines the window position as it moves by the data. The mother-wavelet $\psi_{ab}(t_{wt})$ is computed using function $w(t_{wt})$, i.e.:

$$\psi_{ab}(t_{wt}) = \frac{1}{\sqrt{a_{wt}}} w\left(\frac{t_{wt} - b_{wt}}{a_{wt}}\right) \tag{3.2.2}$$

In this way, the CWT function will be, by substitution of Equation (3.2.2) in Equation (3.2.1), the following:

$$CWT_{ab} = \frac{1}{\sqrt{a}} \int_{-\infty}^{+\infty} p(t_{wt})\, w\left(\frac{t_{wt} - b_{wt}}{a}\right)\, dt_{wt} \tag{3.2.3}$$

Nevertheless, since the DWT is computed in temporal domain and multiplied by scaled and shifted WT function $\psi_{ab}(t_{wt})$, this will give rise to a number of coefficient series of WT scaled in frequency and time [181], which in practice is not useful, since it requires a high number of scales and translations which consumes a large capacity in computational burden and time [179].To overcome the aforementioned problem, a DWT was created to give in an efficient way the description relative to CWT, and nowadays it is widely used to decompose the time series under study. The DWT is defined as:

$$DWT(m_{wt}, n_{wt}) = 2^{-(m_{wt}/2)} \sum_{t=0}^{H} p(t_{wt}) \varphi\left(\frac{t_{wt} - n_{wt} 2^{m_{wt}}}{2^{m_{wt}}}\right) \tag{3.2.4}$$

where H represents the length $p(t_{wt})$, and the parameters of scaling and translation are changed to integer variables $a_{wt} = 2^{m_{wt}}$ and $b_{wt} = n_{wt} 2^{m_{wt}}$ respectively, with a time-step t_{wt}. An efficient way to use the DWT is by multi-resolution analysis developed by Mallat, using a "father-wavelet" with a complementary "mother-wavelet", where the "father-wavelet" determines the low frequency series components while "mother-wavelets" determine the high frequency series components. However, it is recommended to use orthogonal wavelet functions in order to simplify the orthogonal vector space and the associated coefficients of the wavelets [182].

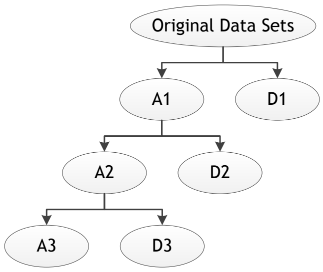

Figure 3.2. Three-level decomposition model of WT.

Furthermore, in this work and following the description cited in [52] and [116] the Daubechies of fourth order, or Db4, was used as mother-wavelet-function. The Db4 has asymmetrical and continuous proprieties, where a higher order level will create a higher level oscillation, which is desirable in forecasting [179] [182]. The coefficients of approximations A_n and details D_n are expressed as:

$$A_n = \sum_n DWT(m_{wt}, n_{wt})\varphi_{mn}(t) \tag{3.2.5}$$

$$D_n = \sum_n DWT(m_{wt}, n_{wt})\psi_{mn}(t) \tag{3.2.6}$$

where $\varphi_{mn}(t_{wt})$ is the father-wavelet and $\psi_{mn}(t_{wt})$ is the mother-wavelet, and $DWT(m_{wt}, n_{wt})$ are the coefficients obtained from Equation (3.2.4) [180]. The Db4 is chosen as mother-wavelet function due to a better trade-off between smoothness and length [52]. Besides, the DWT algorithm used in this work was based on four filters divided into two groups: the decomposition in low-pass and high-pass filters and the reconstruction in low-pass and high-pass filters. The approximations and details of the original sets can be obtained via Mallat's algorithm as referred to in [179] or in [116].

Figure 3.2 shows a three-level decomposition model of WT. In general, the approximations are able to retain the general information of the original sets, i.e., the low-frequency representation and description of the high frequency component. The details are able to explain the difference between successive approximations. It is possible to conclude from Figure 3.2 that the original set was decomposed in two subseries (A_n and D_n) called subseries of approximation and detail, respectively. From this point, the subseries A_n was decomposed again in a second level and repeated in a third level. The procedure will result in (A_1, A_2, A_3) approximation subseries and (D_1, D_2, D_3) details subseries.

3.3. Evolutionary Particle Swarm Optimization

The classical PSO is a research tool where each potential solution can be represented as a particle of a determined population. Theoretically, such particles (individuals) show a similar movement, as do animals that move in large groups.

The position changes in research space and normally the more successful individuals are imitated by the remaining group of individuals. Considering an optimizing problem where the solution space is D-dimensional, the swarm constituted by P particles is initialized with a random initial position x. The position of each particle then converges to the allowable solutions domain of the optimization problem oriented after a continuous of convergence process to the optimal solution. Moreover, in the iteration process, the particle position is changed accordingly with its experience and information shared with its neighboring particles. Besides, the aforementioned position is changing by the velocity v, which represents the mechanism of the optimization process and reflects the information shared between particles. Furthermore, each particle is evaluated by a fitness process which gives a value, and consequently it measures the particle performance to obtain the most convenient solution to the problem [183].

EPSO is a meta-heuristic method where rules and optimization concepts are contained in the evolutionary strategies and self-adaptive properties [184]. In EPSO is usual to call by “generation” the data with alternative solutions and by “individuals” the particles data. Each particle is described by object parameters (the value of the variables describing the solution) and strategic parameters (the mutation coefficients of each variable, angle of correlation of mutation variables, or similar) [185]. In EPSO it should be noted that [186]:

- Each particle is replicated, (with required number of times to find the best solution or until the maximum number of iterations is reached);
- The weight parameter of the particles is transformed by an evolutionary process;
- The object parameters of each particle are transformed into a new generated particle by strategic parameters, again by an evolutionary process;
- The new mutated particles generate new particles;
- For a group constituted by old particles and new particles, the best fit should lead to the generation of a new population of particles. The strongest particles will survive in the evolutionary process helping to provide the optimal result.

Hence, the formulation of EPSO is composed of object parameters X (position) and strategic parameters w that correspond to the weights. The movement rule of EPSO is defined as [187]:

$$X_{i_e}^{new} = X_{i_e} + V_{i_e}^{new} \tag{3.3.1}$$

$$V_{i_e}^{new} = w_{i0}^{*} V_{i_e} + w_{i1}^{*}\left(b_{i_e} - X_{i_e}\right) + w_{i2}^{*}\left(b_g^{*} - X_{i_e}\right) \tag{3.3.2}$$

Note that Equations (3.3.1) and (3.3.2) are similar to the classical PSO algorithm, that is, the movement rule keeps the inertia, memory and cooperation terms of Equation (3.3.1), which can be shown in Figure 3.3. The difference in EPSO is related to the weights $w_{i_e k}^{*}$, which undergo mutation, given as:

$$w_{ik}^{*} = w_{i_e k} + \tau N(0, 1) \tag{3.3.3}$$

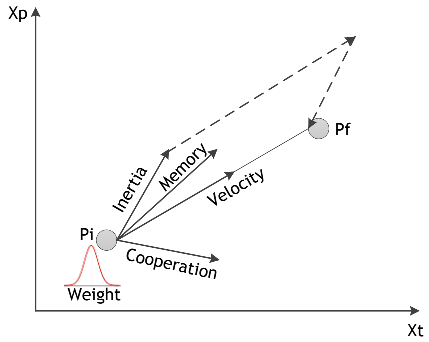

Figure 3.3. EPSO movement rule of a particle.

where $N(0,1)$ is a randomly Gaussian variable with mean 0 and variance 1. Furthermore, the global best b_g^* is changed according to:

$$b_g^* = b_g + \tau' N(0,1) \tag{3.3.4}$$

In Equations (3.3.1)-(3.3.4), the parameters $\{X_{i_e},\ V_{i_e},\ b_{i_e},\ k,\ \tau,\ \tau'\}$ represent the position X_{i_e}, velocity V_{i_e}, best point b_{i_e} found at generation k, the learning parameters τ and the mutated learning parameter τ'. EPSO usually presents better convergence characteristics than PSO due to the fact that only the stronger particles survive in the evolutionary process [184]. Moreover, the inertial weight, beyond the acceleration constant, determines the previous velocity in the new velocity, acquiring a trade-off between a local search and global search in D-dimensional solution space. The inertial weight correction along iterations can reduce the number of iterations, increasing the convergence speed of the system to the optimal solution. In other words, it can reduce the computational burden of providing a timely solution. The inertial weight can be determined by the following expression [52]:

$$w_{IN} = w_{mx} - \frac{w_{mx} - w_{mn}}{i_{mx}} \times i_e \tag{3.3.5}$$

where w_{mx} and w_{mn} are the maximum and minimum inertial weights found from successive simulations, i_e is the actual iteration and i_{mx} is the maximum iteration. Moreover, comparatively to a classical PSO, the evolutionary concepts behind of EPSO can make a real difference in terms of convergence properties. EPSO is self-adaptive, more robust and less sensitive to parameter initialization, comparatively to classical PSO The EPSO algorithm used in this work is described as [188]:

- Start the swarm with P particles and for each particle p the position X_{i_e} and velocity V_{i_e} will randomly start;
- Evaluate the fitness of each particle using the actual position X_{i_e};
- Evaluate the performance of each particle until the actual iteration, and evaluate the performance of each particle until the actual position b_g;
- Update the velocity of each particle provided by Equation (3.3.2).
- Update the position of each particle provided by Equation (3.3.1).

- Update the iteration number and compare it with the maximum It_{mx} chosen. If the optimal solution is found, stop the iteration and save the information; otherwise, update the weights and restart from the evaluation of fitness of each particle.

3.4. Adaptive Neuro-Fuzzy Inference System

ANFIS is a successful hybrid combination of NN and fuzzy algorithms. This is possible due to the low computational requirements of well-structured NN architectures, which can be useful to deal with a large quantity of data, combined with a high response given by fuzzy algorithms. Furthermore, the NN algorithm has the self-learning capability that is combined with the fuzzy algorithm to self-adjust its parameters [49]. The ANFIS system is often used in industrial applications for the following reasons [189]:

- Easy of application of learning algorithms coming from a developed NN techniques;
- Integrate and promote the implicit and explicit knowledge of fuzzy logic;
- Knowledge extraction possibility in rules, from data sets supported by fuzzy logic.

The ANFIS system uses a conversion machine to convert the input data into linguistic variables and vice versa, where the elements of fuzzy sets have membership levels that interpret the uncertainty level of whether some sets are related to the system or not. In this way, let X a set and $x \in X$, and let $\mu_A(x)$ be the membership level of x of fuzzy set Fz, where $\mu_A(\bullet)$ is a membership function that $\mu_A : X \to \{0, 1\}$. The previous membership function indicates the uncertainty level of some element of x belonging to set A. Moreover, a fuzzy set is defined by a membership function and domain of this function. In Figure 3.4 shows the membership functions most commonly used in ANFIS systems. In [190] it was proved that the triangular membership function presents a good computational efficiency, but it depends where it is applied. In this work, as proved in [52] and in [116], the triangular membership function in the ANFIS system was applied in forecasting electricity market prices and wind power.

Figure 3.5 also presents an inference system architecture where the input data is converted into fuzzy language and afterwards the inference and rules process will be converted again into the original language data. The fuzzification process is where the numerical data is changed to fuzzy language variables, the inference mechanism defines the way the rules are combined, and the defuzzification process is where the fuzzy results variables are changed to numerical values. The mechanism most often used in this field is based on the Takagi-Sugeno system [191].

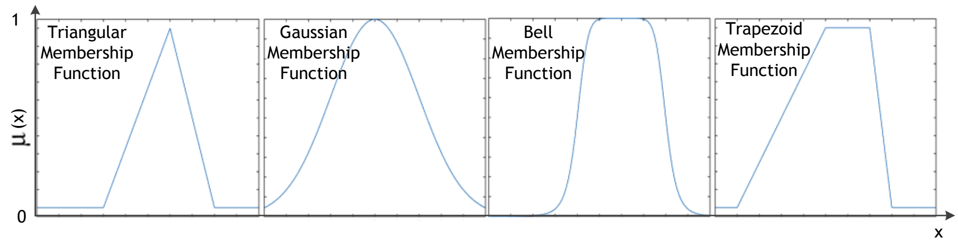

Figure 3.4. Most used ANFIS membership functions.

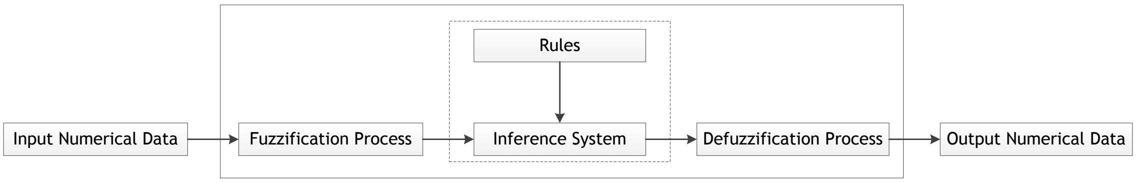

Figure 3.5. Inference system architecture.

Some techniques that are generally applied in the defuzzification process are as follows [191]:

- Maximum first technique, where the first maximum of membership function is determined;
- Maximum average technique, where the average of all results of the membership function that achieved the maximum is determined; i.e.:

$$M_{avg} = \sum_{i=1}^{m} \frac{x_i}{m} \tag{3.4.1}$$

- Centroid technique, determined under the membership function area and in the defuzzification process, considered as the centroid axes, i.e.:

$$M_{cen} = \begin{cases} \dfrac{\sum_x \mu_A(x) \times x}{\sum_x \mu_A(x)}, & if\ x\ is\ discrete \\ \dfrac{\int_x \ \mu_A(x) \times x\ dx}{\int_x \ \mu_A(x)\ dx}, & if x\ is\ continuous \end{cases} \tag{3.4.2}$$

The general ANFIS architecture used in this work consists of fuzzification, rules, normalization data, defuzzification, and signal reconstruction by the respective layers, i.e., it is composed by five layers, thus also called multi-layer feed-forward network, described in general terms in Figure 3.6 [191]. Each layer Ln_i is the output of the i_{th} node in layer n. Each layer also has a specific purpose, as described below [87]:

- In Layer 1 all nodes i are adaptive nodes with node function $L1_i$ given by:

$$L1_i = \mu A_i(x), \qquad i = 1, 2, \tag{3.4.3}$$

or

$$L1_i = \mu B_{i-2}(y), \qquad i = 3, 4, \tag{3.4.4}$$

where x or y is the input of the i_{th} node and A_i or B_{i-2} are the linguistic labels associated with these nodes.

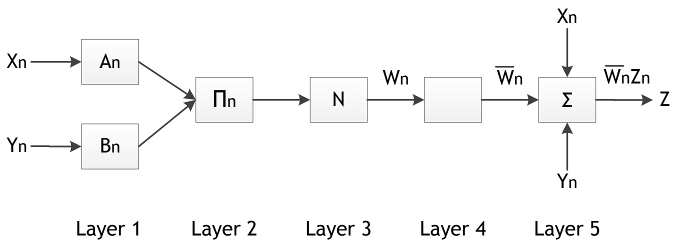

Figure 3.6. General ANFIS architecture.

The memberships function in A or B are described in this work as a triangular membership function [52] where $\{p_i,\ q_i,\ r_i\}$ are set parameters, due to being a continuous and piecewise differentiable function. It is generally described by:

$$\mu A_i(x) = \frac{1}{1 + \left|\frac{x - r_i}{p_i}\right|^{2q_i}} \tag{3.4.5}$$

- In Layer 2 all output nodes represent the firing strength of the rule w_i, where each node is represented by Π, i.e., the output signals are multiplied by the previous inputs signals.

$$L2_i = w_i = \mu A_i(x)\mu B_i(y), \qquad i = 1, 2 \tag{3.4.6}$$

- In Layer 3 every node N calculates the ratio of firing rules strength i_{th} with the sum of all firing strength rules:

$$L3_i = \overline{w}_i = \frac{w_i}{w_1 + w_2}, \qquad i = 1, 2 \tag{3.4.7}$$

- In Layer 4 all nodes compute the contribution of the rule i_{th} to the global output, where $\{a_i,\ b_i,\ c_i\}$ are parameters sets and $\overline{w}_i$ is the layer output:

$$L4_i = \overline{w}_i z_i = \overline{w}_i(a_i x + b_i y + c_i), \qquad i = 1, 2 \tag{3.4.8}$$

- Finally, Layer 5 corresponds to the output node of ANFIS tool where the summation Σ is made:

$$L5_i = \sum_i \overline{w}_i z_i = \frac{\sum_i w_i z_i}{\sum_i w_i} \tag{3.4.9}$$

Furthermore, as stated in [87] the ANFIS tool used in this work employs the least-squares and back-propagation gradient descent method. EPSO assists in the tuning of the membership function parameters.

3.5. Proposed Forecasting Tool

The HEA tool is a successful combination of MI, WT, EPSO and ANFIS advanced techniques applied to forecast electricity market prices and wind power in the short-term. The MI is used to eliminate randomness in the selection data series (electricity market prices or wind power) as inputs. The WT is employed to decompose the sets of aforementioned data series into new constitutive sets with better behavior. The forthcoming values of those constitutive sets are then forecasted with the ANFIS. The EPSO augments the performance of ANFIS by tuning their membership functions to attain a lesser error. The HEA tool is described in successive steps. Figure 3.7 provides the structure of the HEA tool in the form of a detailed flowchart.

- Step 1. Initialize the HEA approach with an historical data matrix of wind power or electricity market prices, considering the previous days/weeks;

- Step 2. The matrix will be normalized in $\{0,\ 1\}$ intervals, to find the set of historical data in the same scale, which will be later used by the MI in the candidate selections procedure. This step is important to avoid the loss of relevant information;
- Step 3. Constitute data groups for the MI. The number of these groups is defined by combinatorial optimization in order to avoid compromising the computational burden. The formation of these groups must be performed in a balanced way, thus avoiding compromising ANFIS performance;
- Step 4. Compute the entropy and conditional entropy of each group by using Equations (3.1.2) and (3.1.8), where $P(X_n)$ is given by binomial distribution function;
- Step 5. Compute MI given by Equation (3.1.10) of each group;
- Step 6. Compute the best group subset data. The best group found will be recombined in original data-sets. These selected data-sets will be inputs for the WT;
- Step 7. Train the ANFIS with the previous constitutive data-sets. The optimization of the membership function parameters is achieved by EPSO. Table 3.1 shows the parameters considered for MI, ANFIS and EPSO. These parameters result from the expertise acquired in the simulations, taking also into account previous publications. The approach developed in this work uses A_3, along with D_3 and D_1, as inputs for the ANFIS (Data-sets coming from WT tool). The inference rules of ANFIS are put into automatic mode to achieve the best performance. This is done due to the nature of the data, which requires a large number of inference rules to obtain the best results;
- Step 8. Until the best results or convergence are not reached:
    - Step 8.1. Jump to Step 7 in case of electricity market prices forecasting. When the best results are found or convergence is reached, the inverse WT is applied and the output of the proposed HEA tool is attained, that is, the electricity prices are forecasted;
    - Step 8.2. Jump to Step 1 in case of wind power forecasting. When the best results are found or convergence is reached, the inverse WT is applied and the output of the proposed HEA tool is attained, that is, the wind power data are forecasted. This is repeated with new and refreshing sets of historical wind power data till the short-term time horizon selected is completed;
- Step 9. Compute the forecasting errors with different criteria to validate the proposed HEA tool for each case study, i.e., for electricity market prices and wind power results.

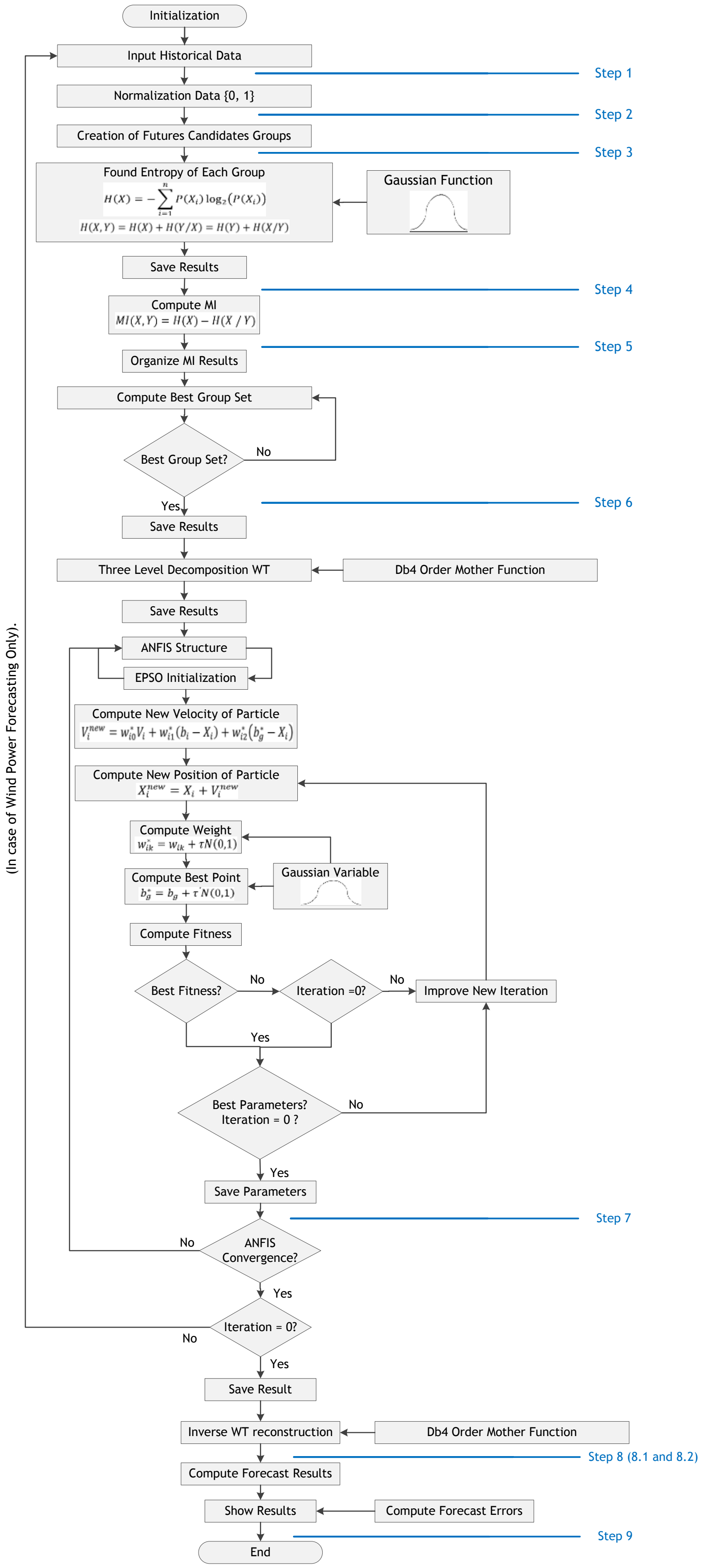

Figure 3.7. Flowchart of proposed HEA tool.

Table 3.1. Parameters of MI, EPSO and ANFIS.

Technique	Parameters	Type or Size	
		Electricity Market Prices	Wind power
MI	Best Lower Bound of Set	0.15	0.20
	Best Upper Bound of Set	0.65	0.86
ANFIS	Membership Function	2-7	
	Necessary Iterations	3-50	2-25
	Membership Function	Triangular Format	
EPSO	Fitness Acceleration	2	
	Sharing Acceleration	2	
	Initial Inertia of Population	0.9	
	Final Inertia of Population	0.4	
	Population Size	24-168	96
	Maximum Generation	48-326	192
	Number of New Particles	24-168	12
	Generation for New Particle	2	
	Necessary Iterations	48-326	192
	Min. Value of New Position	20	5
	Max. Value of New Position	70-120	2000

3.6. Case Studies and Results

The HEA tool was first used to forecast the electricity market prices for the next 24h/168h-ahead for mainland Spain in 2002, which is difficult to forecast due to the changes in prices that occurred as a result of the strategies of the dominant player. The HEA methodology is also utilized to predict electricity market prices for the next 24h/168h-ahead for the PJM market in 2006. Like the Spanish market, no exogenous data such as load, oil prices or other exogenous sets are taken into account. Also, the same test days/weeks used in previously published studies have been used, to allow a clear and fair comparison with the results already obtained using other published methodologies. Otherwise a fair comparison would not be possible. Moreover, the HEA tool has been applied for forecasting the whole wind power in Portugal. The numerical results presented take into account the wind farms that have telemetry with the Portuguese transmission system operator (TSO), that is, *Redes Energéticas Nacionais* (REN).

To compare the proposed tool with other methodologies/tools used for forecasting electricity market prices and wind power in the short-term horizon previously published in the specialized literature, we also used some commonly used criteria accepted by the scientific community to report the proficiency of the proposed approaches. These criteria are described in the following section.

3.6.1. Forecasting Accuracy Evaluation

The HEA tool has been compared with other published methodologies/tools applied in forecasting short-term electricity market prices and wind power. The most well-known criteria accepted and used in the specialized literature are: mean absolute percentage error (MAPE), error variance, normalized mean average error (NMAE), and normalized root mean square error (NRMSE). The MAPE criterion is given as:

$$MAPE = \frac{100}{N}\sum_{h=1}^{N}\frac{|\hat{p}_h - p_h|}{\bar{p}} \tag{3.6.1}$$

$$\bar{p} = \frac{1}{N}\sum_{h=1}^{N} p_h \tag{3.6.2}$$

where $\hat{p}_h$ is the data forecast (electricity market prices or wind power) at hour h; p_h is the actual data (electricity market prices or wind power) at hour h; $\bar{p}$ is the average value for the forecasting horizon N.

Moreover, in electricity prices forecasting the average of electricity market prices is used in Equation (3.6.1) to elude the instability caused when the electricity market prices are near to zero [55].

The uncertainty of the proposed tool is also evaluated using the error variance estimation. The smaller the value for this criterion, the more exact is the tool in its forecasting results [56]. In accordance with the MAPE criterion, the error variance criterion is given by:

$$\sigma_{e,t}^2 = \frac{1}{N}\sum_{h=1}^{N}\left(\frac{|\hat{p}_h - p_h|}{\bar{p}} - e_t\right)^2 \tag{3.6.3}$$

$$e_t = \frac{1}{N}\sum_{h=1}^{N}\frac{|\hat{p}_h - p_h|}{\bar{p}} \tag{3.6.4}$$

Moreover, for the wind power forecasting results, this study used the NMAE criterion, where P_{ins} corresponds to the total wind power capacity installed. The NMAE is determined by:

$$NMAE = \frac{100}{N}\sum_{h=1}^{N}\frac{|\hat{p}_h - p_h|}{P_{ins}} \tag{3.6.5}$$

Finally, the NRMSE criterion (applied only in wind power forecasting results) is determined by [101], [192], [193]:

$$NRMSE = \sqrt{\frac{1}{N}\sum_{h=1}^{N}\left(\frac{\hat{p}_h - p_h}{P_{ins}}\right)^2} \times 100 \tag{3.6.6}$$

3.6.2. Short-Term Electricity Market Prices Results

3.6.2.1. Spanish Market

The HEA tool is used first to forecast the electricity market prices for the next 24h/168h for the mainland Spain electricity market. The historical data of electricity market prices are available in [8]. As mentioned in [56], this market is difficult to forecast due to the changes in prices that occur as a result of the strategies of the dominant player. The electricity market price sets used for the Spanish market date back to the year 2002, to allow a clear and fair comparison with the results already obtained using other published methodologies, i.e., the same four test weeks of the year 2002 were selected, each corresponding to a different season (winter, spring, summer, and fall). Moreover, for a clear and fair comparison with the results already obtained using other published methodologies, only historical data sets of electricity market prices were used, i.e., no exogenous sets, such as load, oil prices, or others are taken into account. Otherwise a fair comparison would not be possible. Moreover, demand data does not significantly improve the results of forecasts [180],

The HEA tool forecasts the next 168h electricity market prices taking into account the previous 1008h, (i.e. six weeks or 42 days for each season), which in turn will be the input sets. Very large training sets are not used to avoid over-training during the learning process. The output of the HEA tool corresponds directly to a set with 168 values, equal to the forecasting horizon. For day-ahead (24h) forecasts, the previous six days are considered. The results with the HEA tool are initially provided in Figures 3.8–3.11 for the four test weeks of 2002 in Spanish market.

Table 3.2 shows the MAPE criterion comparative results between the HEA tool and 18 other methodologies. The enhancements between HEA and the other methodologies are 58.0%, 55.1%, 53.1%, 48.5%, 48.1%, 44.4%, 43.7%, 40.0%, 38.1%, 37.1%, 36.3%, 27.2%, 21.4%, 19.9%, 18.7%, 18.5%, 17.6% and 15.6%,respectively. The MAPE criterion using HEA has an average value of just 4.18%, the lowest of all, which is significant. Even if each week is analyzed *per se*, the results are always better.

Although the proposed methodology is not specifically designed for price spike forecasting, which is the main goal of other studies such as [176], [194], it behaves quite well in their presence with excellent overall results. Table 3.3 shows the comparative results for the error variance criterion between the HEA tool and fourteen other methodologies. The enhancements between HEA and the other methodologies are 83.7%, 78.6%, 76.6%, 72.2%, 68.8%, 59.5%, 58.3%, 58.3%, 57.1%, 54.5%, 44.4%, 28.6%, 28.6% and 28.6% respectively. The average value is only 0.0015, again the lowest of all, indicating reduced uncertainty in the forecasts, which is another important feature. Error variance results for the mixed model, fuzzy NN (FNN) [58], pattern sequence-based forecasting (PSF) [82] and Elman network or simple recurrent network (SRN) [195] are not available in the respective papers.

More recent data (year 2006) for the Spanish market has also been considered. Moreover, the best and worst forecasts generated by the PSF and HEA methodologies for year 2006 data have been compared. The best forecast for the PSF methodology occurred on June 23, 2006, in which the MAPE was 3.10%, while using the HEA tool the MAPE decreases to 2.31%. The worst forecast for PSF methodology occurred on May 8, 2006, in which the MAPE was 9.39%, while using the HEA tool (as illustrated in Figure 3.12) the MAPE decreases to 4.37%. Hence, the forecasting trends for the year 2006 are in agreement with those previously observed for the year 2002: enhancements range from 25.5% to 53.5%, which is significant.

Figure 3.13 shows the daily error between the HEA tool results and the results previously reported for the NN, NNWT and WPA methodologies for the four seasons of the year. It can be seen that, for most days, the HEA tool presents better forecasting results, i.e., lower errors, compared with the other three methodologies.

Furthermore, the HEA tool requires a low computational burden: the average computation time for a 168h forecast is less than 40 seconds using MATLAB platform on a standard PC with a 1.8GHz-based-processor and 1.5GB RAM. Not only is the training time less, but also the accuracy is higher and the uncertainty is lower with the HEA tool. This is the major added value this study provides. The proposed HEA tool presents, indeed, the best trade-off between computation time and average MAPE, which is crucial for real-life and real-time applications.

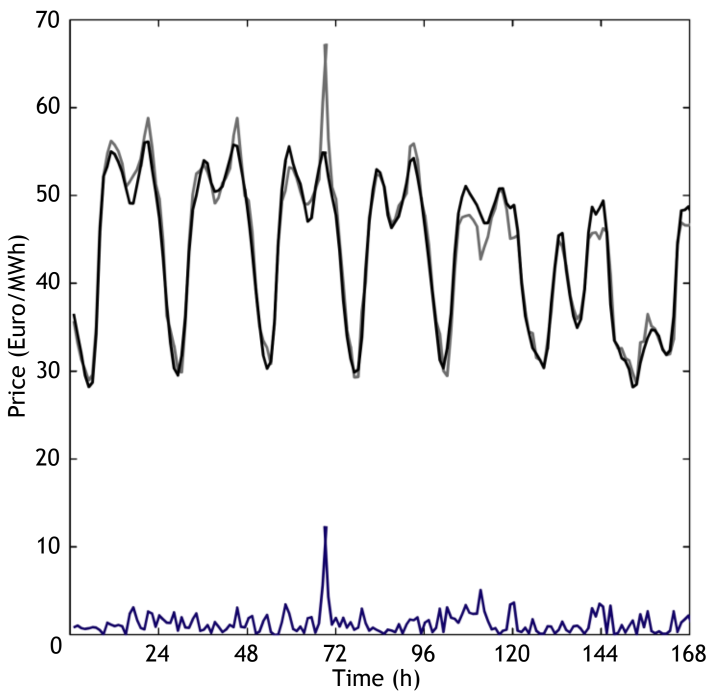

Figure 3.8. Winter week 2002 results for the Spanish market. The gray and black lines represent the actual and forecasted prices, respectively, while the dark-blue line at the bottom represents the errors in absolute value.

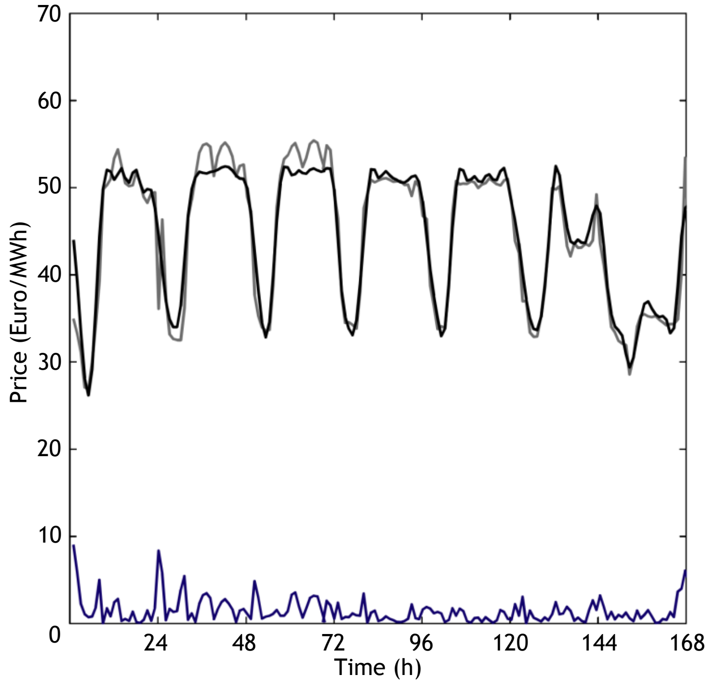

Figure 3.9. Spring week 2002 results for the Spanish market. The gray and black lines represent the actual and forecasted prices, respectively, while the dark-blue line at the bottom represents the errors in absolute value.

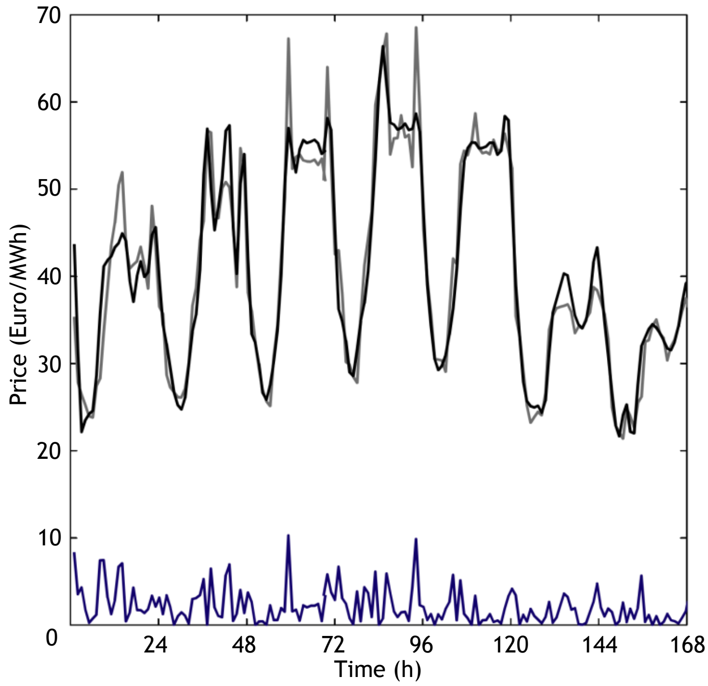

Figure 3.10. Summer week 2002 results for the Spanish market. The gray and black lines represent the actual and forecasted prices, respectively, while the dark-blue line at the bottom represents the errors in absolute value.

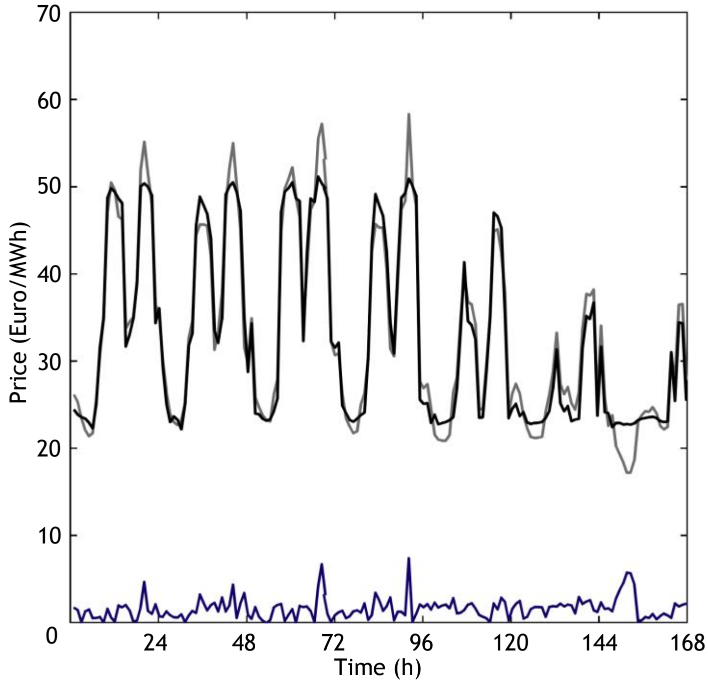

Figure 3.11. Fall week 2002 results for the Spanish market. The gray and black lines represent the actual and forecasted prices, respectively, while the dark-blue line at the bottom represents the errors in absolute value.

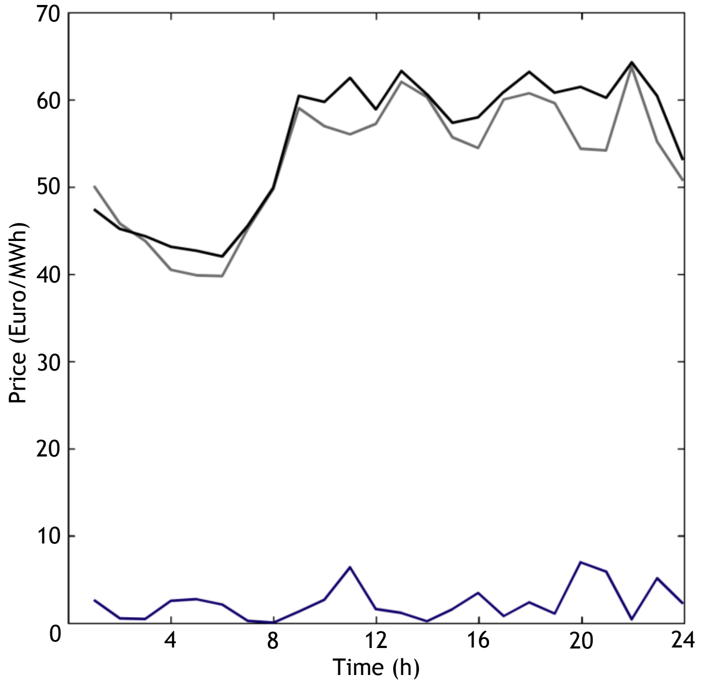

Figure 3.12. May 8, 2006, results for the Spanish market. The gray and black lines represent the actual and forecasted prices, respectively, while the dark-blue line at the bottom represents the errors in absolute value.

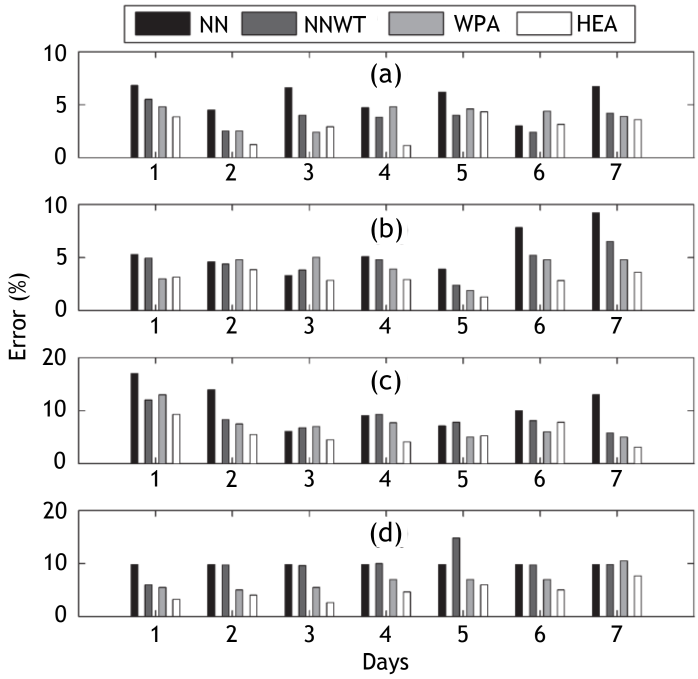

Figure 3.13. Daily error comparative results between NN, NNWT, WPA and HEA methodologies, regarding the four seasons of year 2002 for the Spanish market: (a) winter; (b) spring; (c) summer; (d) fall.

Table 3.2. MAPE criterion: Comparative results for Spanish market.

Methodologies	Winter	Spring	Summer	Fall	Average
ARIMA [55], 2003	6.32	6.36	13.39	13.78	9.96
Mixed Model [196], 2007	6.15	4.46	14.90	11.68	9.30
NN [60], 2005	5.23	5.36	11.40	13.65	8.91
Wavelet-ARIMA [56],2005	4.78	5.69	10.70	11.27	8.11
WNN [62], 2007	5.15	4.34	10.89	11.83	8.05
FNN [58], 2006	4.62	5.30	9.84	10.32	7.52
PSF [82], 2011	5.98	4.51	9.11	10.07	7.42
HIS [59], 2009	6.06	7.07	7.47	7.30	6.97
AWNN [66], 2008	3.43	4.67	9.64	9.29	6.75
NNWT [75], 2010	3.61	4.22	9.50	9.28	6.65
SRN [195], 2013	4.11	4.37	9.09	8.66	6.56
RBFN [54], 2011	4.27	4.58	6.76	7.35	5.74
CNEA [69], 2009	4.88	4.65	5.79	5.96	5.32
CNN [68], 2009	4.21	4.76	6.01	5.88	5.22
HNES [74], 2010	4.28	4.39	6.53	5.37	5.14
MI+CNN [84],2012	4.51	4.28	6.47	5.27	5.13
WPA [52], 2011	3.37	3.91	6.50	6.51	5.07
MI-MI+CNN [84], 2012	4.29	4.20	6.31	5.01	4.95
HEA, 2013	3.04	3.33	5.38	4.97	4.18

Table 3.3. Weakly error variance criterion: Comparative results for Spanish market.

Methodologies	Winter	Spring	Summer	Fall	Average
ARIMA [55], 2003	0.0034	0.0020	0.0158	0.0157	0.0092
NN [60], 2005	0.0017	0.0018	0.0109	0.0136	0.0070
Wavelet-ARIMA [56],2005	0.0019	0.0025	0.0108	0.0103	0.0064
FNN [58], 2006	0.0018	0.0019	0.0092	0.0088	0.0054
AWNN [66], 2008	0.0012	0.0031	0.0074	0.0075	0.0048
NNWT [75], 2010	0.0009	0.0017	0.0074	0.0049	0.0037
HIS [59], 2009	0.0034	0.0049	0.0029	0.0031	0.0036
CNEA [69], 2009	0.0036	0.0027	0.0043	0.0039	0.0036
CNN [68], 2009	0.0014	0.0033	0.0045	0.0048	0.0035
RBFN [54], 2011	0.0015	0.0019	0.0047	0.0049	0.0033
WPA [52], 2011	0.0008	0.0013	0.0056	0.0033	0.0027
MI+CNN [84],2012	0.0014	0.0014	0.0033	0.0022	0.0021
HNES [74], 2010	0.0013	0.0015	0.0033	0.0022	0.0021
MI-MI+CNN [84], 2012	0.0014	0.0014	0.0032	0.0023	0.0021
HEA, 2013	0.0008	0.0011	0.0026	0.0014	0.0015

3.6.2.2. PJM Market

The HEA tool is also used to forecast the electricity market prices for the next 24h/168h for the PJM market. The historical data of electricity prices are available in [197]. As in the Spanish electricity market case study, no exogenous data such as load, oil prices, and other sets are taken into account. The results with the HEA tool for the PJM market are provided in Figures 3.14-3.20 for five days and two weeks of the year 2006.

The same test days/weeks as in the previous studies have been considered to allow a clear and fair comparison with the results already obtained using other published methodologies. Otherwise a fair comparative study would not be possible. Tables 3.4 and 3.5 show the MAPE and error variance results, respectively, for the HEA methodology and five other methodologies.

The MAPE enhancements between HEA and the other methodologies are 59.1%, 40.2%, 28.2%, 25.9% and 25.7%, respectively. The error variance enhancements between HEA and the other methodologies are 75.5%, 64.7%, 45.5%, 42.9% and 25.0%, respectively. The HEA tool clearly outperforms, again, all other methodologies in every day/week analyzed.

Moreover, the results of electricity market price forecasts for 168h are provided in about 40 seconds, while 24h forecasts require even less computation time. Hence, this second case study further and unequivocally demonstrates and validates the proficiency of the proposed methodology.

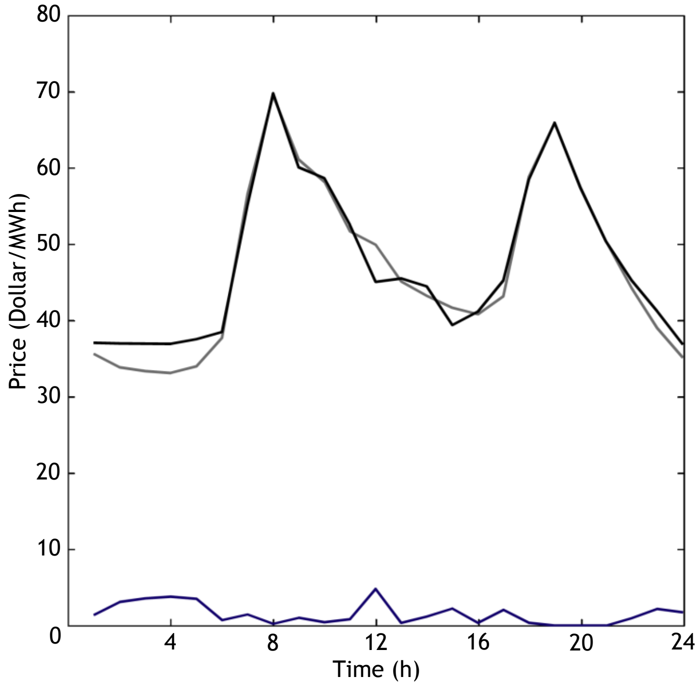

Figure 3.14. January 20, 2006, results for the PJM market. The gray and black lines represent the actual and forecasted prices, respectively, while the dark-blue line at the bottom represents the errors in absolute value.

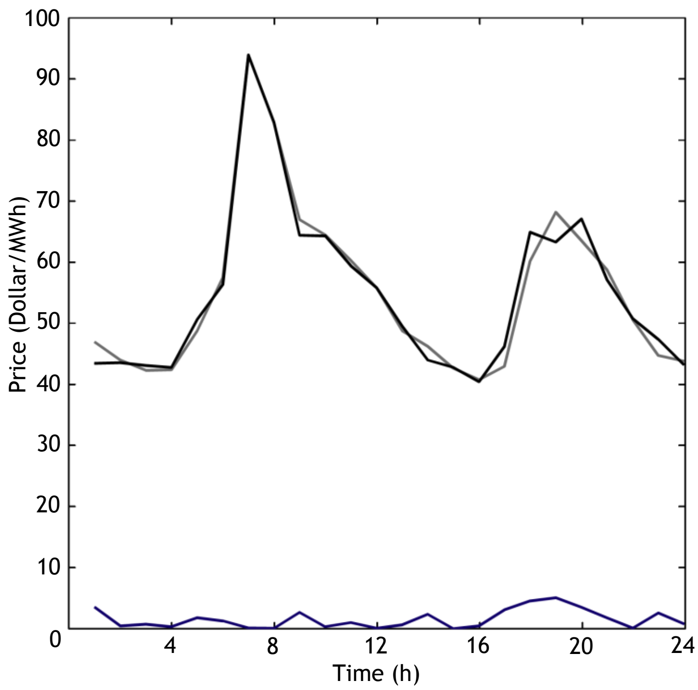

Figure 3.15. February 10, 2006, results for the PJM market. The gray and black lines represent the actual and forecasted prices, respectively, while the dark-blue line at the bottom represents the errors in absolute value.

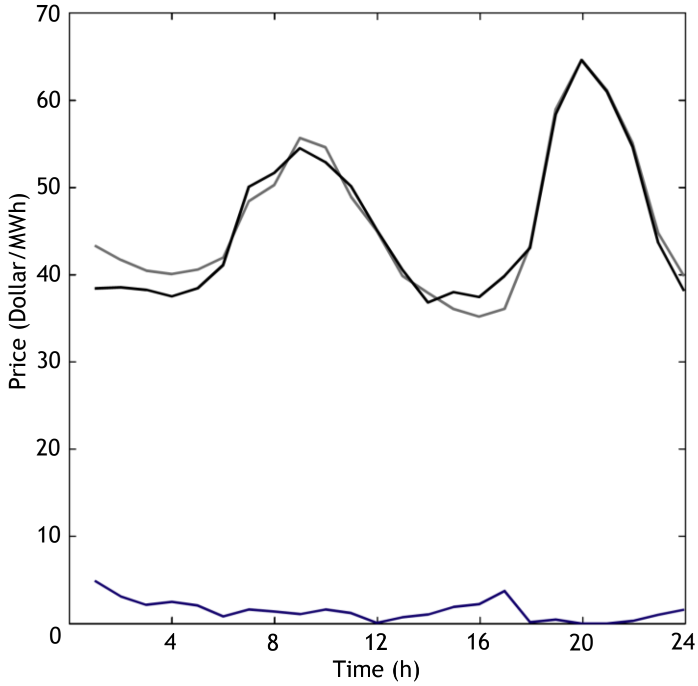

Figure 3.16. March 5, 2006, results for the PJM market. The gray and black lines represent the actual and forecasted prices, respectively, while the dark-blue line at the bottom represents the errors in absolute value.

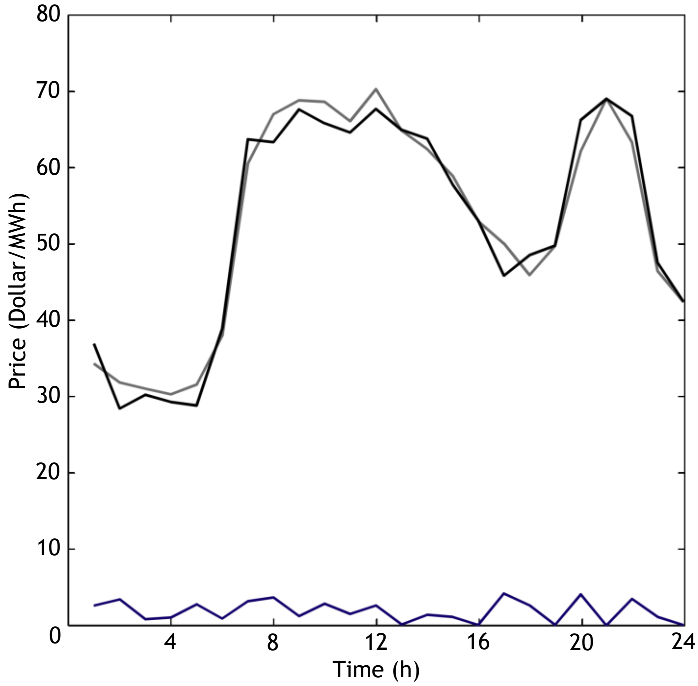

Figure 3.17. April 7, 2006, results for the PJM market. The gray and black lines represent the actual and forecasted prices, respectively, while the dark-blue line at the bottom represents the errors in absolute value.

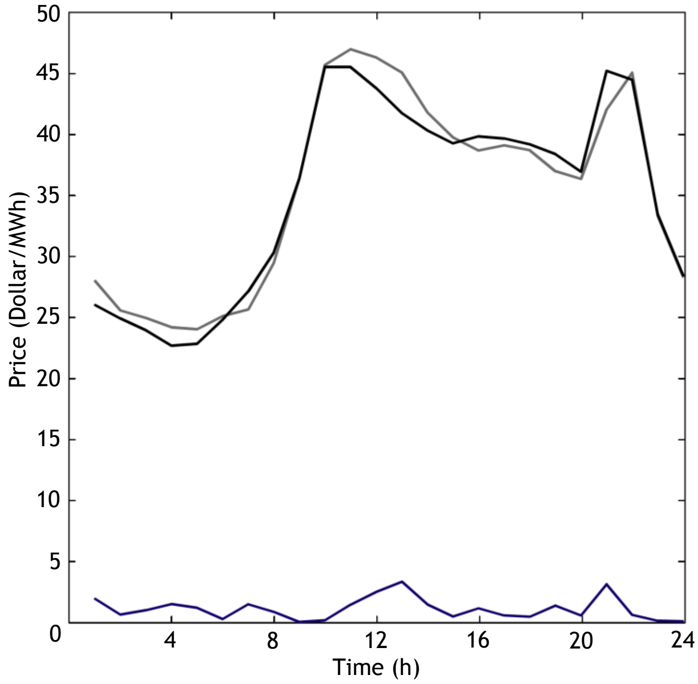

Figure 3.18. May 13, 2006, results for the PJM market. The gray and black lines represent the actual and forecasted prices, respectively, while the dark-blue line at the bottom represents the errors in absolute value.

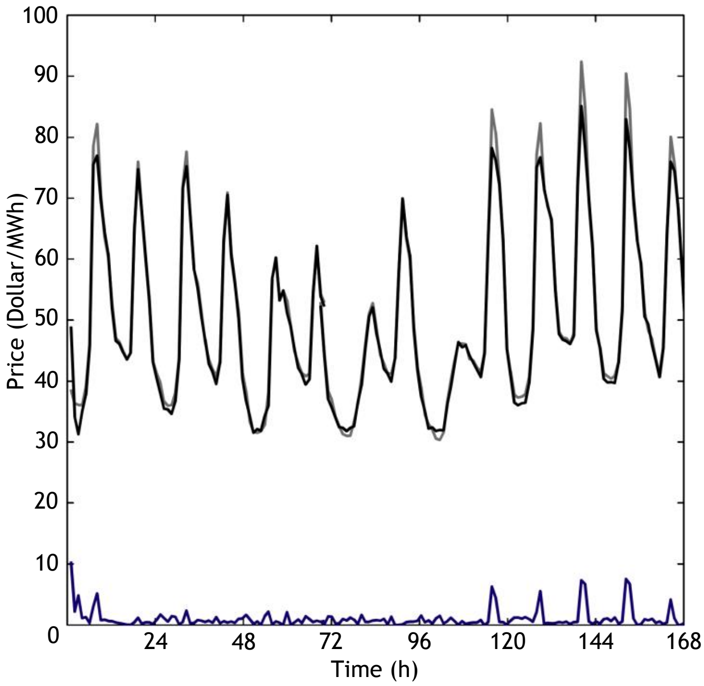

Figure 3.19. February 1–7, 2006, results for the PJM market. The gray and black lines represent the actual and forecasted prices, respectively, while the dark-blue line at the bottom represents the errors in absolute value.

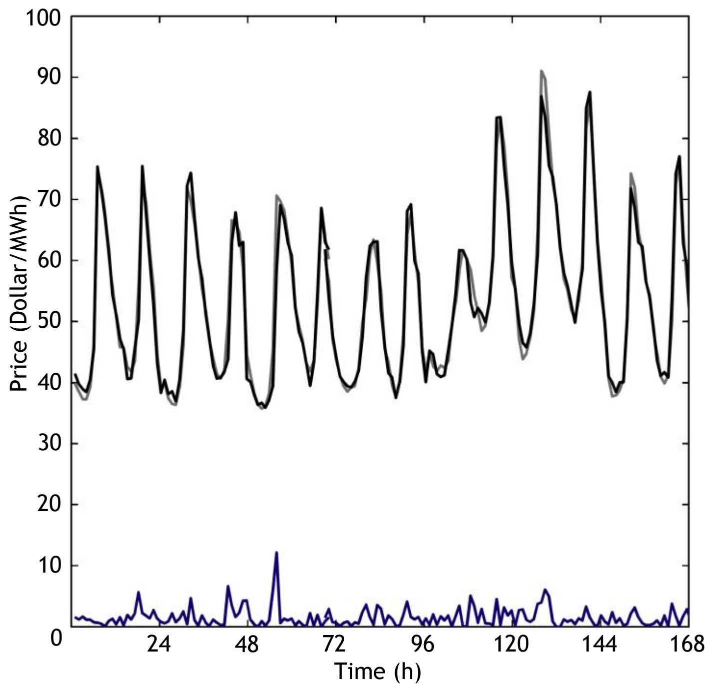

Figure 3.20. February 22–28, 2006, results for the PJM market: The gray and black lines represent the actual and forecasted prices, respectively, while the dark-blue line at the bottom represents the errors in absolute value.

Table 3.4. MAPE criterion: Comparative results for PJM market.

Days/Weeks	SDNN [61], 2007	WT+FF+FA [91], 2013	HNES [74], 2010	Hybrid [79], 2010	CNEA [69], 2009	HEA, 2013
January 20	6.93	5.04	4.98	3.71	4.73	3.29
February 10	7.96	5.43	4.10	2.85	4.50	2.80
March 5	7.88	4.82	4.45	5.48	4.92	3.32
April 7	9.02	6.24	4.67	4.17	4.22	3.55
May 13	6.91	4.11	4.05	4.06	3.96	3.43
February 1-7	7.66	6.07	4.62	5.27	4.02	3.11
Feb. 22-28	8.88	6.12	4.66	5.01	4.13	3.08
Average	7.89	5.40	4.50	4.36	4.35	3.23

Table 3.5. Error variance criterion: comparative results for PJM market.

Days/Weeks	SDNN [61], 2007	CNEA [69], 2009	WT+FF+FA [91], 2013	Hybrid [79], 2010	HNES [74], 2010	HEA, 2013
January 20	0.0034	0.0031	0.0016	0.0010	0.0020	0.0010
February 10	0.0050	0.0036	0.0021	0.0015	0.0012	0.0009
March 5	0.0061	0.0042	0.0032	0.0033	0.0015	0.0011
April 7	0.0038	0.0022	0.0019	0.0013	0.0018	0.0011
May 13	0.0049	0.0027	0.0016	0.0015	0.0013	0.0012
February 1-7	0.0066	0.0044	0.0023	0.0037	0.0016	0.0012
Feb. 22-28	0.0047	0.0035	0.0024	0.0025	0.0017	0.0017
Average	0.0049	0.0034	0.0022	0.0021	0.0016	0.0012

3.6.3. Short-Term Wind Power Forecasting Results

The HEA tool has also been applied for forecasting wind power in Portugal. The numerical results presented take into account the wind farms that have telemetry with the Portuguese TSO (REN) in 2006 and 2007; these are available in [23]. Our forecaster predicts the value of the wind power subseries for 3h-ahead taking into account the wind power data of the previous 12h with a time-step of 15 minutes. Numerical results with HEA tool are provided in Figures 3.21 - 3.24 for the four seasons of the year (winter, spring, summer and fall). The forecasting bias may be considered rather neutral, in the sense that when the errors start to go more to the positive side, the methodology immediately corrects itself and drives them to the negative side to compensate, and vice versa. This behavior is associated with the evolutionary characteristics of EPSO, on the one hand, and the adaptive characteristics of ANFIS, on the other.

Table 3.6 provides a comparison between the HEA tool and eight other previously published methodologies, regarding the MAPE criterion. The MAPE criterion using the HEA tool has an average value of just 3.75%, the lowest one of all. The MAPE enhancements between HEA and the other methodologies are 80.3%, 80.3%, 63.7%, 48.3%, 46.2%, 43.5%, 37.4% and 24.7%, respectively, always above 24%, which is significant.

Table 3.7 provides a comparison between the HEA tool and the eight other methodologies, regarding the error variance criterion. The average value is 0.0013, again the lowest of all, indicating less uncertainty in the forecasts. The error variance enhancements between HEA and the other methodologies are 94.4%, 94.4%, 83.8%, 74.5%, 72.3%, 69.8%, 59.4% and 38.1%, respectively, always above 38%, even more significant since it is related to the uncertainty in the forecasts, representing a major improvement.

Table 3.8 shows the NMAE criterion results comparing the HEA tool and the eight other methodologies. The enhancements between the HEA tool and the other methodologies regarding the NMAE criterion are 83.1%, 83.0%, 69.0%, 55.1%, 53.3%, 51.1%, 46.5% and 36.3%, respectively, always above 35%, and again significant.

Furthermore, Table 3.9 shows the NRMSE criterion results of the HEA tool for the four seasons. The NRMSE criterion using the HEA methodology has an average value of 2.66%. Statistically results demonstrative for the full year 2009 using the HEA tool are provided in Table 3.10 and Table 3.11 concerning the MAPE and NMAE criterions, respectively. The HEA tool clearly outperforms all other methodologies.

Furthermore, the HEA tool presents a relatively low computational burden; the CPU time is less than 40 seconds per iteration, on average, working with MATLAB on a standard PC with 1.8GHz-based processor and 1.5GB of RAM. Not only is the training time almost negligible, but also the accuracy is higher and the uncertainty is lower.

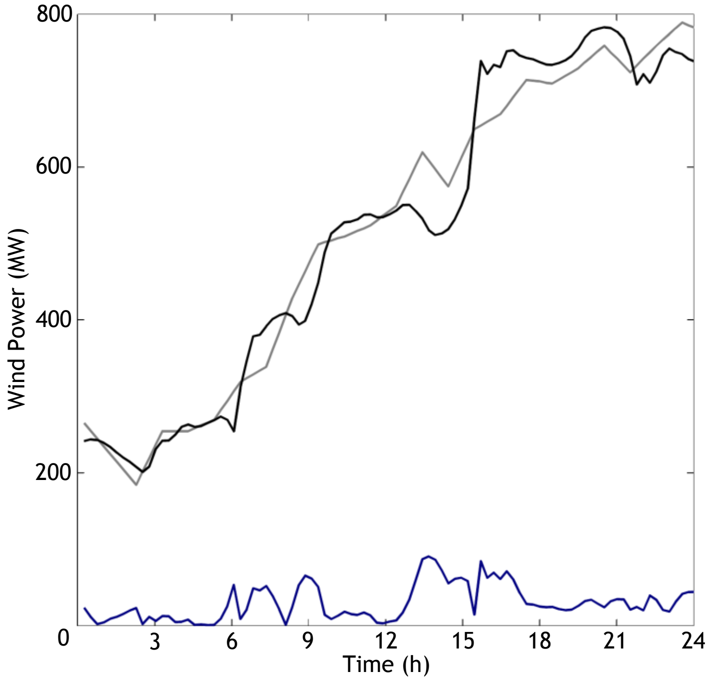

Figure 3.21. Measured and forecasted results (15 minutes intervals) for the Winter season. Gray and black lines represent actual and forecasted wind power, respectively, while dark-blue line represents errors in absolute value.

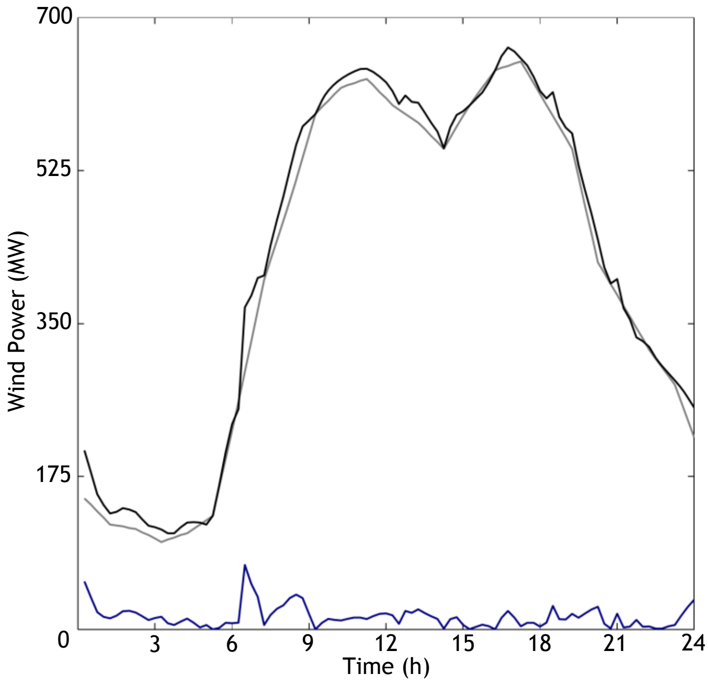

Figure 3.22. Measured and forecasted results (15 minutes intervals) for the Spring season. Gray and black lines represent actual and forecasted wind power, respectively, while dark-blue line represents errors in absolute value.

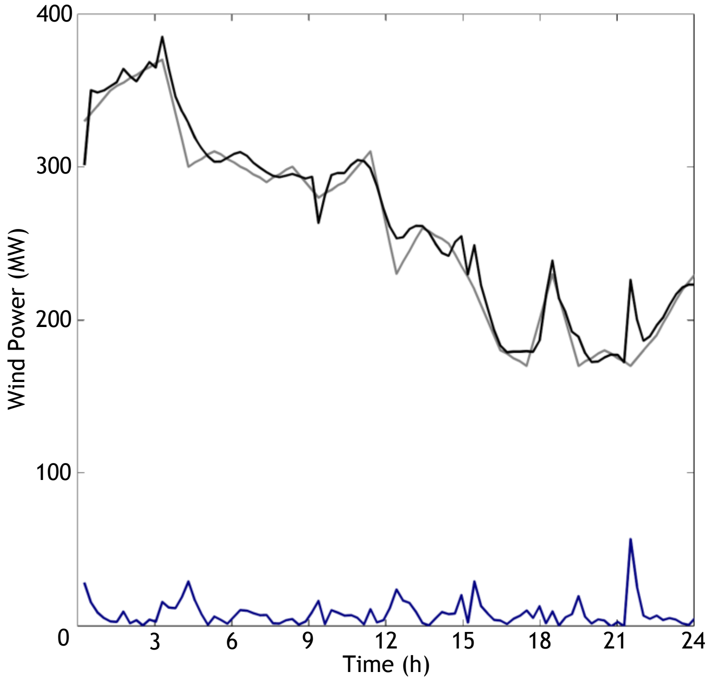

Figure 3.23. Measured and forecasted results (15 minutes intervals) for the Summer season. Gray and black lines represent actual and forecasted wind power, respectively, while dark-blue line represents errors in absolute value.

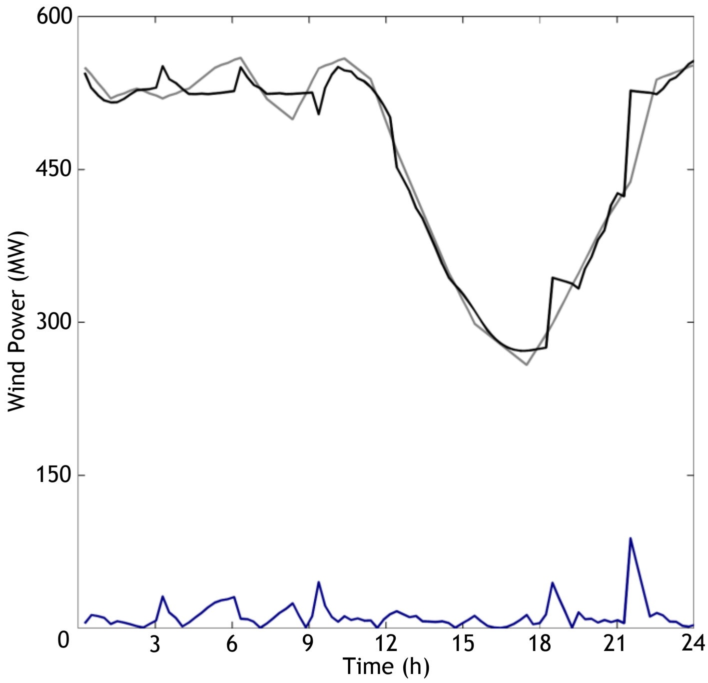

Figure 3.24. Measured and forecasted results (15 minutes intervals) for the Fall season. Gray and black lines represent actual and forecasted wind power, respectively, while dark-blue line represents errors in absolute value.

Table 3.6. MAPE outcomes for all methodologies.

Methodologies	Winter season	Spring season	Summer season	Fall season	Average
Persistence [109]	13.89	32.40	13.43	16.49	19.05
NRM [116]	13.87	32.38	13.43	16.43	19.03
ARIMA [109]	10.93	12.05	11.04	7.35	10.34
NN [109]	9.51	9.92	6.34	3.26	7.26
NNWT [111]	9.23	9.55	5.97	3.14	6.97
NF [113]	8.85	8.96	5.63	3.11	6.64
WNF [198]	8.34	7.71	4.81	3.08	5.99
WPA [116]	6.47	6.08	4.31	3.07	4.98
HEA	5.74	3.49	3.13	2.62	3.75

Table 3.7. Error variance outcomes for all methodologies.

Methodologies	Winter season	Spring season	Summer season	Fall season	Average
Persistence [109]	0.0078	0.0592	0.0085	0.0179	0.0233
NRM [116]	0.0074	0.0590	0.0079	0.0180	0.0231
ARIMA [109]	0.0025	0.0164	0.0090	0.0039	0.0080
NN [109]	0.0044	0.0106	0.0043	0.0010	0.0051
NNWT [111]	0.0055	0.0083	0.0038	0.0012	0.0047
NF [113]	0.0041	0.0086	0.0038	0.0008	0.0043
WNF [198]	0.0046	0.0051	0.0021	0.0011	0.0032
WPA [116]	0.0021	0.0035	0.0016	0.0011	0.0021
HEA	0.0019	0.0015	0.0010	0.0008	0.0013

Table 3.8. Comparative NMAE results.

Methodologies	Winter season	Spring season	Summer season	Fall season	Average
Persistence [109]	7.64	12.15	4.98	10.88	8.91
NRM [116]	7.62	12.14	4.98	10.84	8.90
ARIMA [109]	6.01	4.52	4.09	4.85	4.87
NN [109]	5.22	3.72	2.35	2.15	3.36
NNWT [111]	5.07	3.58	2.21	2.07	3.23
NF [113]	4.86	3.36	2.09	2.05	3.09
WNF [198]	4.58	2.89	1.78	2.03	2.82
WPA [116]	3.56	2.28	1.60	2.02	2.37
HEA	2.73	1.48	0.74	1.10	1.51

Table 3.9. NRMSE results.

Methodology	Winter season	Spring season	Summer season	Fall season	Average
HEA	3.60	3.18	1.78	2.07	2.66

Table 3.10. Comparative MAPE outcomes for 2009.

	Persis. [109]	NRM [116]	ARIMA [109]	NN [109]	NNWT [111]	NF [113]	WNF [198]	WPA [116]	HEA
January	17.44	16.83	16.03	13.62	12.22	10.69	8.16	6.71	6.14
February	22.84	22.81	20.56	14.55	12.92	11.68	8.64	7.05	6.05
March	19.70	18.99	13.01	12.04	11.05	8.76	7.51	6.19	5.61
April	22.77	22.53	13.26	9.43	9.19	8.78	7.82	6.57	5.55
May	17.20	16.78	11.98	9.86	8.85	8.29	6.87	5.94	4.52
June	36.70	36.37	27.96	14.18	12.52	11.60	8.85	7.23	6.98
July	21.20	20.86	15.98	13.53	12.28	11.16	8.42	7.06	7.02
August	13.94	13.55	11.94	8.42	7.48	6.18	5.09	4.66	4.58
September	24.51	24.20	16.65	10.60	10.28	9.95	8.28	7.33	5.55
October	26.45	26.16	18.58	12.92	11.28	10.44	8.67	7.26	7.20
November	17.16	16.88	14.47	12.72	12.15	11.36	8.65	6.99	5.10
December	16.90	16.86	12.14	10.03	9.54	8.98	7.02	5.99	5.43
Average	21.41	21.07	16.05	11.83	10.81	9.82	7.83	6.58	5.81

Table 3.11. Comparative NMAE outcomes for 2009.

	Persis. [109]	NRM [116]	ARIMA [109]	NN [109]	NNWT [111]	NF [113]	WNF [198]	WPA [116]	HEA
January	3.23	3.12	2.97	2.53	2.26	1.98	1.51	1.24	1.16
February	8.34	8.37	7.51	5.31	4.71	4.27	3.16	2.58	2.24
March	1.91	1.84	1.26	1.17	1.07	0.85	0.73	0.60	0.55
April	4.07	4.02	2.37	1.69	1.64	1.57	1.40	1.17	0.99
May	5.91	5.76	4.11	3.39	3.04	2.85	2.36	2.04	1.59
June	7.86	7.79	5.99	3.04	2.68	2.48	1.89	1.55	0.72
July	4.05	3.96	3.04	2.57	2.33	2.12	1.60	1.34	0.69
August	4.73	4.60	4.05	2.86	2.54	2.10	1.73	1.58	1.55
September	4.85	4.79	3.29	2.10	2.03	1.97	1.64	1.45	1.09
October	5.36	5.31	3.77	2.62	2.29	2.12	1.76	1.47	1.35
November	7.02	6.90	4.08	5.20	4.97	4.65	3.54	2.86	1.98
December	5.54	5.53	3.98	3.29	3.13	2.95	2.30	1.97	1.81
Average	5.24	5.17	3.87	2.98	2.72	2.49	1.97	1.65	1.31

Chapter 4

Economic Dispatch Problem

The optimal scheduling considering the uncertainty introduced by wind generation and failure events is a challenging task. Many of the methodologies presented in the literature are based on a limited number of scenarios, assuming the same probability of occurrence for all of them, which could be an important source of error. As a consequence, the obtained scheduling depends on the methodology used for the scenario generation (ARMA, Markov process, among others). Regarding the probabilistic approaches, many of them represent the effects of ramp constraints (limitation of power generation capacity) indirectly by means of penalty factors (cost of spinning reserve used to compensate the wind power forecasting error). For these reasons, the development of a new probabilistic model capable of considering all possible changes in wind power generation, as well as the effects of ramp constraints in the stochastic optimization problem, is required, avoiding the use of a MCS tool.

In this thesis, the solution of the ED problem, considering the uncertainty of wind power generation, is set out below:

- Unlike the probabilistic models presented in [153], [138], [139] and [140], in this work the wind power forecasting error is represented as a discretized beta PDF;
- The power production at the previous time-step $(t-1)$ is represented as a discretized PDF and it is incorporated in the ramp constraints of the probabilistic ED problem;
- The incorporation of generators reliability is made by means of discretized joint PDF of power production and failure events. The discretized PDF of energy not supplied (ENS) as a consequence of wind power forecasting error and generators reliability is incorporated by means of a convolution process.

4.1. Probabilistic Economic Dispatch Problem and Proposed Approach

The probabilistic ED problem consists of finding the optimal power generation of each unit committed, taking into account the uncertainty related to wind power forecasting error. The system under analysis is shown in Figure 4.1, where the aggregated wind power generation has been represented by only one wind farm. The power system is supposed to have a dump load, which is used to dissipate the energy surplus produced during those periods of low load. ENS is represented by a big unit capable of supplying any amount of power that cannot be supplied by thermal units.

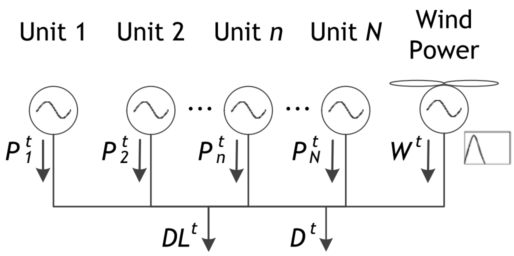

Figure 4.1. Power system under study.

The proposed approach consists of four main steps which are listed below:

- Step 1: Discretization of the PDF of forecasted wind power generation;
- Step 2: Simplification of PDF of initial power production;
- Step 3: Incorporation of wind power forecasting error;
- Step 4: Incorporation of generators reliability.

In the first step, discretization of the PDF that represents the wind power forecasting error is carried out, assumed in this work as a beta PDF. In the second step, in order to make the optimization problem tractable, the PDF of power production at time instant $t-1$ is simplified, so that only some specific power production situations are taken into account. In the third step, the discretized PDF obtained in the first step is incorporated in the optimization problem considering the simplification carried out in second step. In the fourth step, generator reliability is incorporated by estimating the joint PDF of power production and failure events for each unit; while a convolution process is carried out between the PDF of ENS obtained in the third step from the incorporation of wind power forecasting error and the results obtained from the reliability analysis of each unit.

4.1.1. Discretization of the PDF of Forecasted Wind Power Generation

To illustrate the methodology proposed to solve the probabilistic ED problem, the beta PDF has been adopted. Assuming that the corresponding parameters are known, the discretization of this PDF is carried out by applying the methodology proposed in [199]. Figure 4.2 shows the main characteristics of discretized beta PDF in interval $\{0,1\}$, where the corresponding discretized PDF could be mathematically expressed in terms of discrete state r according to Equation (4.1.1):

$$S=\{s_r, \qquad P_r\{s_r\}, \qquad r=0,1,2,\dots,R\} \tag{4.1.1}$$

The value (s_r) that corresponds to each discrete state r is estimated by means of Equation (4.1.2) in the interval $\{0,1\}$:

$$s_r=\begin{cases}\max\left(\left\{\dfrac{r}{R}-\dfrac{\sigma_p}{R}, \quad 0\right\}, \quad \dfrac{r}{R}-\dfrac{\sigma_p}{R}+\dfrac{1}{R}\right), & r=0,1,2,\dots,R-1\\ \left[\dfrac{r}{J}-\dfrac{\sigma_p}{J}, \quad 1\right], & J=R\end{cases} \tag{4.1.2}$$

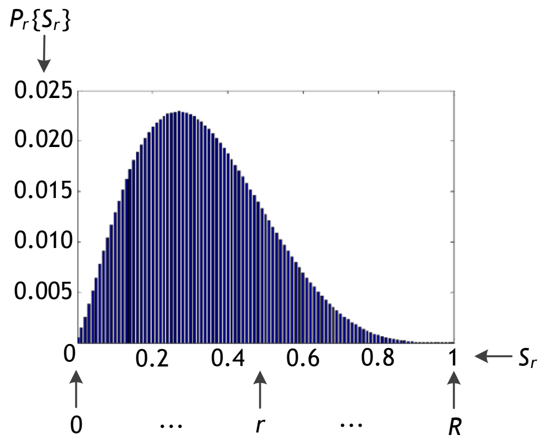

Figure 4.2. Characteristics of the discretized beta PDF.

The corresponding probability value ($P_r\{s_r\}$) that corresponds to the discrete state r is calculated by using Equation (4.1.3).

$$P_r\{s_r\} = \frac{(1+r)^{\alpha_{pdf}-1}(R+1-r)^{\beta_{pdf}-1}}{\sum_{av_0=0}^{R}(1+av_0)^{\alpha_{pdf}-1}(R+1-av_0)^{\beta_{pdf}-1}}, \qquad r = 0, 1, 2, \dots, R \tag{4.1.3}$$

In order to allocate the discretized PDF obtained from Equations (4.1.1)-(4.1.3) in the range of interest of wind power generation $\{W_{min}^t, W_{max}^t\}$, a new discrete state (j) is introduced in terms of state r, which is related through the expression $j = r + 1$. The PDF of available wind power generation is estimated from discretized PDF in interval $\{0, 1\}$, using Equation (4.1.4):

$$AWP^t = \left\{awp_j^t = (W_{max}^t - W_{min}^t)s_{j-1} + W_{min}^t, \qquad j = 1,2, \dots, J\right\} \tag{4.1.4}$$

The notation of discretized PDF of wind power generation is presented in Equation (4.1.5). Note that Equation (4.1.4) represents the available wind power generation which is obtained from the forecasting process, while Equation (4.1.5) represents the wind power produced, which is obtained from the solution of the ED problem. This formulation allows wind power curtailment to be considered from a probabilistic point of view.

$$W^t = \left\{w_j^t, \qquad P_r\{w_j^t\}, \qquad j = 1, 2, \dots, J\right\} \tag{4.1.5}$$

4.1.2. Simplification of PDF of Initial Power Production

The discretized PDF of power production at time $t-1$ is considered as the input data available to solve the probabilistic ED problem. The incorporation of all possible combinations of power generation between the different units of the system leads to an infinite number of cases that should be evaluated, which make the optimization problem intractable. If the discretized PDF of unit $n = 1$ at time $t-1$ is divided in B bins, the number of combinations that results from considering the power generation of this unit and the possible power production of other units of the system ($n = 2, \dots, N$) could lead to a large amount of cases to be evaluated. To deal with this problem, a simplification is introduced.

Considering a determined significance level (γ), the interval $\{\gamma, 1-\gamma\}$ is swept with a determined step (sampling increment) $\Delta\theta$, obtaining I values described in Equation (4.1.6).

$$\theta = \{\theta_{i_s} \epsilon\, [\gamma, 1-\gamma], \qquad i_s = 1, 2, \cdots, I\} \tag{4.1.6}$$

Using the values defined in Equation (4.1.6), the discretized PDF of power generation at time $t-1$ and its corresponding CDF presented in Figure 4.3, some selected power production values $\left(P_{n,i_s}^{t-1}\right)$ can be selected by evaluating the inverse CDF of each element of set θ. Note that when $\theta_{i_s} = 0.5$, power production at $t-1$ is the mean value of power production, which corresponds to the result obtained from evaluation of the ED problem in the mean value of forecasted power generation. This methodology uses the concept of quantile to select and consider the power production values at time $t-1$. Another characteristic to take into account is when $\theta_{i_s} \rightarrow \gamma$, low load conditions at $t-1$ are considered; on the contrary, when $\theta_{i_s} \rightarrow 1-\gamma$, high conditions of load are considered. This allows extreme conditions, of low and high load, to be considered.

From the application of the methodology previously described, a similar table to that shown in Figure 4.4 is obtained; where the power production at time $t-1$ according to the sampling point could be easily recognized. Something important to note is that the probabilities of occurrence of each column in Figure 4.4 do not add up to 1, due to all possible combinations not being considered. To solve this problem, the corresponding probability $(P_r\{\bullet\})$ is substituted by normalized probability $(NP_r\{\bullet\})$ of Equation (4.1.7), whose sum is equal to 1 for any amount of sampling points I.

$$NP_r\{P_n^{t-1} = P_{n,i_s}^{t-1}\} = \frac{\prod_{n=1}^{N}\left(P_r\{P_n^{t-1} = P_{n,i_s}^{t-1}\}\right)}{\sum_{i_s=1}^{I}\prod_{n=1}^{N}\left(P_r\{P_n^{t-1} = P_{n,i_s}^{t-1}\}\right)} \tag{4.1.7}$$

4.1.3. Incorporation of Wind Power Forecasting Error

Once the discretized PDF of available wind power generation and power production at time $t-1$ are obtained, wind power forecasting error is incorporated in the probabilistic ED problem by following the algorithm described next:

- Step 1: Select the number of bins (B) to be considered in the discrete PDF of all variables of interest (power production of thermal units, wind power generation, energy not supplied and energy surplus). The maximum value of power (P^{max}) to be considered is chosen as well in this step, while the minimum value (P^{min}) is assumed to be zero. The corresponding bin is identified by the index $b\, \epsilon\, \{1, B\}$;
- Step 2: Using the parameters selected in Step 1, the increment of the discrete representation of power values (ΔP) is calculated by using Equation (4.1.8):

$$\Delta P = \frac{P^{max} - P^{min}}{B-1} \tag{4.1.8}$$

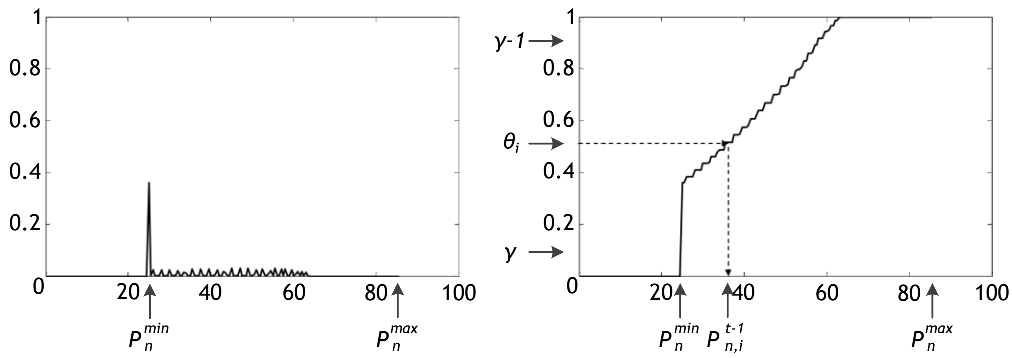

Figure 4.3. PDF of P_n^{t-1} (left side) and CDF of P_n^{t-1} (right side).

Sampling Point

Unit	1	2	…	i_s	…	…	I
1	$P_{1,1}^{t-1}$	$P_{1,2}^{t-1}$	…	P_{1,i_s}^{t-1}	…	…	$P_{1,I}^{t-1}$
⋮	⋮	…	…	…	…	…	⋮
n	$P_{n,1}^{t-1}$	…	…	P_{n,i_s}^{t-1}	…	…	$P_{n,I}^{t-1}$
⋮	⋮	…	…	…	…	…	⋮
N	$P_{N,1}^{t-1}$	$P_{N,2}^{t-1}$	…	P_{N,i_s}^{t-1}	…	…	$P_{M,I}^{t-1}$

Figure 4.4. Selected cases of power production at time $t-1$.

After this, the power value (P_b) that corresponds to discrete state b is obtained. This is implemented as a vector $P_b = P_1, P_2, \dots, P_b, \dots, P_B$, where $P_1 = P^{min} = 0$ and $P_B = P^{max}$. Then, any continuous power value obtained from the optimization process can be represented in a discrete manner, selecting the corresponding discrete state;

- Step 3: Create a table of B rows and M columns $(T_{b,n})$. This table is the discrete PDF of power generation of thermal units. All elements in this table are initialized as zero;
- Step 4: In this step, the first case of power generation at time $t-1$ (see Figure 4.4) is selected. This is carried out by setting the index i_s equal to 1 $(i_s \leftarrow 1)$;
- Step 5: The first discrete state of available wind power generation is selected. This is carried out by setting j equal to 1 $(j \leftarrow 1)$;
- Step 6: Solve the EC problem for the corresponding combination $(i_s,\ j)$. This is carried out by solving the optimization problem of Equations (4.1.9) - (4.1.14) [200]:

$$z_{i_s,j} = \sum_{n=1}^{N} \left(a_n + b_n\left(P_{n,i_s}^t\right) + c_n\left(P_{n,i_s}^t\right)^2\right) + VOWE\left(DL_{i_s}^t\right) + VOLL\left(ENS_{i_s}^t\right) \tag{4.1.9}$$

$$\sum_{n=1}^{N} P_{n,i_s}^t + w_j^t = D^t \tag{4.1.10}$$

$$P_{n,i_s}^t - P_{n,i_s}^{t-1} \leq UR_n \tag{4.1.11}$$

$$P_{n,i_s}^{t-1} - P_{n,i_s}^t \leq DR_n \tag{4.1.12}$$

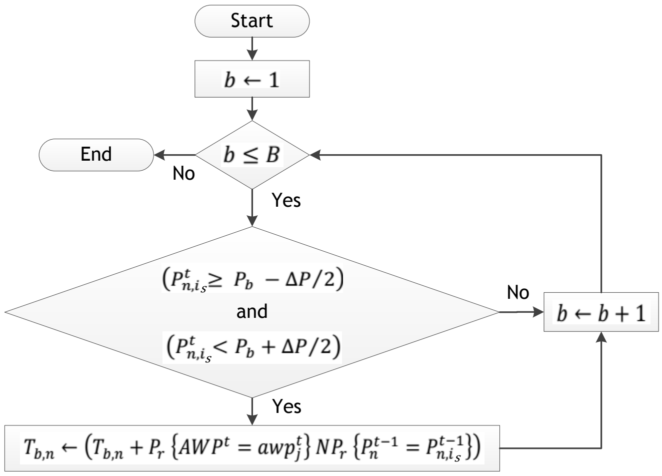

Figure 4.5. Allocation of power generation(P_{n,i_s}^t) in the PDF of P_n^t .

$$P_n^{min} \leq P_n^t \leq P_n^{max} \tag{4.1.13}$$

$$0 \leq w_j^t \leq awp_j^t \tag{4.1.14}$$

- Step 7: From the solution of optimization problem in Step 6, variables w_j^t and P_{n,i_s}^k are determined. Then, the corresponding probability values are calculated and allocated in the discrete PDF using the algorithm presented in Figure 4.5 (available at the top of the present page). In similar manner, discretized PDF of ENS and generation cost are built;
- Step 8: If $j < J$, set $j \leftarrow j+1$ and go back to Step 6; else go to Step 9;
- Step 9: If $i < I$, set $i_s \leftarrow i_s + 1$ and go back to step 5; else end.

4.1.4. Incorporation of Generators Reliability

For a determined unit n, the estimation of power production considering the failure events could be estimated by using the algorithm presented next. This algorithm was adapted from the methodology proposed in [201] to the estimation of joint PDF of power production and failure modes.

- Step 1: Using the discrete representation of any power value ($P_b\ \epsilon \{P^{min}, P^{max}\}$), find the bin ($b_n$) that corresponds to the rated power of unit n (P_n^{max}). It can be carried out by adapting the algorithm presented in Figure 4.5;
- Step 2: Create the state h, i.e., $(h = 0, 1, 2, \dots, H)$, using the state b by means of expression $h + 1 = b$ to represent a determined state of power production and failure events. The value of power production of state h can be estimated as $P_h = P_{b-1}$. This change in states name is required to the estimation of join PDF of power production and failure events;
- Step 3: In this step, the discrete PDF of failure events (F_h^n) of determined unit n is represented by Equation (4.1.15):

$$F_h^n = \begin{cases} FOR_n\,, & h = 1 \\ 1 - FOR_n\,, & h = b_n \\ 0\,, & otherwise \end{cases} \tag{4.1.15}$$

- Step 4: Once discrete PDF of power production (P_h) and discrete PDF of failure events (F_h^n) have been estimated, the discrete join PDF of power production and failure events can be built. The event of power production and failure events are considered as two independent variables, so that the join PDF can be obtained by multiplication of the occurrence probability of each event $(P_r\{P_n^t = P_h\}; P_r\{F_h^n = P_h\})$. The joint PDF is represented by a table similar to the table presented in Figure 4.6;
- Step 5: Create the discrete state l of power production when generators reliability is considered, state $l = 0, 1, 2, \dots, L$, where $L = (H+1)^2 = B^2$. The corresponding power value associated with the state l (P_l) is defined according to equation (4.1.16):

$$P_l = l\left(\frac{\Delta P}{b_n - 1}\right) \tag{4.1.16}$$

- Step 6: In this step, the probability of state $l = 0$, i.e., $(P_{l=0})$ is estimated. This probability is calculated summing the elements $(1,1)$, the elements of row 1 from 2 until B, and the elements of column 1 from 2 until B of the table presented in Figure 4.6;
- Step 7: The estimation of probabilities that corresponds to states $l = 1, 2, \dots, L$ is carried out by using the algorithm presented as follow:
  - Step 7.1: Create the table $E_{(l,n)}$ of B^2 rows and M columns. Initialize all its elements to zero;
  - Step 7.2: Set $av_1 \leftarrow 0$;
  - Step 7.3: Set $av_2 \leftarrow 0$;
  - Step 7.4: Calculate $av_3 = av_1 av_2$;
  - Step 7.5: If $av_3 > 0$, $E_{(av_3,n)} \leftarrow E_{(av_3,n)} + P_r\{P_n^t = P_h\}\, P_r\{F_h^n = P_h\}$; else go to Step 7.6;
  - Step 7.6: If $av_2 < L$, set $av_2 \leftarrow av_2 + 1$ and go to Step 7.4; else go to Step 7.7;
  - Step 7.7: If $av_1 < L$, set $av_1 \leftarrow av_1 + 1$ and go to Step 7.3; else end.

The discrete PDF of power production incorporating the forecasting error of wind power generation and generator reliability is represented by discrete states l, the power associated with corresponding state (P_l) and the probabilities of table $E_{l,n}$. Regarding the ENS, the discrete PDF of this variable could be estimated by using the methodology explained in Sub-Section 4.1.3, representing ENS as the generation unit.

The component of ENS due to generator reliability could be estimated by using the recursive expression of Equation (4.1.17) [202]:

$$F_b^e(P_b) = (1 - FOR_n)\, F_b^e(P_b) + FOR_n\, F_b^e\,(P_b - P_n^{max}) \tag{4.1.17}$$

where F_b^e is the CDF of ENS due to any failure event in the generation system. From this result the required PDF could easily be estimated. Both of them are shown in Figure 4.7. Finally, the discrete PDF of ENS taking into account wind power forecasting error and generator reliability is estimated as the convolution between the discrete PDF obtained from the procedure explained in Sub-Section 4.1.3 and that obtained from Equation (4.1.17) and Figure 4.7.

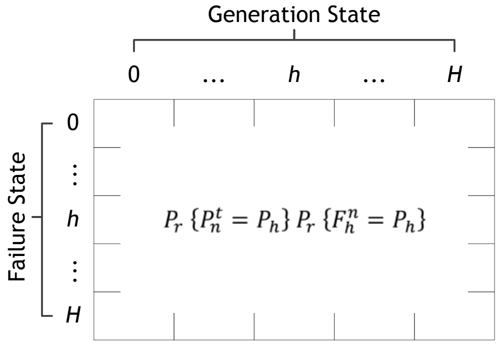

Figure 4.6. Illustration of the join PDF of failure events and power production.

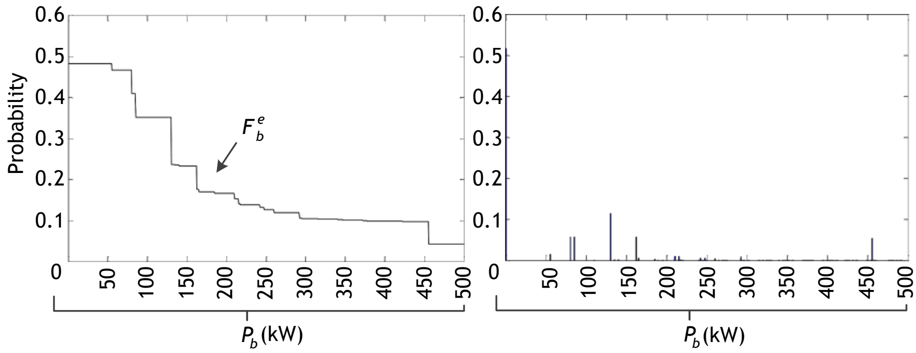

Figure 4.7. CDF of power generation loss (left side) and PDF of power loss (right side) due to failure events.

4.2. Case Studies and Results

The approach proposed in this thesis is illustrated by analyzing two case studies of 5 and 10 units and wind power generation. In order to evaluate the performance of the proposed approach, the results obtained from the approach explained in Section 4.1 were compared with those obtained from the application of MCS methodology. In both cases, the number of trials considered in the MCS was 50,000. The test system based on MCS was built by considering three time instants. The first time instant corresponds to the actual conditions so that the initial power generation was considered as a real value.

In the second and third time instants, the conditions of available wind power generation were randomly generated, while the power generation of each unit and wind farm was obtained from the solution of the corresponding optimization problem by a quadratic programming approach [200]. Using the results obtained from the second time instant, the PDF of initial power generation of each unit required by the proposed approach was then obtained. The results obtained from the third time instant were used to build the PDF of power generation of each unit, which is employed as a reference of comparison between the proposed methodology and the MCS methodology. The number of bins considered to build the required PDFs was 1500 ($B = 1500$), the significance level was 0.05 and the sampling increment used was 0.15, obtaining seven sampling points ($I = 7$).

The discretization of the PDF of available wind power generation was carried out by considering $\sigma = 0.01$ and $R = 3500$. The results obtained from the analysis of each case study are presented next in Sub-sections 4.2.1 and 4.2.2. The proposed approach was implemented in MATLAB using a computer with i7-3630QM CPU at 2.40GHz, 8GB of memory and 64-bit operating system.

4.2.1. Analysis of 5-Unit Power System

The power system under analysis corresponds to a typical diesel-powered system of an island. The main characteristics such as rated capacity and generation costs are presented in Table 4.1, the minimum output power of each unit was assumed to be 50% of corresponding rated power. This data was obtained from the analysis of information provided by the manufacturers. Available wind power generation was modeled as a beta PDF with parameters $\alpha_{pdf} = 1.4$, $\beta_{pdf} = 3.1$, $W_{min}^{t} = 0$kW, and $W_{max}^{k} = 600$kW. The maximum power value considered was $P^{max} = 1000$kW. Finally, load demand was assumed to be 892kW at time t.

Figure 4.8 shows the PDF of wind farm (W^t) obtained from the solution of the optimization problem. It is observed how wind power generation is curtailed to about 424kW due to the minimum output power of thermal units. This is an important problem in the integration of renewable energy sources to a power grid and which could be probabilistically analyzed by means of the approach proposed in this work. Figure 4.9 shows the PDF of power production of unit 1. Due to this unit being one of the cheapest in the system, this unit responds to the fluctuations from wind power generation. It is possible to observe how the probability of high wind power generation leads this unit to reduce its output power at its minimum value, while the probability of power production at high values is influenced by the PDF of available wind power generation. Similar results were obtained for the other units and were not reported here.

Through the analysis of Figures 4.8 - 4.10, it is possible to observe the excellent performance of the proposed approach compared with MCS. It could be quantified by means of a comparison between the expected values obtained from the application of each methodology; such a comparison is shown in Table 4.2. The proposed approach could be used to evaluate the GHE of each thermal unit.

Table 4.1. Description of 5-Unit system.

n	P_n^{max}(kW)	a_n (\$/h)	b_n (\$/kWh)	c_n (\$/kW^{2}h)
1	350	10.3904	0.1472992	0.00012224
2	300	8.6332	0.1534112	0.00012224
3	125	3.5908	0.1842768	0.00009168
4	100	3.2852	0.1815264	0.00012224
5	60	2.2156	0.2270608	-0.00030560

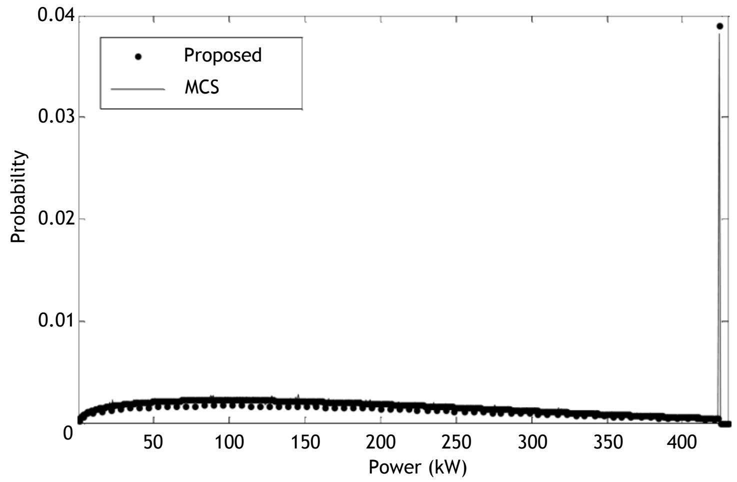

Figure 4.8. PDF of wind power generation (5-Unit system).

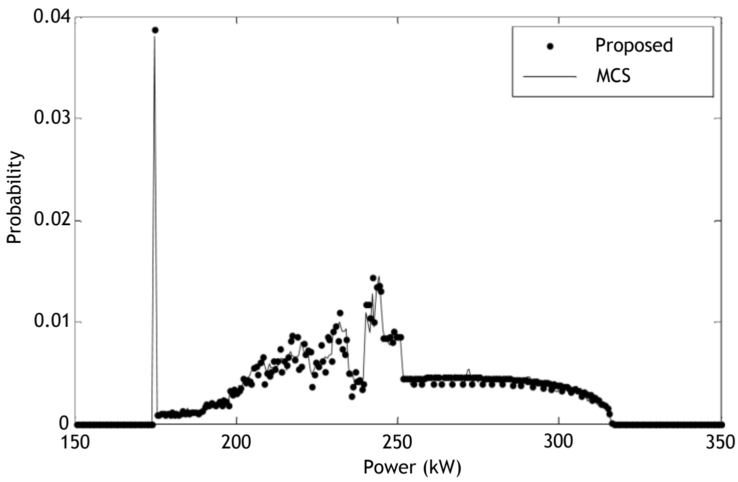

Figure 4.9. PDF of power generation of unit 1.

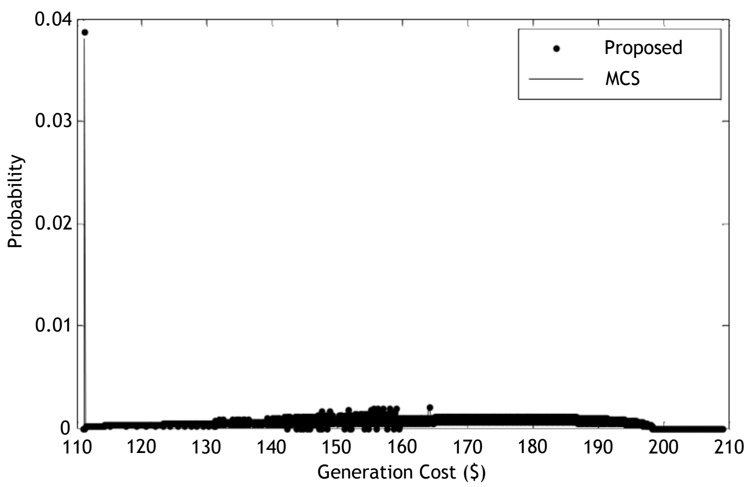

Figure 4.10. PDF of generation cost.

To illustrate this application, the CO_2 emission of each unit has been modeled by using the quadratic expression of Equation (4.2.1).

$$GHE_n = U_n + X_n\left(P_{n,i_s}^t\right) + V_n\left(P_{n,i_s}^t\right)^2 \tag{4.2.1}$$

The corresponding parameters of Equation (4.2.1) were obtained by fitting the experimental measurements presented in [203] related to CO_2 emissions to the Equation (4.2.1). The obtained results are presented in Table 4.3. Furthermore, Table 4.4 presents the expected value of CO_2 emissions for each unit. It is possible to observe how the forecasting error of available wind power generation highly influenced the probability of emission of a determined amount of CO_2. Figure 4.11 presents the PDF of CO_2 emissions of unit 1, which was obtained by evaluating the PDF power production of Figure 4.9 in Equation (4.2.1).

Table 4.2. Expected value comparison between MCS and proposed approach.

Comparison	MCS	Proposed
Wind farm (kW)	185.788939	184.988933
Unit 1 (kW)	243.892262	244.178446
Unit 2 (kW)	218.904510	219.191016
Unit 3 (kW)	107.157612	107.361965
Unit 4 (kW)	88.606244	88.752082
Unit 5 (kW)	47.612342	47.486873
Total cost ($)	159.023486	159.189200
Time (s)	787.462000	149.976000

Table 4.3. CO_2 emission model.

n	P_n^{max}(kW)	U_n (kg/h)	X_n (kg/kWh)	V_n (kg/kW^{2}h)
1	350	28.062	0.5075	0.0004
2	300	24.104	0.5626	0.0002
3	125	16.244	0.4506	0.0010
4	100	11.148	0.5544	0.0006
5	60	9.163	0.6201	-0.0014

Table 4.4. Expected value of CO_2 emissions.

n	CO_2 emissions (kg)
1	176.313261
2	157.271476
3	76.610344
4	65.232853
5	35.148854

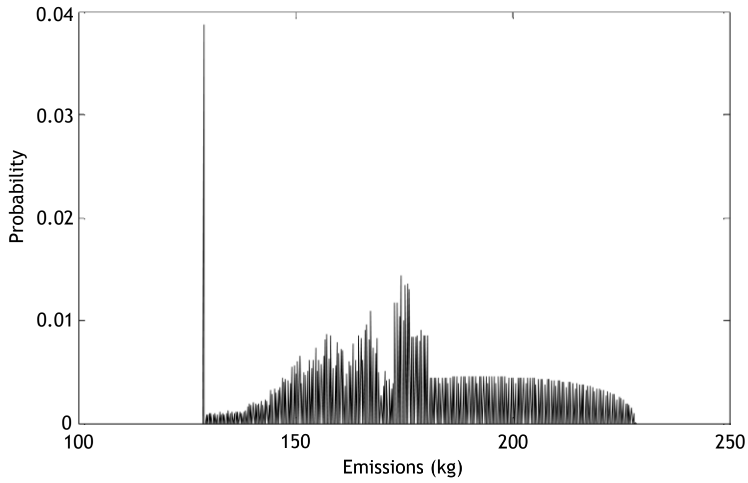

Figure 4.11. PDF of CO_2 emissions of unit 1.

4.2.2. Analysis of 10-Unit Power System

In this case study, the power system described in [162] has been adapted by adding the values of forced outage rates (FOR) presented in Table 4.5, estimated according to the corresponding role of the unit (base-unit, cycling-unit, and peak-unit). Available wind power generation was modeled with the parameters $\alpha_{pdf} = 1.6$, $\beta_{pdf} = 6.3$, $W_{min}^{k} = 150$MW, and $W_{max}^{k} = 500$MW. The maximum power value considered was $P^{max} = 1700$MW. Finally, load demand was assumed to be 1600MW at time t. This system has been used to analyze the performance of the proposed approach when ramp constraints and failure events are considered. The results obtained are presented in Sub-Section 4.2.2.1 and 4.2.2.2.

4.2.2.1. Analysis of 10-Unit System Incorporating Generators Reliability

The methodologies explained in Sub-Sections 4.1.3 and 4.1.4 were used in the analysis of the system taking into account the reliability of generation units. The corresponding comparison with the MCS approach in Figure 4.12 shows the PDF of power generation of unit 4. Note that this unit has a high probability of being committed at its maximum output power (130MW). Due to its generation cost and technical characteristics, this unit does not respond to the fluctuations of wind power or failure events of other units. Otherwise, there is a probability of 0.1 of being de-committed as a consequence of a failure event. According to these results, the proposed approach offer excellent performance.

Figure 4.13 shows the PDF of power generation of unit 6. As can be observed, this unit responds to any failure event of other units by increasing its power production, which produces important differences between the PDF obtained from the proposed approach and the MCS approach. The approach proposed in this work does not take into account this increment in power generation as a consequence of any failure in other units. Figure 4.14 shows the PDF of generation cost related to the fuel consumption (without considering the value of lost load (VOLL)). As in the previous case study, this cost is strongly influenced by the PDF of available wind power forecasting error.

Table 4.5. Description of 10-Unit system.

n	P_n^{max} (MW)	FOR_n
1	455	0.05
2	455	0.05
3	130	0.10
4	130	0.10
5	162	0.10
6	80	0.10
7	85	0.10
8	55	0.01
9	55	0.01
10	55	0.01

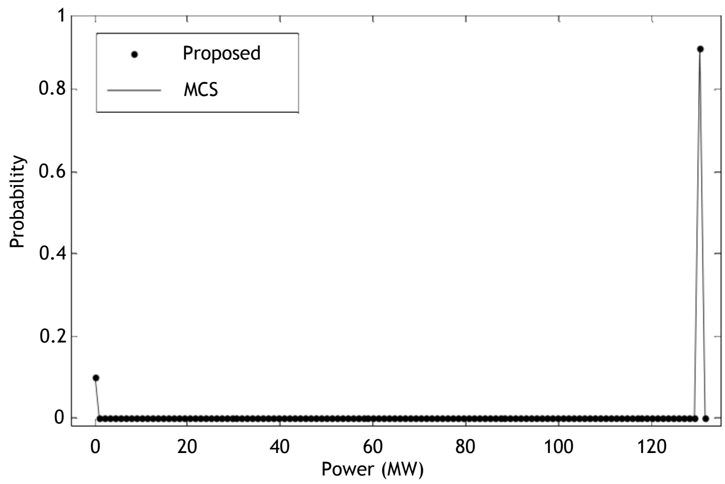

Figure 4.12. PDF of power generator of unit 4.

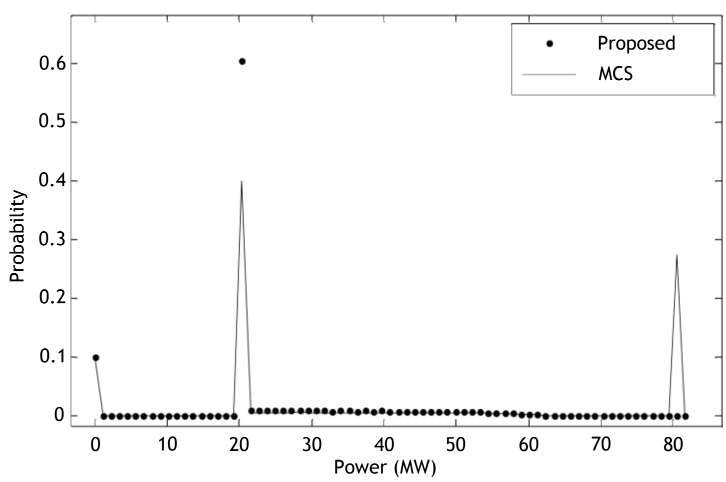

Figure 4.13. PDF of power generator of unit 6.

Table 4.6 shows the expected value of power production, ENS, and fuel consumption cost. It is possible to observe how the proposed approach can reasonably model those units used to provide base-load, which operate continuously at their maximum output power (units 1 - 4). However, the proposed approach has difficulties modeling the behavior of those units that increase their power production under any failure of other units (units 5 - 10) that are used as cycling and peak units. This reasoning justifies the important differences in estimation of ENS observed. Figure 4.15 presents the PDF of ENS, where important differences can be observed. The results obtained from the proposed approach suggest higher values of ENS due to increment in power production of those units that provide spinning reserve not being considered.

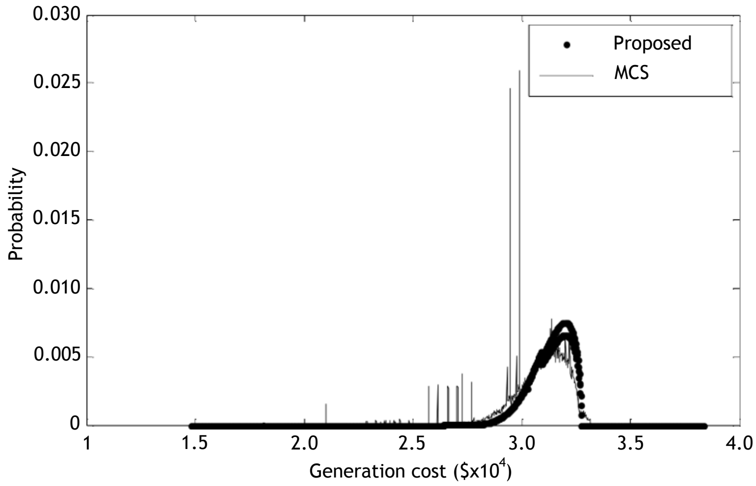

Figure 4.14. PDF of generation cost related with fuel consumption.

Table 4.6. Expected value comparison between MCS and proposed approach.

Comparison	MCS	Proposed
Unit 1 (MW)	432.286025	432.031354
Unit 2 (MW)	432.248759	431.392345
Unit 3 (MW)	117.740821	117.378252
Unit 4 (MW)	117.866024	117.378252
Unit 5 (MW)	125.958954	115.711446
Unit 6 (MW)	39.962974	23.878370
Unit 7 (MW)	31.075342	22.455013
Unit 8 (MW)	22.839449	10.104748
Unit 9 (MW)	20.058911	10.104736
Unit 10 (MW)	15.733109	10.104736
ENS (MWh)	24.049636	106.069599
Fuel cost ($)	30736.441648	31313.845805
Time (s)	1194.889000	228.262000

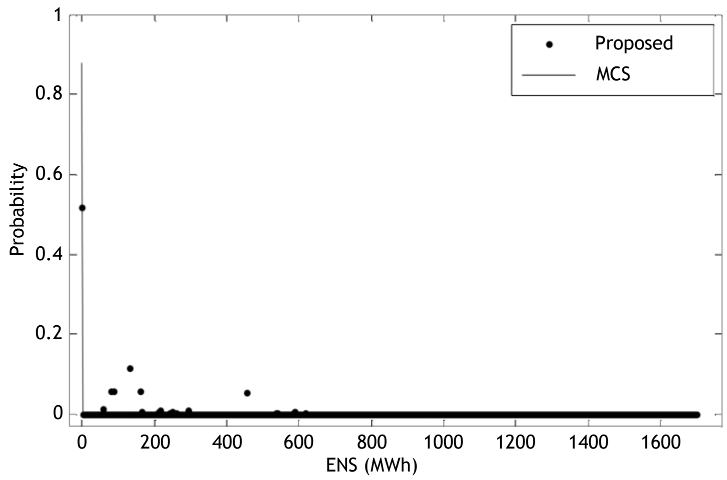

Figure 4.15. PDF of energy not supplied.

4.2.2.2. Analysis of 10-Unit System Without Incorporating Generators Reliability

In this sub-section, the results obtained from the analysis of the ten unit system without considering the generator reliability are presented. Figure 4.16 shows the PDF of wind power generation, which is totally accepted by the system without any curtailment. Figure 4.17 shows the PDF of power production of unit 6, where it is possible to observe how under these conditions (without considering unit reliability) the proposed approach can reasonably reproduce the PDF obtained from the MCS approach.

Figure 4.18 shows the PDF of generation cost and the impact of forecasting error of wind power generation. The increment in generation cost is directly related to the decrement in wind power generation previously presented in Figure 4.16. Table 4.7 summarizes the comparison between the expected value of power production and generation cost. As can be observed, the proposed methodology presents excellent performance compared with the results obtained from the MCS approach.

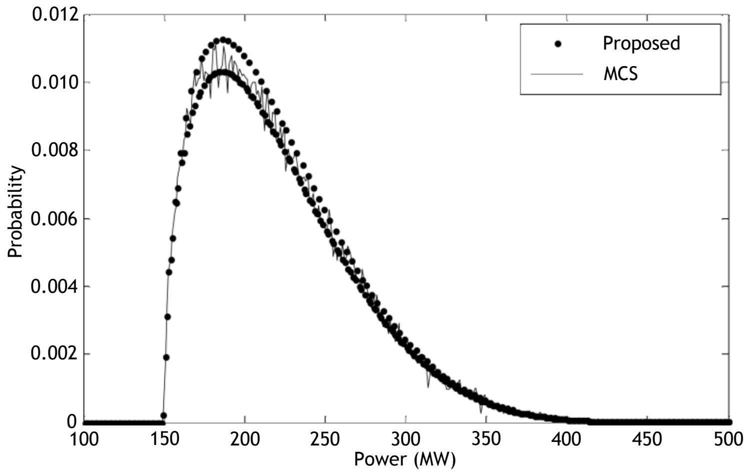

Figure 4.16. PDF of wind power generation.

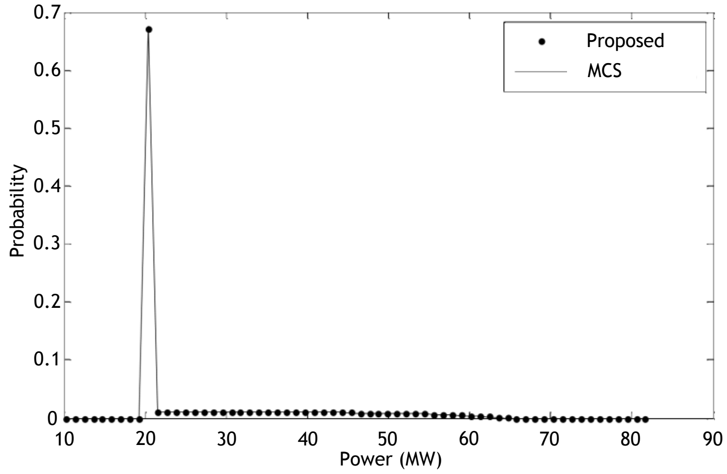

Figure 4.17. PDF of power generation of unit 6.

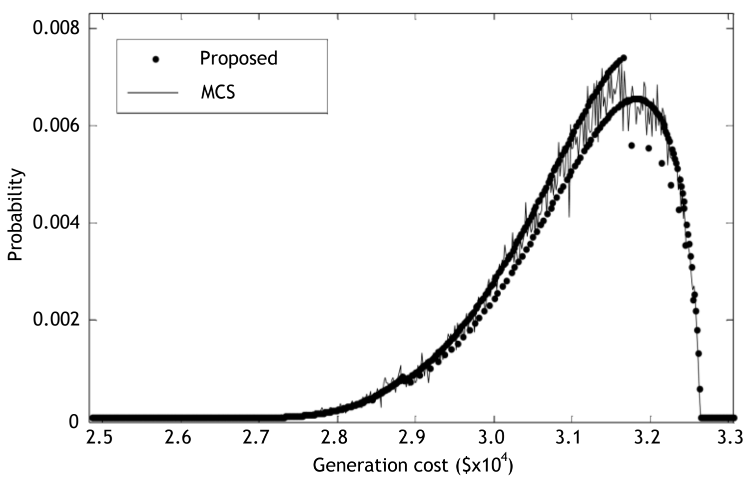

Figure 4.18. PDF of generation cost.

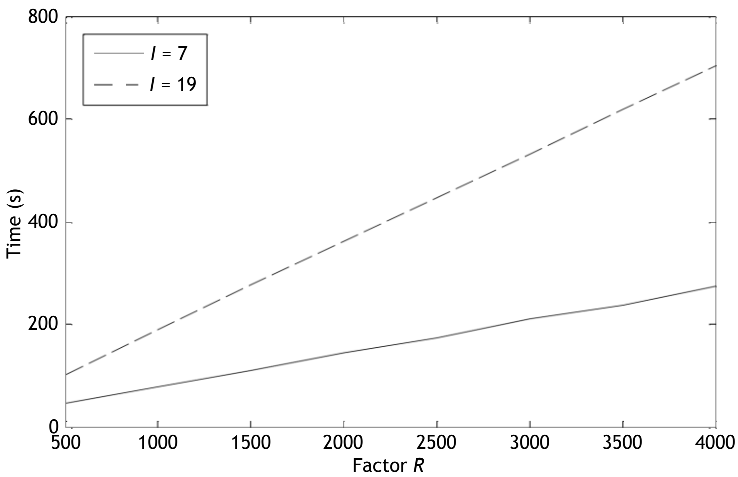

Figure 4.19. Behavior of computational time.

In the proposed approach, the trade-off between the accuracy of results obtained and computational time is carried out by adjusting the parameters I and R, which represents the total number of possible power production combinations at time $t-1$, and the amount of discretization levels of PDF of available wind power generation. These factors can be adjusted according to the computational resources available and the size of the system under analysis. Figure 4.19 presents the behavior of computational time as a function of the factor R for two different values of parameter I. According to these results, computational time has a linear behavior, which facilitates the selection of the factor R taking into account the computational resources.

Table 4.7. Expected value comparison between MCS and proposed approach incorporating generator reliability.

Comparison	MCS	Proposed
Wind power (MW)	220.910611	220.877230
Unit 1 (MW)	454.769847	454.769847
Unit 2 (MW)	454.075239	454.097234
Unit 3 (MW)	130.420280	130.420280
Unit 4 (MW)	130.420280	130.420280
Unit 5 (MW)	128.632910	128.303661
Unit 6 (MW)	26.490740	26.665282
Unit 7 (MW)	24.949967	24.949967
Unit 8 (MW)	10.206805	10.206805
Unit 9 (MW)	10.206805	10.206805
Unit 10 (MW)	10.206805	10.206805
Total cost ($)	31087.151684	31087.762562
Time (s)	1222.937000	235.965000

Chapter 5

Unit Commitment Problem

The optimal operation of power systems with high integration of renewable energy sources is challenging due to the random nature of some sources like wind energy and photovoltaic energy. Nowadays this problem is solved using the MCS approach, which allows the consideration of important statistical characteristics of wind and solar power production, such as the correlation between consecutive observations, the diurnal profile of the forecast power production, and the forecasting error.

In this thesis, a new model of the unit scheduling of power systems with significant renewable power generation based on scenario generation/reduction method combined with the priority list (PL) method is proposed, which finds the PDF of a determined generator being committed or not. This approach allows the recognition of the role of each generation unit on the day-ahead UC problem with a probabilistic point of view, which is important for acquiring a cost-effective and reliable solution. The capabilities and performance of the proposed approach are illustrated through the analysis of a case study, where the spinning reserve requirements are probabilistically verified with success.

The new approach proposed is based on the scenario generation and reduction approach. By solving the deterministic UC problem for each scenario, the PDF of committing a particular generator at a particular time is determined. In the next step, the definitive solution to the stochastic UC problem is carried out by selecting those generators with a probability of being committed higher than a predefined value. Finally, the solution obtained is probabilistically checked by evaluating the selected UC solution, using the scenarios previously generated.

5.1. Scenario Generation Process

Recently, several methods for scenario generation and reduction have been developed. In [204] a methodology that combines Latin hypercube sampling (LHS) with Cholesky decomposition (LHS-CD) is proposed. The joint PDF of wind power generation is modeled as a Gaussian one, assuming the forecast values to be the mean values, while standard deviation depends on the forecasting error. Undesired correlations are then reduced by means of the Cholesky decomposition method. In [205] a methodology was proposed that introduces forecasting error through empirical distributions, while assuming the PDF of wind power variability as a t location-scale distribution.

Scenarios are generated by using an inverse transformation from the joint PDF, which is assumed to be a Gaussian-multivariate distribution.

The methodology used in this work for scenario generation is able to consider the most important features that describe the temporal behavior of the wind power time series, such as the autocorrelation that exists between consecutive observations, the hourly profile of the expected wind power production, and its corresponding forecasting error. For the scenario generation, the first step consists of randomly generating a set of scenarios, taking into account the intrinsic autocorrelation of the hourly wind power production. In the second step, a subset of the scenarios previously generated is chosen according to the forecasting error.

Finally, the scenarios to be used for the solution of the stochastic UC problem are selected by applying the k-means clustering algorithm to the set of scenarios obtained in the second step. To reproduce the original forecast wind power production, synthetically generated scenarios have to incorporate the correlated behavior of the wind power generation and its hourly profile. On the one hand, autocorrelation is introduced by generating a random series, assuming a first-order autoregressive Markov process according to Equation (5.1.1):

$$x_m^t = \emptyset x_m^{t-1} + \epsilon \tag{5.1.1}$$

where x_m^t is the time series which saves the autocorrelation nature of the original wind power profile, index m refers to scenario generated $(m = 1, 2, \dots, M)$ and index t refers to the time $(t = 1, 2, \dots, H)$, $\emptyset$ is the one-lag autocorrelation parameter, and ϵ is a Gaussian white noise with mean zero and standard deviation of $\sqrt{1 - \emptyset^2}$. On the other hand, the hourly wind power profile is introduced by normalizing the forecast wind power production according to Equation (5.1.2):

$$y^t = \frac{W^t - \mu}{\sigma} \tag{5.1.2}$$

where y^t is the normalized wind power profile, W^t is the time series of the total wind power generation, while μ and σ are its mean and standard deviation, respectively. Thus, a normalized time series of wind power generation that simultaneously incorporates the autocorrelation of the predicted wind power generation and its hourly profile is obtained with the addition of time series previously obtained in Equations (5.1.1) and (5.1.2) [206]:

$$z_m^t = x_m^t + y^t \tag{5.1.3}$$

where z_m^t is the normalized total wind power generation of scenario m at time t. Finally, the total wind power generation (W_m^t) is obtained by applying the probability transformation described in Equation (5.1.4), Equation (5.1.5) and Figure 5.1:

$$A(z_m^t) = h_m^t = A_w(W_m^t) \tag{5.1.4}$$

$$W_m^t = A_W^{-1}\big(A(z_m^t)\big) \tag{5.1.5}$$

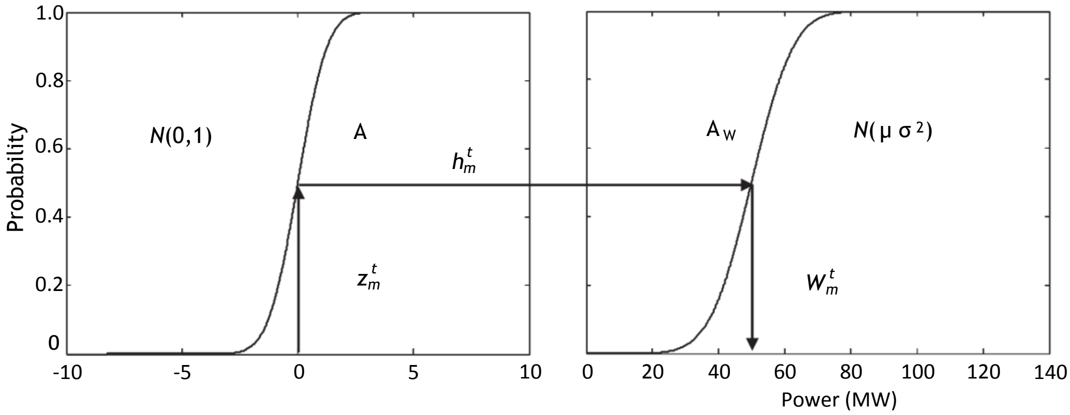

Figure 5.1. Probability transformation.

where A is the continuous distribution function (CDF) of time series z_m^t, having mean 0 and standard deviation 1, and A_w is the CDF of time series W^t. A and A_w are assumed to be Gaussian PDF. According to Figure 5.1, curve A presented on the left side corresponds to the CDF of a normalized Gaussian PDF, which is the PDF of the time series obtained in Equation (5.1.3), while curve A_w presented on the right side corresponds to the CDF of the original predicted wind power profile modeled as a Gaussian PDF with mean μ and standard deviation σ. h_m^t is an intermediate time series that has uniform PDF within the interval $\{0, 1\}$ [207].

Scenarios obtained from the implementation of the procedure described previously could lead to unrealistic situations, in which scenarios with extremely high or low values are obtained. To deal with this problem, an algorithm to select those scenarios with reliable values is introduced. Assuming a determined PDF for the hourly forecasting error, a determined value for the significance level (α) is fixed and the corresponding confidence interval is calculated for each hour. A vector of H binary elements (F_m) is then created, as a storage vector if the corresponding scenario m at time t is within the corresponding confidence interval. In the case that W_m^t is inside, the confidence interval value of 1 is assigned and if it is outside a value of 0 is assigned. Once vector F_m has been built for each scenario, an index (I_m) that reflects the degree to which the scenario under analysis (m) fulfills the hourly forecasting error is calculated. This index is defined according to Equation (5.1.6):

$$I_m = \left(\sum_{t=1}^{H} F_m\right) \Big/ H \tag{5.1.6}$$

If I_m is equal to 1 it means that during all hours each value of scenario m is within the confidence level. On the other hand, a value of this index lower than 1 means that during some hours the scenario generated is outside the corresponding confidence interval. In the next step, by establishing a determined limit to this index (β) all scenarios that correspond to the specified forecasting error are selected. As an example, if a value $\beta = 0.9$ is chosen, those scenarios with I_m higher than β should be selected. Finally, the scenarios required to be used in the solution of the stochastic UC problem are found by applying the *k*-means clustering algorithm [208] on the set of scenarios previously selected by using the parameter β.

5.2. Problem Description

In the following subsection the mathematical formulation of the UC problem integrating the uncertainty related to the net load is presented. Net load is defined as the difference between load demand and wind power generation. Solving the stochastic UC problem consists of finding out the optimal combination of generators that should be committed and their corresponding power production in order to minimize the generation costs over the scheduling horizon, considering the possible fluctuations of the different sources of uncertainty (wind power generation and load demand, among others). An important barrier to the successful solution of this optimization problem and the accommodation of wind power generation is the set of constraints that characterize the operation of the thermal generation units, such as generation limits, operating ramp rate constraints, startup and shutdown ramp rate constraints, reserve constraints and minimum up and down time constraints.

5.2.1. Objective Function

UC is an optimization problem that consists of minimizing the expected operating cost. This cost could be divided into fuel-consumption cost and starting-up cost. Traditionally, fuel-consumption cost has been modeled by using a quadratic expression in terms of the corresponding power production, while starting-up cost has been modeled by using a piecewise expression that depends on the number of hours that a specific generator has been de-committed. The mathematical expression for generation cost is presented in Equation (5.2.1):

$$f = \sum_{m=1}^{M} P_r\{m\}\left\{\sum_{t=1}^{T}\sum_{n=1}^{N} a_n U_{n,m}^t + b_n P_{n,m}^t U_{n,m}^t + c_n\left(P_{n,m}\right)^2 + SUC_n^t\left(1 - U_{n,m}^{t-1}\right)U_{n,m}^t\right\} \tag{5.2.1}$$

where f is the expected value of total operating cost, $P_r\{m\}$ is the probability of occurrence of a determined scenario (m), and $P_{n,m}^t$ is the power production of generator n, at time t, in scenario m. $U_{n,m}^t$ is a binary variable to represent if generator n, at time t, and in scenario m is committed or de-committed, and $SUC_{n,m}^t$ is the starting-up cost of generator n, parameters a_n, b_n, and c_n correspond to the fuel-consumption of generator n. The ED problem is solved by means of a quadratic programming approach, an approximation of the starting-up cost is presented in Equation (5.2.2):

$$SUC_n^t = \begin{cases} HSU_n, & OFF_{n,m}^t \leq MDT_n + CST_n \\ CSU_n, & OFF_{n,m}^t > MDT_n + CST_n \end{cases} \tag{5.2.2}$$

where $HSU_{n,m}^t$ is the hot startup cost, $CSU_{n,m}^t$ is the cold startup cost, and $CST_{n,m}^t$ is the cold startup time of generator n. $OFF_{n,m}^t$ is an integer variable that saves the cumulative account of the number of hours that generator n has been de-committed. In a similar manner, $ON_{n,m}^t$ saves the number of hours that generator n has been committed. The definition of these variables is presented in Equation (5.2.3) and Equation (5.2.4):

$$ON_{n,m}^{t} = \begin{cases} ON_{n,m}^{t-1} + 1, & U_{n,m}^{t} = 1 \\ 0, & U_{n,m}^{t} = 0 \end{cases} \tag{5.2.3}$$

$$OFF_{n,m}^{t} = \begin{cases} OFF_{n,m}^{t-1} + 1, & U_{n,m}^{t} = 0 \\ 0, & U_{n,m}^{t} = 1 \end{cases} \tag{5.2.4}$$

5.2.2. Generation Limit Constraints

If the generator n is committed, its power production should be limited by its minimum (P_n^{min}) and maximum (P_n^{max}) production. This is mathematically expressed in Equation (5.2.5):

$$P_n^{min} \leq P_{n,m}^{t} \leq P_n^{max}, \qquad U_{n,m}^{t} = 1 \tag{5.2.5}$$

5.2.3. Operating Ramp rate Constraints

Many of the technologies used nowadays have important limitations on sudden change of power production. These limitations are expressed through the set of constrains of Equation (5.2.6) and Equation (5.2.7):

$$P_{n,m}^{t} - P_{n,m}^{t-1} \leq UR_n, \qquad U_{n,m}^{t} = 1;\ U_{n,m}^{t-1} = 1 \tag{5.2.6}$$

$$P_{n,m}^{t-1} - P_{n,m}^{t} \leq DR_n, \qquad U_{n,m}^{t} = 1;\ U_{n,m}^{t-1} = 1 \tag{5.2.7}$$

where UR_n and DR_n are the ramp up and ramp down rates of generator n.

5.2.4. Startup and Shutdown Ramp Rate Constraints

The effects of the ramping limitations during the starting process are considered by the inclusion of Equation (5.2.8) and Equation (5.2.9) in the optimization problem:

$$P_{n,m}^{t} \leq SUR_n + P_n^{min}, \qquad U_{n,m}^{t} = 1;\ U_{n,m}^{t-1} = 0 \tag{5.2.8}$$

$$P_{n,m}^{t} \leq SDR_n + P_n^{min}, \qquad U_{n,m}^{t} = 1;\ U_{n,m}^{t+1} = 0 \tag{5.2.9}$$

where SUR_n and SDR_n are the startup and shutdown ramp rates.

5.2.5. Reserve Requirements Constraint

Reserve is a specification that allows a system operator to face unexpected situations and failure events; this specification is incorporated through the variable SR in the constraint of Equation (5.2.10):

$$\sum_{n=1}^{N} P_n^{t,max} U_{n,m}^{t} - \sum_{n=1}^{N} P_{n,m}^{t} U_{n,m}^{t} \geq (SR)L^{t}, \qquad U_{n,m}^{t} = 1 \tag{5.2.10}$$

where L^t is the value of load demand at time t, and $P_n^{t,max}$ is maximum power that could be generated taking into account the effects of the ramp constraints.

5.2.6. Power Balance

This constraint guarantees the balance between total power production and its consumption. This idea is mathematically expressed in Equation (5.2.11):

$$\sum_{n=1}^{N} P_{n,m}^{t} U_{n,m}^{t} + W_{m}^{t} = L^{t}, \qquad U_{n,m}^{t} = 1 \tag{5.2.11}$$

Note that the wind power generation is assumed to be completely integrated.

5.2.7. Minimum Up/Down Time Constraint

Another important limitation of the generators used for electricity generation is that they have to be online for at least a determined number of hours. Generation units, however, have to be offline for at least another determined number of hours. These required times are known as minimum up time (MUT_n) and minimum down time (MDT_n) of generator n. These constraints are presented in Equation (5.2.12) and Equation (5.2.13):

$$ON_{n,m}^{t} \geq MUT_n \tag{5.2.12}$$

$$OFF_{n,m}^{t} \geq MDT_n \tag{5.2.13}$$

5.3. Priority List Method to the Unit Scheduling

Among the methodologies developed to solve the UC problem, MILP has been generally accepted due to the fact that, in a determined number of steps, it is able to find solutions that are guaranteed to converge to the global-optimal solution [209]. However, recent studies have found that, under high integration of renewable resources, and consequently low values of net load, the MILP method has difficulty finding a feasible solution in a reasonable computational time [210].

PL is a methodology for solving the UC problem which is able to give a near-optimal solution in a reduced computational time. This method has undergone important developments. In [211] a stochastic PL method was introduced. In this approach, generators are committed according to a determined PDF that depends on the characteristics of the system under analysis. In [212] the PL method has been adapted to the management of power systems with ESS. In [213] the PL method was adapted to the management of power systems with ESS. In [214] the combination of an improved PL and an augmented Hopfield Lagrange (AHL) neural network was proposed. In [214] improved pre-prepared power demand (IPPD) was combined with the Muller method. In [215] a combination of improved Lagrangian relaxation (ILR) and ALH embedded in the PL method was proposed.

The PL method is composed of several processes that jointly arrive at a feasible and cost-effective solution to the UC problem. The processes involved are primary unit scheduling, minimum up/down time repair, spinning reserve repair, shutdown repair, unit substitution, and shutdown excess of power generation. All these processes are detailed in the next sub-sections.

5.3.1. Primary Unit Scheduling

The order in which each generator is committed depends on its average production cost (G_n) which is defined according to Equation (5.3.1) and Equation (5.3.2) [213]:

$$G_n = \frac{a_n + b_n q_n + c_n (q_n)^2}{q_n} \tag{5.3.1}$$

$$q_n = \frac{P_n^{max}}{2}\left(1 + \frac{P_n^{min}}{P_n^{max}}\right) \tag{5.3.2}$$

where q_n is the average power production of generator n. The procedure for developing a primary approximation to the solution is as follow:

- Step 1: Create the matrix of primary unit scheduling $\left(PUS_{n,m}^t\right)$. Set $PUS_{n,m}^t = 0$ for $n = 1, 2, \dots, N$ and $t = 1, 2, \dots, H$;
- Step 2: Using the values obtained from Equation (5.3.1) and Equation (5.3.2), build the priority list.
- Step 3: Set $t \leftarrow 1$;
- Step 4: Select the first generator of the priority list built in Step 2, i.e., set $n \leftarrow 1$.
- Step 5: Set $PUS_{n,m}^t \leftarrow 1$;
- Step 6: If the committed capacity is not enough to fulfill the reserve requirements and $n \leq N$, set $n \leftarrow n + 1$ and go back to Step 5, else if $t \leq H$ set $t \leftarrow t + 1$ and go to Step 4; else stop.

5.3.2. Minimum Up/Down Time Repairing

The solution obtained from primary unit scheduling should fulfill minimum up/down time constraints. To solve this problem an additional process is applied. An example of the repair process is shown in Figure 5.2 where the first approximation resulting from primary scheduling (mathematically modeled by the matrix $PUS_{n,m}^t$) is repaired by committing generator n to two additional hours to fulfill the condition $MUT_n = 3$.

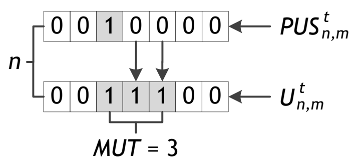

Figure 5.2. Repairing process of minimum up time constraint.

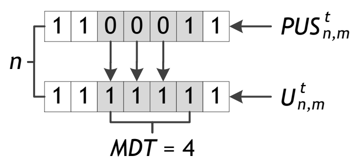

Figure 5.3. Repairing process of minimum down time constraint.

Figure 5.3 shows the repairing process for the situation in which minimum down time constraint is violated, and the repair algorithm commits generator n during three hours in order to fulfill the condition $MDT_n = 4$. The algorithm to the minimum up/down time constraint presented in [213] has been used in this work; this algorithm consists of the next steps:

- Step 1: Using the results of primary unit scheduling, calculate $ON_{n,m}^{t}$ and $OFF_{n,m}^{t}$ matrices according to Equation (5.2.3) and Equation (5.2.4). Then, create the matrix scheduling for each scenario $U_{n,m}^{t}$ and set it to $U_{n,m}^{t} = 0$.
- Step 2: Set $t \leftarrow 1$;
- Step 3: Set $n \leftarrow 1$;
- Step 4: If $\left(PUS_{n,m}^{t} = 0\right)$ and $\left(PUS_{n,m}^{t-1} = 1\right)$ and $\left(ON_{n,m}^{t-1} < MUT_n\right)$, set $U_{n,m}^{t} \leftarrow 1$;
- Step 5: If $\left(PUS_{n,m}^{t} = 0\right)$ and $\left(PUS_{n,m}^{t-1} = 1\right)$ and $(t + MDT_n - 1 \leq H)$ and $\left(OFF_{n,m}^{t+MDT_n-1} < MDT_n\right)$, set $U_{n,m}^{t} \leftarrow 1$;
- Step 6: If $\left(PUS_{n,m}^{t} = 0\right)$ and $\left(PUS_{n,m}^{t-1} = 1\right)$ and $(t + MDT_n - 1 > H)$ and $\left(\sum_{j=t}^{H} PUS_{n,m}^{j} > 0\right)$, set $U_{n,m}^{t} \leftarrow 1$;
- Step 7: Calculate the elements of the matrices $ON_{n,m}^{t}$ and $OFF_{n,m}^{t}$ that correspond to generator n using Equation (5.2.3) and Equation (5.2.4);
- Step 8: If $n < N$, set $n \leftarrow n + 1$ and go back to Step 4;
- Step 9: If $t < H$, set $t \leftarrow t + 1$ and go back to Step 3, else stop.

5.3.3. Spinning Reserve Repairing

The total generation capacity of the system could be considerably reduced by the incorporation of operating ramp rate constraints and startup and shutdown ramp rate constraints; as a consequence, these limitations reduce the spinning reserve estimated previously in the primary unit scheduling process. To deal with this problem, using the results obtained from the primary unit scheduling and minimum up/down time repairing processes, more generation capacity is committed following the next algorithm:

- Step 1: For each time instant $(t = 1, 2, \ldots, H)$ the reserve requirements are checked by using Equation (5.2.9);
- Step 2: Then, those hours at which spinning reserve requirements are insufficient are determined. These hours (in combination with the priority list) are used to determine those points (n, t in $U_{n,m}^{t}$) at which generation capacity should be added. All these points are saved in a list of two columns; the first column saves the generators, while the second column saves the time intervals;
- Step 3: If the list created in Step 2 is not empty, go to Step 4, in other case stop;
- Step 4: Then, the list developed in Step 2 is sorted according to its second column in ascending order;

- Step 5: In this step, the first point of the sorted list developed in Step 4 is selected; the status of the generator n at hour t corresponding to this point is changed from 0 to 1;
- Step 6: Apply minimum up/down time repairing in order to avoid the violation of these constraints;
- Step 7: Go to Step 1.

5.3.4. Shutdown Repairing Process

In order to fulfill the shutdown ramp rate constraint, it is likely that additional hours are required so that generator n may have enough time to be effectively de-committed. In order to overcome this situation, those generators in problems are committed during more time in order to get the adequate level of generation. This is done following the next algorithm:

- Step 1: For each generator $(n = 1, 2,..., N)$ and time interval $(t = 1, 2,..., H)$, the shutdown ramp rate constraint is checked by application of Equation (5.2.8);
- Step 2: Then, a list of all those points at which this constraint is violated is created. All those hours at which the operation of the corresponding generators should be extended are saved in a list of two columns; the first column saves the generators, while the second column saves the time intervals;
- Step 3: If the list created in Step 2 is not empty, go to Step 4, in other case stop;
- Step 4: Then, the list created in Step 2 is sorted according to its second column in ascending order;
- Step 5: In this step, the first point of the sorted list developed in Step 4 is selected; the status of the generator n at hour t corresponding to this point is changed from 0 to 1;
- Step 6: Apply minimum up/down time repairing in order to avoid the violation of these constraints;
- Step 7: Go to Step 1.

5.3.5. Unit Substitution Process

After the minimum up/down time repair process has been carried out, some generators are committed during more hours than required. This situation is illustrated in Figure 5.2, where generator n is required during only one hour; however, due to the minimum up-time constraint it is committed during three hours. In order to achieve cost-effective scheduling, this generator with $MUT_n = 3$ is substituted by another one with a lower MUT_n.

To recognize the generators under this situation, i.e., generators to be substituted, a matrix $(CH_{n,m}^t)$ that store the changes in the primary scheduling due to minimum up/down time repair is created. This matrix is obtained by the subtraction of the matrices $U_{n,m}^t$ and $PUS_{n,m}^t$. The matrix $D_{n,m}^t$ is created to save the generators and the times at which they are going to be substituted. The elements of this matrix are binary so that $D_{n,m}^t = 1$ means that generator n should be substituted at hour t, while the contrary situation is represented by using $D_{n,m}^t = 0$.

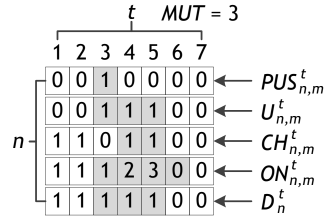

Figure 5.4. Selection of generators in unit substitution process.

Figure 5.4 extends the example previously described in Figure 5.2. In Figure 5.4, the row of generator n of the matrices $PUS_{n,m}^{t}$, $U_{n,m}^{t}$, $CH_{n,m}^{t}$, $ON_{n,m}^{t}$, and $D_{n,m}^{t}$ between $t = 1$ and $t = 7$ are shown. From the analysis of this figure, the reader can note that in $t = 3$, the matrix element $CH_{n,m}^{3} = 0$; this means that during the initial moment any change in the scheduling can be found. Otherwise, $ON_{n,m}^{3} = 1$ and $ON_{n,m}^{6} = 0$, which means that effectively generator n is committed only during its MUT_n, and $\sum_{t}^{6} CH_{n,m}^{t} = 2 > 0$, which means that there is a change in the scheduling due to minimum up/down time repair. As was stated before, $D_{n,m}^{t}$ indicates the generators and times to be used in the unit substitution process so that, for the example, the elements of $D_{n,m}^{t}$ become 1 between $t = 3$ and $t = 5$. From the analysis of this situation, an algorithm to recognize the generators that could be substituted and their corresponding times is presented as follows:

- Step 1: Estimate the matrix $CH_{n,m}^{t}$ as the subtraction between $U_{n,m}^{t}$ and $PUS_{n,m}^{t}$;
- Step 2: Create and initialize the matrix $D_{n,m}^{t}$ by assigning $D_{n,m}^{t} = 0$ for $n = 1, 2, \ldots, N$ and $t = 1, 2, \ldots, H$;
- Step 3: Set $n \leftarrow 1$;
- Step 4: Set $t \leftarrow 1$;
- Step 5: If $\left(CH_{n,m}^{t} = 0\right)$ and $\left(ON_{n,m}^{t} = 1\right)$ and $(t + MUT_n < H)$ and $\left(ON_{n,m}^{t+MUT_n} = 0\right)$ and $(MUT_n > 1)$ and $\left(\sum_{t}^{t+MUT_n-1} CH_{n,m}^{t} > 0\right)$, the elements of $D_{n,m}^{t}$ from t to $t + MUT_n - 1$ become 1. Else if $\left(CH_{n,m}^{t} = 0\right)$ and $\left(ON_{n,m}^{t} = 1\right)$ and $(t + MUT_n - 1 = H)$ and $\left(ON_{n,m}^{t+MUT_n-1} = MUT_n\right)$ and $(MUT_n > 1)$ and $\left(\sum_{t}^{t+MUT_n-1} CH_{n,m}^{t} > 0\right)$, the elements of $D_{n,m}^{t}$ from t to $t + MUT_n - 1$ become 1; else go to Step 6;
- Step 6: If $t < H$, set $t \leftarrow t + 1$ and go to Step 5; else go to Step 7;
- Step 7: If $n < N$, set $n \leftarrow n + 1$ and go to Step 4, else stop.

Once the matrix $D_{n,m}^{t}$ has been created, the generators to be substituted can be easily recognized. Considering each of these generators one by one, all processes described in the previous sections are then repeated. If the substitution of a determined generator leads to an increment in the generation cost, the unit substitution process is stopped.

5.3.6. Shutdown Excess of Generation

Minimum up/down time repair and spinning reserve repair could lead to an excess of spinning reserve in some hours, which increases the generation costs.

In order to achieve cost-effective unit scheduling, shutdown of excess of generation is carried out following the next algorithm:

- Step 1: Using Equation (5.2.9), the excess of spinning reserve is checked over the entire horizon scheduling and a list is created by saving the corresponding hours. This list is assumed to have R elements;
- Step 2: Set $r \leftarrow 1$;
- Step 3: The point r of the list created in Step 1 is chosen. To this hour the most expensive generator is selected. Then, if $ON_{n,m}^{t}$ is higher than the corresponding MUT_n, the status of this generator is changed from 1 to 0;
- Step 4: Using the scheduling obtained in the Step 3, minimum up/down time repairing is carried out in order to get a feasible solution;
- Step 5: Using the scheduling obtained in the Step 4, startup/shutdown ramp rate constraints and spinning reserve requirements are checked by using Equation (5.2.8) and Equation (5.2.9), respectively. If both of these constraints are not violated, the element $U_{n,m}^{t}$ becomes 0, in other case it becomes 1;
- Step 6: If $(r < R)$, set $r \leftarrow r + 1$ and go back to Step 3, else stop.

5.4. Proposed Approach

The proposed approach consists of building the PDF of the situation at which a determined generator (n) be committed or not at a determined time (t). Those generators and hours (n, t in $U_{n,m}^{t}$) with a high probability of being committed are then selected. However, the scheduling obtained from this procedure could be unfeasible due to the violation of minimum up/down time constraints, so that this solution is repaired by means of the corresponding process. The methodology proposed in this paper to the solution of the stochastic UC problem is implemented by following the next algorithm:

- Step 1: In this step M scenarios of wind power production and load demand are built following the methodology presented in Section 5.1;
- Step 2: Solve UC problem for each scenario (m) using the mathematical formulation presented in Section 5.2 and the PL method described in Section 5.3;
- Step 3: Estimate histogram of frequency of unit scheduling $\left(HF_{n,m}^{t}\right)$ and its corresponding PDF (PDF_{n}^{t}) using Equation (5.4.1) and Equation (5.4.2). The matrices $HF_{n,m}^{t}$ and PDF_{n}^{t} have the same dimensions of matrix $U_{n,m}^{t}$;

$$HF_{n}^{t} = \sum_{m=1}^{M} U_{n,m}^{t}, \qquad t = 1, 2, \dots, H \tag{5.4.1}$$

$$PDF_{n}^{t} = \frac{HF_{n}^{t}}{M} \tag{5.4.2}$$

- Step 4: Create the probabilistic primary scheduling, which is a matrix ($PPUS_n^t$) with N rows and H columns. Set all elements of this matrix to zero ($PPUS_n^t = 0,\ n = 1,\ 2, \dots, N$ and $t = 1, 2, \dots, H$). Then, according to a determined significance level (α), those generators and hours so that $PDF_n^t > \alpha$ are chosen and their status is changed from 0 to 1.
- Step 5: Solution obtained in Step 4 ($PPUS_n^t$) could be infeasible due to the violation of minimum up/down time constraint. For this reason minimum up/down time repairing is carried out, obtaining the solution to the stochastic UC problem U_n^t. (Note that variable $U_{n,m}^t$ represents the deterministic solution of UC problem for the scenario m, while U_n^t represents the scheduling suggested to solve stochastic UC problem taking into account all scenarios previously generated).

5.5. Case Study and Results

The proposed approach to the solution of the UC problem, incorporating the uncertainty related to wind power generation, is illustrated by analyzing the power system whose characteristics are presented in Table 5.1 and Table 5.2, while Table 5.3 presents hourly load and wind power forecasting, as described in [204], [209], and [212]. In our illustrative case study, spinning reserve requirements of 10% ($SR = 0.1$) have been considered in order to guarantee the power system's reliability against any failure event. Results from the scenario generation and reduction process described in Section 5.1 are shown in Figure 5.5. Initially, 2000 scenarios were randomly generated. Thus, considering a forecasting error of 20%, $\alpha = 0.05$ and $\beta = 0.05$, 250 scenarios were used in the optimization process ($M = 250$) obtained from the application of the *k*-means clustering algorithm. Table 5.4 shows the probability of obtaining a spinning reserve higher than 10% for the entire horizon scheduling. It could be noted that except for $t = 12$ (which was discussed before), the probability of fulfilling this constraint is higher than 95%. Table 5.5 presents PDF of unit scheduling (PDF_n^t) for the case under analysis, while Table 5.6 presents the average power production of each generator along the horizon of scheduling. In Table 5.5, the probability that corresponds to the selected scheduling is in bold, which are those generators and hours with probabilities higher than $\alpha = 0.05$. Note how those generators that are in base and cycling condition are committed in all the scenarios and consequently the probability of them being committed is equal to 1. Moreover, peak units have a probability lower than 1 according to the requirements for supplied sudden changes in wind power generation.

These results could be understood as those decision variables that correspond to stages 1 and 2 in the stochastic programming framework, i.e., the generators with probabilities equal to 1 could be understood as those generators to be committed before the uncertainty is realized, while those generators with probabilities lower than 1 could be understood as those generators for which the decision to commit is taken in stage 2 (fast start generators). From these results, it is possible to observe how the proposed approach offers a probabilistic perspective of the role of each generation unit in the solution of the stochastic UC problem.

Table 5.1. Description of the power system under analysis (part 1).

n	P_n^{min} (MW)	P_n^{max} (MW)	a_i ($/h)	b_i ($/MWh)	c_i ($/MW^{2}h)	DR (MW/h)	UR (MW/h)
1	150	455	1000	16.19	0.00048	130	130
2	150	455	970	17.26	0.00031	130	130
3	25	162	450	19.70	0.00398	90	90
4	20	130	680	16.50	0.00211	60	60
5	20	130	700	16.60	0.00200	60	60
6	20	80	370	22.26	0.00712	40	40
7	20	80	370	22.26	0.00712	40	40
8	25	85	480	27.74	0.00079	40	40
9	25	85	480	27.74	0.00079	40	40
10	10	55	660	25.92	0.00413	40	40

Table 5.2. Description of the power system under analysis (part 2).

n	P_0 (MW)	IS (h)	MUT_n (h)	MDT_n (h)	CSC ($)	HSC ($)	CST (h)
1	455	8	8	8	9000	4500	5
2	163	8	8	8	10000	5000	5
3	0	-6	6	6	1800	900	4
4	0	-5	5	5	1120	560	4
5	0	-3	5	5	1100	550	4
6	0	-3	3	3	340	170	2
7	0	-3	3	3	340	170	2
8	0	-3	3	3	520	260	2
9	0	-3	3	3	520	260	2
10	0	-1	1	1	60	30	0

Table 5.3. Load demand and wind power forecasting.

Time (h)	Wind (MW)	Load (MW)	Time (h)	Wind (MW)	Load (MW)
1	93	700	13	60	1400
2	107	750	14	115	1300
3	100	850	15	68	1200
4	100	950	16	70	1050
5	117	1000	17	117	1000
6	103	1100	18	135	1100
7	108	1150	19	110	1200
8	80	1200	20	121	1400
9	60	1300	21	123	1300
10	57	1400	22	110	1100
11	78	1450	23	88	900
12	72	1500	24	47	800

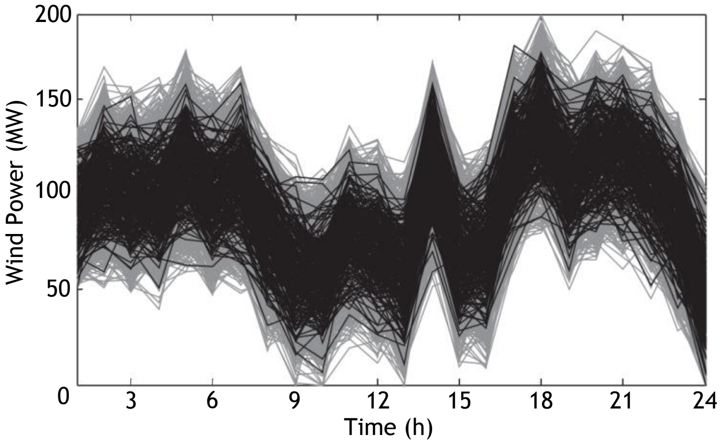

Figure 5.5. Results from de scenario generation and reduction process.

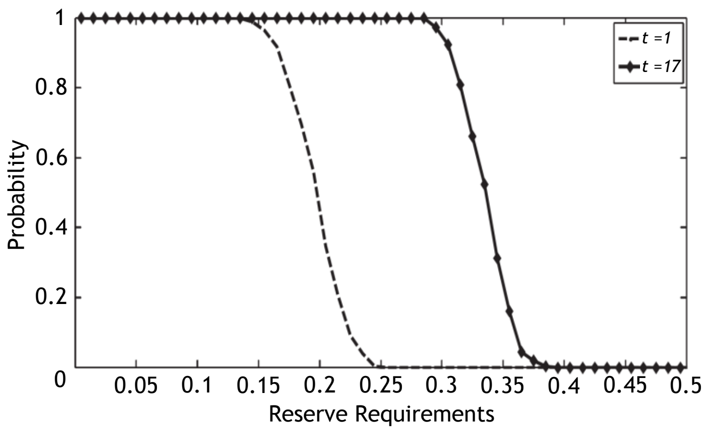

Figure 5.6. CDF of supply reserve requirements for $t = 1$ and $t = 17$.

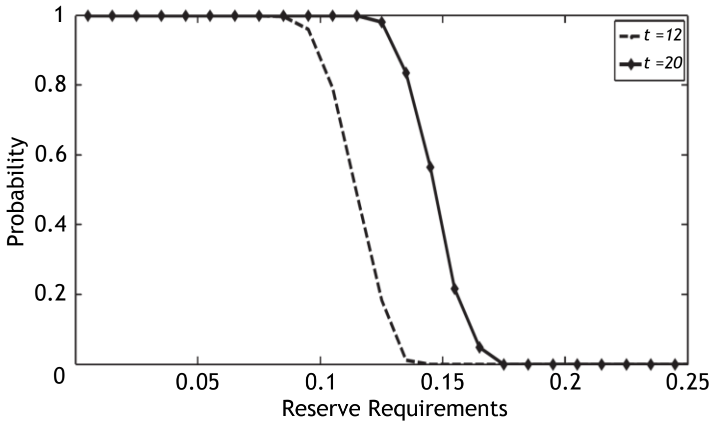

Figure 5.7. CDF of supply reserve requirements for $t = 12$ and $t = 20$.

Moreover, the expected value of generation cost is $525,220.604. This value is higher than that obtained by evaluation of the scheduling suggested in [204], i.e. $516,115.05. It is important to take into account that the mathematical formulation used here to check and measure the reserve requirements is different from that used in [204]; the formulation used in [204] is expressed in terms of P_n^{max}, while the expression used in this work was carried out in terms of maximum power generation considering the ramp rate constraints (see Equation(5.2.9)), which requires more generation capacity and consequently higher generation costs.

Figure 5.6 presents the CDF for fulfilling the spinning reserve requirements for $t = 1$ and $t = 17$, which correspond to the situation of low load. For these hours, the specified spinning reserve requirements are guaranteed. On the other hand, Figure 5.7 shows the CDF for $t = 12$ and $t = 20$, each of which corresponds to the hours of high energy demand. For $t = 12$, all the generation capacity of the system has been committed, but the required reserve requirements cannot be totally guaranteed due to the effects of ramp rate constraints. This result shows the negative effects of the ramp rate constraints on the accommodation of wind power generation. However, for $t = 20$ the committed specified reserve level can be guaranteed.

The proposed approach was implemented in MATLAB programming language. The computer used has an i7-3630QM CPU at 2.40GHz with 8GB of memory and 64-bit operating system. The computational time required to solve this illustrative example was 1403 seconds.

Table 5.4. Probability of supply the required reserve.

Time (h)	$P_r\ \{SR \geq 0.1\}$	Time (h)	$P_r\ \{SR \geq 0.1\}$
1	1.000	13	0.974
2	1.000	14	1.000
3	0.954	15	0.954
4	1.000	16	1.000
5	1.000	17	1.000
6	1.000	18	0.986
7	1.000	19	0.956
8	1.000	20	1.000
9	0.960	21	1.000
10	0.956	22	1.000
11	0.960	23	1.000
12	0.876	24	1.000

Table 5.5. PDF of unit scheduling.

n	Time (h)																							
	1	2	3	4	5	6	7	8	9	10	11	12	13	14	15	16	17	18	19	20	21	22	23	24
1	**1.00**	**1.00**	**1.00**	**1.00**	**1.00**	**1.00**	**1.00**	**1.00**	**1.00**	**1.00**	**1.00**	**1.00**	**1.00**	**1.00**	**1.00**	**1.00**	**1.00**	**1.00**	**1.00**	**1.00**	**1.00**	**1.00**	**1.00**	**1.00**
2	**1.00**	**1.00**	**1.00**	**1.00**	**1.00**	**1.00**	**1.00**	**1.00**	**1.00**	**1.00**	**1.00**	**1.00**	**1.00**	**1.00**	**1.00**	**1.00**	**1.00**	**1.00**	**1.00**	**1.00**	**1.00**	**1.00**	**1.00**	**1.00**
3	0	**0.06**	**1.00**	**1.00**	**1.00**	**1.00**	**1.00**	**1.00**	**1.00**	**1.00**	**1.00**	**1.00**	**1.00**	**1.00**	**1.00**	**1.00**	**1.00**	**1.00**	**1.00**	**1.00**	**1.00**	**1.00**	**0.30**	0
4	0	0	0	**0.08**	**0.08**	**1.00**	**1.00**	**1.00**	**1.00**	**1.00**	**1.00**	**1.00**	**1.00**	**1.00**	**1.00**	**1.00**	**1.00**	**1.00**	**1.00**	**1.00**	**1.00**	**0.98**	0	0
5	0	0	0	0	0	**0.56**	**0.68**	**1.00**	**1.00**	**1.00**	**1.00**	**1.00**	**1.00**	**1.00**	**1.00**	**1.00**	**1.00**	**1.00**	**1.00**	**1.00**	**1.00**	**0.24**	0	0
6	0	0	0	0	0	0	0	**0.15**	**1.00**	**1.00**	**1.00**	**1.00**	**1.00**	**0.20**	0.01	0	0	0	**0.94**	**0.98**	**0.98**	0.04	0	0
7	0	0	0	0	0	0	0	0	**0.92**	**1.00**	**1.00**	**1.00**	**1.00**	0	0	0	0	0	0	0.01	0.01	0.01	0	0
8	0	0	0	0	0	0	0	0	0.01	**1.00**	**1.00**	**1.00**	**0.89**	0	0	0	0	0	0.01	**0.99**	**0.05**	0	0	0
9	0	0	0	0	0	0	0	0	0	**0.88**	**0.67**	**1.00**	0.02	0	0	0	0	0	0	**0.95**	0	0	0	0
10	0	0	0	0	0	0	0	0	0	0.01	0	**0.91**	0	0	0	0	0	0	0	**0.10**	0	0	0	0

Table 5.6. Average power production results (MW).

n	Time (h)																							
	1	2	3	4	5	6	7	8	9	10	11	12	13	14	15	16	17	18	19	20	21	22	23	24
1	449.8	453.2	455.0	455.0	455.0	455.0	455.0	455.0	455.0	455.0	455.0	455.0	455.0	455.0	455.0	455.0	455.0	455.0	455.0	455.0	455.0	455.0	455.0	455.0
2	157.2	165.6	269.3	291.1	275.3	308.6	303.2	360.1	447.7	455.0	455.0	455.0	455.0	417.5	391.7	262.1	154.9	225.3	329.5	450.1	407.7	351.3	331.7	297.5
3	0	25.0	25.3	25.0	25.0	25.0	25.0	25.0	32.1	106.2	135.7	161.4	114.8	32.0	25.0	25.0	25.0	25.0	25.4	63.6	25.0	25.0	25.0	0
4	0	0	0	80.0	130.0	130.0	130.0	130.0	130.0	130.0	130.0	130.0	130.0	130.0	130.0	125.8	128.5	130.0	130.0	130.0	130.0	80.0	0	0
5	0	0	0	0	0	80.0	130.0	130.0	130.0	130.0	130.0	130.0	130.0	130.0	130.0	111.5	119.6	130.0	130.0	130.0	130.0	80.0	0	0
6	0	0	0	0	0	0	0	20.0	20.0	21.1	20.4	40.7	20.2	20.0	0	0	0	0	20.0	20.0	20.0	0	0	0
7	0	0	0	0	0	0	0	0	25.0	25.0	25.0	25.0	25.0	0	0	0	0	0	0	0	0	0	0	0
8	0	0	0	0	0	0	0	0	0	10.0	10.0	11.0	10.0	0	0	0	0	0	0	10.0	10.0	0	0	0
9	0	0	0	0	0	0	0	0	0	10.0	10.0	10.0	0	0	0	0	0	0	0	10.0	0	0	0	0
10	0	0	0	0	0	0	0	0	0	0	0	10.0	0	0	0	0	0	0	0	10.0	0	0	0	0

Chapter 6

Control Strategy with Energy Storage System

Nowadays, the optimal management and control of ESS is an important topic that has been widely analyzed in the technical literature. From a global perspective, the potential for the installation of ESS based on batteries in isolated power systems is estimated at 5300MWh in the next few years [160]. In this thesis, a new control strategy to be used in the weekly scheduling of insular power systems with ESS is presented. The methodology described here incorporates the effects of the most relevant components such as thermal generators, wind power generation, power converter, charge controller and an ESS based on batteries, namely Vanadium Redox batteries (VRB). The joint effect of these elements in the scheduling process of insular power systems has not been considered properly, so the development of new control strategies incorporating this feature is of the utmost importance. The proposed methodology consists of two major steps. In the first step the UC problem is solved without taking into account ESS; from this procedure the total energy available to charge ESS is estimated, while in the second step, using the estimated energy available obtained in the first step, the ESS is incorporated into the UC problem.

6.1. Power System under Analysis

The structure of the insular power system with the ESS to be analyzed is presented in Figure 6.1. The system consists of several thermal generators that could be steam turbines, combined-cycle gas turbines, diesel engines, or open-cycle gas turbines. These units could be powered by different types of fuel oils (heavy fuel oil (HFO) and light fuel oil (LFO)). Another important component of this type of system is renewable energy sources, which in this case study is considered to be obtained from the wind.

The ESS is composed of the power converter, the charge controller, and the storage system itself, which, as stated before, is assumed to be a VRB system. A VRB allows the storage of the excess of electricity generated by thermal and renewable units. A charge controller guarantees the correct use of the VRB, to prevent its overcharging or undercharging, and the power converter carried out the DC-to-AC conversion, and vice versa. Furthermore, under a high penetration of renewable sources it is possible to produce an excess of electricity that could not be stored in a VRB. In order to preserve system stability, this excess of energy has to be consumed by the dump load. In the next subsections, each element of the insular power system is described in detail.

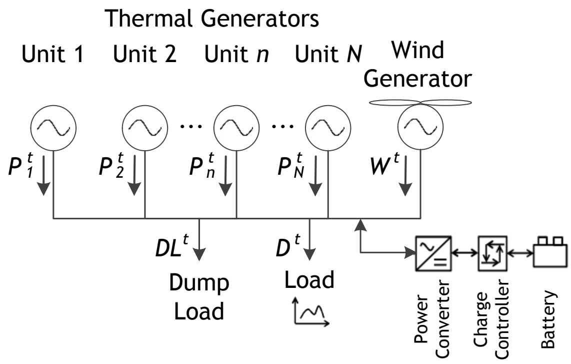

Figure 6.1. Architecture CDF of the power system under analysis.

6.1.1. Thermal and Renewable Generation Units

In the framework of the UC problem, thermal generation units are modeled through their estimated fuel consumption, starting-up cost, power generation limits, startup and shutdown ramp rates, operating ramp rates, and minimum up/down time constraints. Typically, fuel consumption is modeled by using the quadratic expression of Equation (6.1.1):

$$f_n^t = a_n + b_n P_n^t + c_n (P_n^t)^2 \tag{6.1.1}$$

where a_n, b_n and c_n are parameters related to the fuel consumption of the unit n, f_n^t is the fuel consumption of unit n, and P_n^t is the power generation of unit n at time t $(n = 1, 2, \ldots, N)$ and $(t = 1, 2, \ldots, H)$. The cost related to the start-up of a determined generator could be modeled by using the simplified expression of Equation (6.1.2):

$$SUC_n^t = \begin{cases} HSU_n; \; T_{off,n}^t \leq MDT_n + CST_n \\ CSU_n; \; T_{off,n}^t > MDT_n + CST_n \end{cases} \tag{6.1.2}$$

where SUC_n^t is the starting-up cost, HSU_n^t is the hot startup cost, and CSU_n^t is the cold startup cost of unit n at time t. Variables $T_{on,n}^t$ and $T_{off,n}^t$ are calculated by Equation (6.1.3) and Equation (6.1.4):

$$T_{on,n}^t = \begin{cases} T_{on,n}^t + 1, & U_n^t = 1 \\ 0, & U_n^t = 0 \end{cases} \tag{6.1.3}$$

$$T_{off,n}^t = \begin{cases} T_{off,n}^t + 1, & U_n^t = 0 \\ 0, & U_n^t = 1 \end{cases} \tag{6.1.4}$$

where $T_{on,n}^t$ is the cumulative number of hours until the present instant t that unit n has been online, and $T_{off,n}^t$ is the cumulative number of hours until the present instant t that unit n has been offline. MUT_n and MDT_n are minimum up and down time of unit n, respectively. U_n^t is the status of unit n at time t, where 0 represents de-committing, while 1 represents the committing of the respective unit. In each time-step, power production of a determined unit is constrained by the maximum and minimum capacity of the unit and its corresponding ramp constraint. This is mathematically expressed through Equations (6.1.5) - (6.1.7).

$$P_n^{min} \leq P_n^t \leq P_n^{max}, \qquad U_n^t = 1 \tag{6.1.5}$$

$$P_n^t - P_n^{t-1} \leq UR_n, \qquad U_n^t = 1;\; U_n^{t-1} = 1 \tag{6.1.6}$$

$$P_n^{t-1} - P_n^t \leq DR_n, \qquad U_n^t = 1;\; U_n^{t-1} = 1 \tag{6.1.7}$$

where P_n^{min}, and P_n^{max} are the minimum and maximum power production of unit n, respectively. Meanwhile, UR_n and DR_n are ramp up and down of unit n, respectively. The ramp constraints during starting up and shutting down of a determined unit are represented by using the constraints of Equation (6.1.8) and Equation (6.1.9):

$$P_n^t \leq SUR_n + P_n^{min}, \qquad U_n^t = 1;\; U_i^{t-1} = 0 \tag{6.1.8}$$

$$P_n^t \leq SDR_n + P_n^{min}, \qquad U_n^t = 1\; U_n^{t+1} = 0 \tag{6.1.9}$$

where SUR_n and SDR_n are startup ramp and shutdown ramp of unit n, respectively. Typically, thermal units have to be online or offline during a determined time length; this restriction is incorporated by using Equation (6.1.10) and Equation (6.1.11):

$$T_{on,n}^t \geq MUT_n \tag{6.1.10}$$

$$T_{off,n}^t \geq MDT_n. \tag{6.1.11}$$

Wind power generation is modelled as in in Equation (6.1.12), where the maximum capacity is defined by the available wind power obtained from the forecasting process:

$$0 \leq W^t \leq W_{max}^t \tag{6.1.12}$$

where W^t is the wind power production determined from the optimization process and W_m^t is the forecasted wind power production.

6.1.2. Power Converter

The connection between the ESS and the power grid of the insular system is carried out using electronic power converters. The technology of this connection device can be divided into three different categories: standard, multilevel, and multiport topologies. The standard topology is divided into single-stage and double-stage. Single-stage is the simplest topology, which consists of a bidirectional DC/AC converter, while double-stage consists of a DC/DC stage and a DC/AC stage. The DC/DC stage adjusts the DC voltage to a reasonable level, so that the DC/AC stage can be connected directly to the distribution system. Multilevel topology allows the required AC voltage to be obtained from several levels of DC voltages. On the other hand, multiport topology is provided with a single-stage with multiple ports, which can interface the ESS with the grid in a reduced number of stages, improving the efficiency with a reduced cost and a simple control strategy [216].

In a general sense, the efficiency of the DC/AC conversion process depends on the load to be supplied, DC voltage, and temperature [217]. The model used in this work estimates the efficiency of the power converter by means of Equation (6.1.13) [218]:

$$\eta_v = \frac{P_v}{m_0 P_v^{rated} + (1 + m_1) P_v} \tag{6.1.13}$$

where η_v is the efficiency of the power converter, P_v^{rated} is the rated power of the inverter P_v is the power through the inverter, and m_0 and m_1 are parameters to be determined by using experimental information; the values assumed here are $m_0 = 0.0119$ and $m_1 = 0.0155$.

6.1.3. Vanadium Redox Battery and Charge Controller Model

In VRB storage technology, energy and power are independent of each other, giving more flexibility to improve power system operation. The rated power is determined by the capacity of the VRB stack, while the total energy to be stored is determined by the amount of electrolyte. Hence, state-of-charge (SOC) can be determined with precision by means of the amount of electrolyte remaining. Another important feature is its fast response due to the speed of the chemical reaction [219], [220]. VRB is important to improve the operation of an isolated system as well as grid-connected systems with high penetration of renewable energy sources [221]. In this work, the SOC of VRB is estimated by Equation (6.1.14):

$$SOC_t = SOC_{t-1} + \frac{P_{bt}^t \Delta t}{E_{max}} \eta_b F_c \tag{6.1.14}$$

where SOC_t is the state-of-charge of VRB at time t, P_{bt}^t is the power to charge or discharge VRB, positive for charge and negative during discharge, E_{max} is the maximum energy to be stored on VRB, Δt is the time-step of the simulation, η_b is the efficiency of VRB, and F_c is the control factor; this factor represents the actions carried out by the charge controller during the charge process. Mathematical definition of factor F_c is presented in Equation (6.1.15):

$$F_c = \begin{cases} max\left(1 - e^{\left[\left(\frac{m_2}{\frac{P_{bt}^t}{P_{max}} + m_3}\right)(SOC_t - SOC_{max})\right]}, 0\right), & P_{bt}^t > 0 \\ 1, & P_{bt}^t < 0 \end{cases} \tag{6.1.15}$$

where P_{max} is the rated power of VRB stack, m_2 and m_3 are parameters to define how the charge controller manages the charge process. In this work, considering some experience from lead acid batteries, these parameters were fixed to $m_2 = 20.73$ and $m_3 = 0.55$ [222]. SOC_{min} and SOC_{max} are the minimum and maximum SOC allowed to be reached by the VRB. Typically, according to the suggestions of the manufacturers in this study $SOC_{max} = 0.9$. In order to illustrate the operation of the charge controller, the charging process of a VRB of 7kW/40kWh was simulated. SOC_{min} and SOC_{max} are assumed to be 0.2 and 0.9, respectively, while the charge and discharge efficiencies (η_b) were assumed to be 0.8.

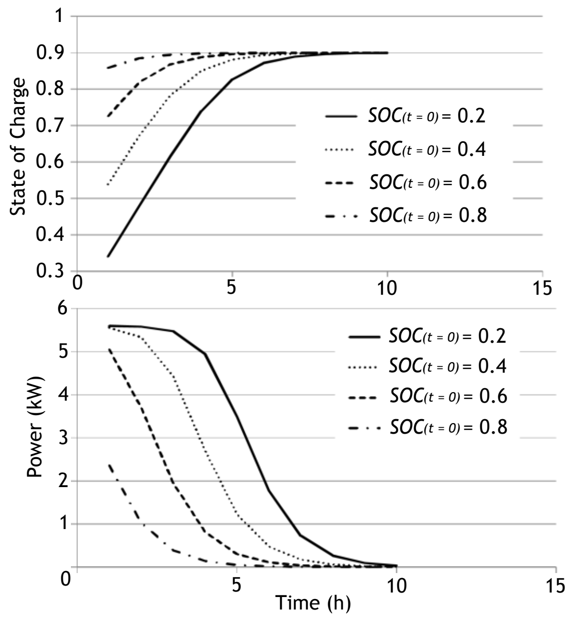

Figure 6.2. SOC and charging power simulation.

The charge process was simulated considering different initial SOC between 0.2 and 0.8. The results from the simulations are presented in Figure 6.2. The proposed model described in Equation (6.1.14) and Equation (6.1.15) was used to estimate the power required from the grid to charge the VRB, considering the effects of the charge controller. It is possible to observe how the charge controller gradually reduces the power absorbed from the grid as the VRB reaches its maximum SOC. This explains the role of the term F_c introduced in Equation (6.1.15).

6.2. Unit Commitment Problem Incorporating Energy Storage System

The proposed methodology consists of two main steps: in the first step, the excess of power generation and the curtailed wind power are estimated from the solution of the UC problem, without taking the ESS into account; then, in the second step, the management of the ESS is carried out considering the excess of energy generated and the curtailed wind power obtained from the first step. In the following subsections, the proposed methodology used to solve the UC problem is described in detail.

6.2.1. Proposed Methodology

The methodology proposed in this work aims to store the excess of power generated and the curtailed wind power during low load periods, in order to be discharged during high energy demand periods. The proposed methodology can be applied by implementing the algorithm presented as follows:

- Step 1: Solve the UC problem by PL method; from the solution determine the excess of thermal power generation (ETG^t) for each time instant t;

- Step 2: Determine the available charging power of ESS, (CP^t), applying Equation (6.2.1):

$$CP^t = ETG^t + (W_{max}^t - W^t) \tag{6.2.1}$$

- Step 3: Create the binary vector of battery state according to the available charging power (BS_{WC}^t). In this vector, 1 means charging and 0 means discharging. If there is power to charge, ESS $(CP^t > 0)$; $BS_{WC}^t = 1$, in other case $BS_{WC}^t = 0$. In other words, if there is power available, ESS should be charged, on the contrary case ESS should be discharged to minimize the fuel consumption. Figure 6.3 illustrates how to build this vector under different operating conditions;
- Step 4: Create the vector of binary state according to the shape of the load profile $\left(BS_{shape}^t\right)$. As it is shown in Figure 6.4, the state of ESS is determined taking into account the geometry of the profile. Let D_{avg} be the average value of the hourly load; if $D^t < D_{avg}$, load should be increased, on the contrary, load should be reduced. This strategy makes uniform the shape of the load profile, while reducing the commitment of thermal units;
- Step 5: Once vectors BS_{WC}^t and BS_{shape}^t have been built, the reference power of ESS (RP^t) is created. This vector is the power set point of ESS for a determined time instant t. For any value of t; if $BS_{shape}^t = 0$ and $BS_{WC}^t = 0$, $RP^t = W_{max}^t - D^t$, else $RP^t = CP^t$. In this step is guaranteed that ESS is discharged only in those periods that the load profile becomes flattened. After this, the signal of reference to the ESS is completed. Positive elements of RP^t correspond to charge periods; while, negative elements correspond to discharge periods. The signal RP^t obtained is illustrated in Figure 6.5;
- Step 6: Using RP^t, the periods of charge and discharge are defined. In the case presented in Figure 6.5, charge period corresponds to the hours between t_i and t_0, while discharge period corresponds to the hours between t_0 and t_f. Considering the initial SOC $(SOC_t = 0)$; if the next period corresponds to charging, SOC at the end of this period is estimated by using the ESS model of Section 6.1.

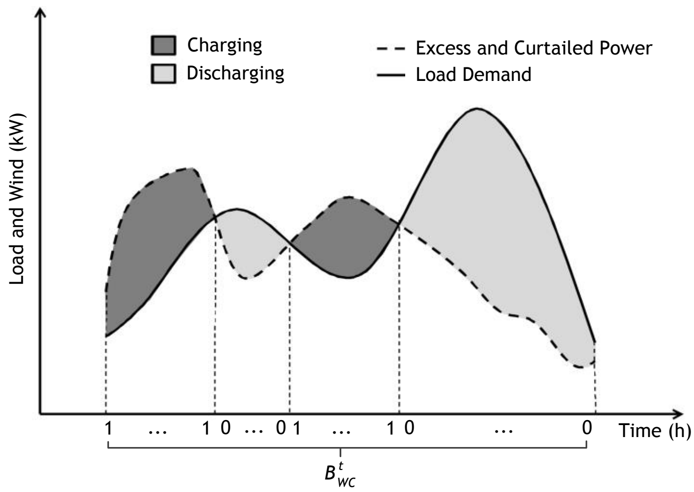

Figure 6.3. Charge and discharge periods according to the wind power curtailed.

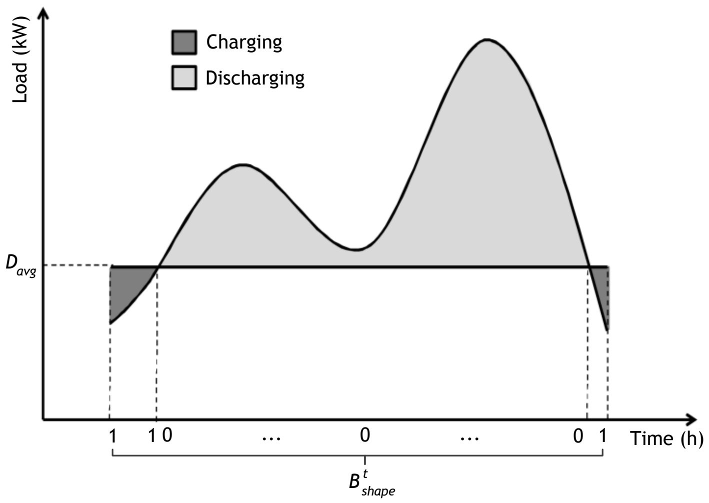

Figure 6.4. Charge and discharge periods according to the load profile.

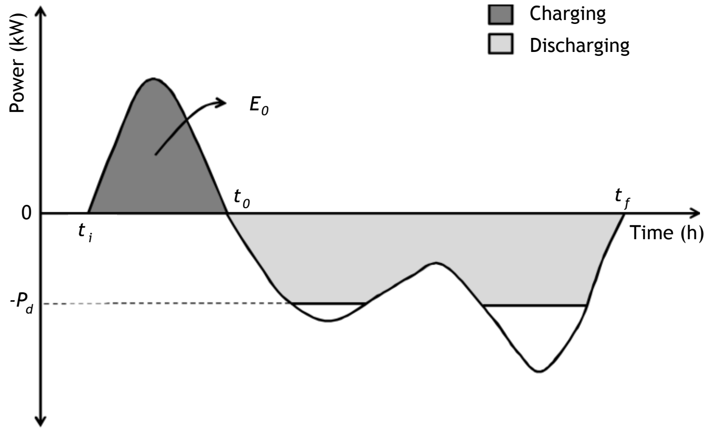

Figure 6.5. Reference power of ESS.

On the contrary, if the next period corresponds to discharge, the energy stored in ESS to be discharged (E_0) is estimated by using Equation (6.2.2):

$$E_0 = (SOC_t - SOC_{min})E_{max} \tag{6.2.2}$$

and the discharge power (P_d) is determined from Equation (6.2.3):

$$\frac{E_o}{\eta_b} = \sum_{t=t_0}^{t=t_f} |max(W^t - D^t - P_d)|\Delta t \tag{6.2.3}$$

where variable P_d is limited between 0 and a determined value $\left(P^0_{d,max}\right)$. In this step, the variable $P^0_{d,max}$ is assumed to be equal to P_{max} i.e., $\left(0 \le P_d \le P^0_{d,max}\right)$;

- Step 7: Using the value of P_d obtained in Step 6 the behavior of ESS is estimated by evaluating the VRB model of Section 6.1. The power exchanged between ESS and the power system obtained from VRB model, Figure 6.2, is represented by the variable P^t_{ESS}. The power absorbed or supplied by VRB considering the effects of charge controller are saved in the variable P^t_{ESS} through the hourly cycle;

- Step 8: When ESS is incorporated to the UC problem, it is assumed to be the unit with highest priority in the system. The power to be supplied by thermal units and wind generator (G^t) is assigned according to the Equation (6.2.4):

$$G^t = D^t + P_{ESS}^t \tag{6.2.4}$$

- Step 9: Now, the UC problem is solved considering the time series (G^t) instead of D^t. The excess of thermal generation (ETG^t) is checked. If there is some excess of electricity, the maximum power to be discharged, previously estimated in Step 6 $\left(P_{d,max}^0\right)$, is limited to a new value $\left(P_{d,max}^f\right)$ and calculated according to Equation (6.2.5):

$$P_{d,max}^f = \left|P_{d,max}^0\right| - max(ETG^t) \tag{6.2.5}$$

  This reduction in the maximum discharging power allows reducing the excess of electricity. After this process, go to Step 6 assigning the value of $P_{d,max}^0$ with the value of $P_{d,max}^f$ previously calculated in Equation (6.2.5), i.e., make the assignment $P_{d,max}^0 \leftarrow P_{d,max}^f$. On the contrary, if the excess of power generation is equal to zero and P_d is different of zero, the scheduling process is finished. However, if excess of electricity is higher than zero and $Pd \rightarrow 0$, this energy surplus will be absorbed by the dump load DL^t.

6.2.2. Solving the Unit Commitment Problem by Priority List Method

The UC is an optimization problem that consists of minimizing the total generation cost, which is expressed by means of the variable (z_b) in Equation (6.2.6):

$$z_b = \sum_{t=1}^{H} \sum_{n=1}^{N} f_n^t + SUC_n^t (1 - U_n^t) U_n^t \tag{6.2.6}$$

This optimization problem is constrained to the general characteristics of thermal units that have been described in Equations (6.1.2)-(6.1.12) in Section 6.1. Other important constraints are related to the spinning reserve and power balance, which are presented in Equation (6.2.7) and Equation (6.2.8):

$$\sum_{n=1}^{N} P_n^{t,max} U_n^t - \sum_{n=1}^{N} P_n^t U_n^t \geq SR(D^t) + WFE(W^t) + BFE(P_{ESS}^t) \tag{6.2.7}$$

$$\sum_{n=1}^{N} P_n^t U_n^t + W^t + P_{bt}^t = D^t + DL^t \tag{6.2.8}$$

where $P_n^{t,max}$ is the maximum power production of unit n at time t, considering the ramp rate constraints. SR is the spinning reserve, WFE is the increment in spinning reserve due to wind power forecasting error, and BFE is the increment in spinning reserve due to the uncertainty in the power to be discharged from ESS.

As stated before, the PL method offers a near-optimal solution to the UC problem in a reduced computational time. In particular, in cases with a high integration of renewable energy sources, where the load to be supplied by thermal generators is low, the PL method can provide a reasonable solution, in contrast with other methodologies that have great difficulty in finding a feasible solution [210]. However, the PL method consists of several steps that allow obtaining a cost-effective and feasible solution to the UC problem. These steps are primary unit scheduling, minimum up/down time repair, spinning reserve repair, shutdown repair, unit substitution, and the shutdown of the power surplus. Descriptions of these steps as presented as follows.

6.2.2.1. Primary Unit Scheduling

In the PL method, all units are committed according to their average production cost (G_n), which is defined by Equation (5.3.1) and Equation (5.3.2). Meanwhile, an initial approximation to the UC problem is obtained by following the next algorithm:

- Step 1: Built the matrix to save the primary unit scheduling (PUS_n^t). This matrix has $N + 1$ rows and T columns; an additional row is added in order to consider the production of the wind generation. The values of all the elements in this matrix that correspond to thermal units are assumed to be zero;
- Step 2: Establish the order at which the units will be committed. This is carried out using (G_n) index presented in Equation (5.3.1);
- Step 3: Set $t \leftarrow 1$;
- Step 4: According to the PL method of Step 2, the first unit of the list is chosen by set $n \leftarrow 1$;
- Step 5: Set $PUS_n^t \leftarrow 1$;
- Step 6: Check the maximum capacity committed in Step 4 without considering the ramp constraints. If the spinning reserve constraint is not fulfilled and $n \leq N$, set $n \leftarrow n + 1$ and go to Step 5; else if $t \leq T$ set $t \leftarrow t + 1$, go to Step 4; otherwise, stop.

6.2.2.2. Minimum Up/Down Time Repairing

As described in the previous sections, the initial approximation obtained from the primary unit scheduling procedure described before does not satisfy the minimum up/down time constraints. For this reason, a repair process has to be introduced. The procedure used in this work follows the details explained in Sub-Section 5.3.2, which consider the repair minimum up/down time constraint developed in [213].

6.2.2.3. Spinning Reserve Repairing

The scheduling obtained from the primary unit scheduling and the repair of minimum up/down time constraint could not fulfill the spinning reserve requirements.

To overcome this problem, more generation is added by the following algorithm:

- Step 1: For $t = 1, 2, \ldots, H$, verify the spinning reserve requirements using Equation (6.2.7);
- Step 2: Create a list with those hours where spinning reserve requirements are not fulfilled. The number of elements of this list is represented by the variable B_h;
- Step 3: If ($B_h > 0$); create a table with B_h rows and two columns. This table will save the units and hours that units should be committed in order to fulfill the spinning reserve requirements. In other case; stop;
- Step 4: The list created in Step 2 is saved in the second column of table created in Step 3;
- Step 5: For each element of the list created in Step 2, identify the potential units to be committed according to the PL method. These units are saved in the first column of the table created in Step 3;
- Step 6: The first two elements (the first element of column one and column two) of the table previously filled are selected. Then, the condition of the corresponding unit is changed from offline to online;
- Step 7: As consequence of previous step, i.e., the condition of corresponding unit has changed, the repairing of minimum up/down time constraint is carried out in order to fulfill these constraints;
- Step 8: Go to Step 1.

6.2.2.4. Shutdown Repairing

At this stage, it is likely that some units could not be shut down because of the violation of the respective condition. To solve this problem, it is necessary to give more time for operation to these units so that units fulfill the offline requirements. The repair process used in this section is explained as follows:

- Step 1: For $t = 1, 2, \ldots, H$, verify the violation of shutdown ramp constraint using Equation (6.1.9);
- Step 2: Create a list with those units at which shutdown ramp constraint is violated and the corresponding hours that should be additionally committed in order to fulfill this constraint. This list is saved in a table whose first column represents the units and second column represents the additional hours that they should be committed;
- Step 3: If the list is not empty, the first two elements (first element of column one and two) of the table previously filled are selected. Then, the condition of the corresponding unit is changed from offline to online. In other case, stop;
- Step 4: As the condition of this unit has changed, the repairing of minimum up/down time constraint is carried out in order to fulfill these constraints;
- Step 5: Go to Step 1.

6.2.2.5. Unit Substitution

As described in previous sections, during peak hours some units are committed during more hours than is required in order to fulfill the minimum up-time constraint. In order to solve this problem, the algorithm described in Sub-Section 5.3.5 is integrally carried out in this procedure to improve the results of the PL process.

6.2.2.6. Shutdown Excess of Committed Capacity

The repair of minimum up-/down-time constraints produces an excess of spinning reserve which increases the total operation cost. In this procedure, this excess of committed capacity is found and shut down to reduce operating costs. This is carried out by applying the algorithm described next:

- Step 1: For $t = 1, 2, \dots, H$, verify the excess of spinning reserve using Equation (6.2.7);
- Step 2: Create a list with those hours with excess of spinning reserve. The number of elements of this list is represented by the variable J_h;
- Step 3: Set $j_h \leftarrow 1$;
- Step 4: Considering the element j_h in the list created in Step 2, the most expensive unit is recognized and chosen as candidate to be de-committed. If $T_{on,n}^{t}$ is higher than MUT_n, the unit n is de-committed;
- Step 5: As consequence of the Step 4, the unit scheduling is changed, so that the minimum up/down time constraint is repaired;
- Step 6: Considering the scheduling obtained from Step 5, start/shutdown ramp constraints and spinning reserve are verified through Equation (6.1.9) and Equation (6.2.8), respectively. If at least one constraint is violated, the condition of the corresponding element is changed from 0 to 1;
- Step 7: If $(j_h < J_h)$, set $j_h \leftarrow j_h + 1$ and go to Step 4; else, stop.

6.3. Case Study and Results

The strategy proposed for the management of an ESS is illustrated by analyzing an insular power system of five diesel units, whose characteristics are presented in Table 6.1. These characteristics were obtained by using information provided by the manufacturers, although other costs, such as starting-up costs, have not been considered. Moreover, start-up and shut-down ramp rates and operating ramp rates have not been taken into account. Thus, it is assumed that these generators can deal with sudden changes in the load to be supplied. For all generators, minimum up/down times were assumed to be equal to 1h. The time horizon of the scheduling process is 168h $H = 168$h corresponding to one week.

Table 6.1. Characteristic of thermal units.

n	P_n^{min} (kW)	P_n^{max} (kW)	a_n (L/h)	b_n (L/h)	c_n (L/kW^{2}h)
1	3150.00	6300	101.95	0.0868	0.000001
2	528.00	1056	45.20	0.1699	0.000040
3	482.50	965	13.10	0.2555	-0.000009
4	600.00	1200	38.80	0.1995	0.000030
5	640.00	1280	53.10	0.1981	0.000020

The wind power forecast is presented in Figure 6.6, while a forecasting error of 15% was assumed. The spinning reserve requirements were assumed to be 10% ($SR = 0.1$). The ESS is composed of a power inverter of 2000kW, and a VRB of 2000kW/8000kWh. The charge controller is settled to maintain SOC between 15% and 90% ($SOC_{min} = 0.15$ and $SOC_{max} = 0.9$), and the efficiency of VRB was assumed to be equal to 80% during charge and discharge processes ($\eta_b = 0.8$). The initial SOC of the VRB was assumed 15%. The increment in the spinning reserve, as a result of the wind power forecasting error (WFE) and uncertainty in the power obtained from ESS (BFE) was assumed to be equal to the forecasting error. Figure 6.7 shows the power interchange (P_{ESS}^t) between the ESS and the insular power system, while Figure 6.8 shows the SOC of the VRB. On the one hand, it is possible to observe how the power available from the curtailed wind power is used to charge the VRB, and how the charge controller limits the SOC to 90% by reducing the charge power, specifically between $t = 147$h and $t = 165$h. On the other hand, it is possible to see how the proposed methodology controls the discharging process by adjusting the discharging power to a fixed value. Something relevant happens between $t = 77$h and $t = 143$h, where the VRB is discharged. However, the power interchanged with the system is almost zero ($P_{ESS}^t \rightarrow 0$), and this loss of power is a result of the low efficiency of the power inverter at this load. Figure 6.9 shows the load to be supplied by the thermal units and the wind generator when the ESS is incorporated. It is possible to see how the controlled discharge of the VRB by means of a uniform discharging power reduces the energy demand, particularly during the second and third days of the schedule under study.

Tables 6.2 and Table 6.3 show the power production of the thermal units and the wind generators during day 2. In these tables it is possible to see how the incorporation of the ESS reduces the power to be supplied by the thermal units, while it improves the accommodation of wind power generation. Those generators removed from the scheduling owing to the operation of the ESS are presented in bold. Over the scheduling horizon, fuel consumption without incorporating the ESS is 115,755.80 liters, while the incorporation of the ESS reduces this value to 113,784.30 liters, which represents a fuel saving of 1971.50 liters, about 2%. Moreover, curtailed wind power without incorporating the ESS is 99,620.70kWh, while after integration of the ESS, wind power curtailment is reduced to 79,340.90kWh. This represents an improvement in the wind power use of about 20%, which is significant.

The proposed approach was implemented in MATLAB programming language, using a standard PC with an i7-3630QM CPU at 2.40GHz, 8GB of memory and 64-bit operating system. The computational time required to carry out this scheduling was only about four minutes.

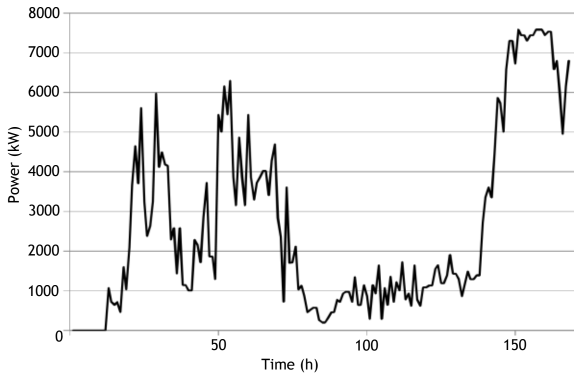

Figure 6.6. Hourly aggregated wind power generations.

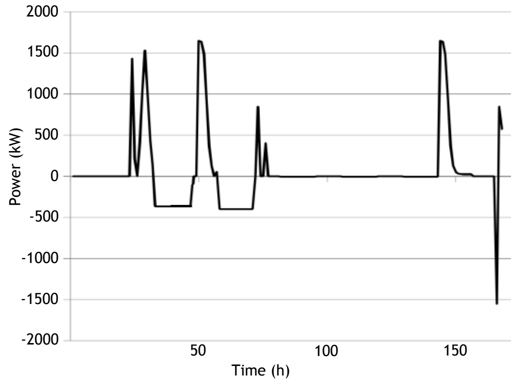

Figure 6.7. Power from/to ESS under study.

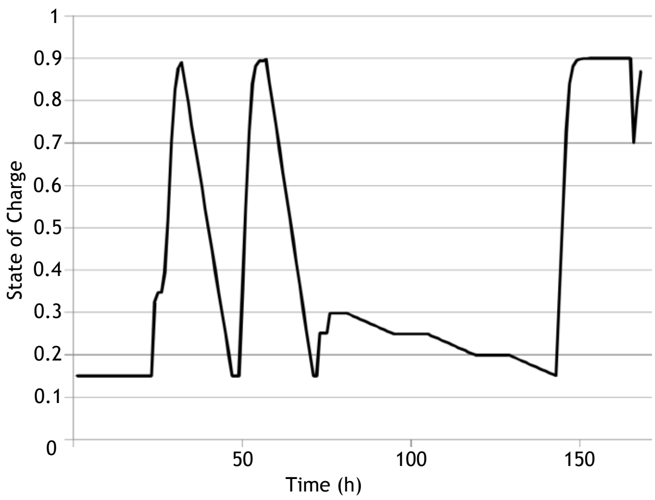

Figure 6.8. State of charge behavior of ESS under study.

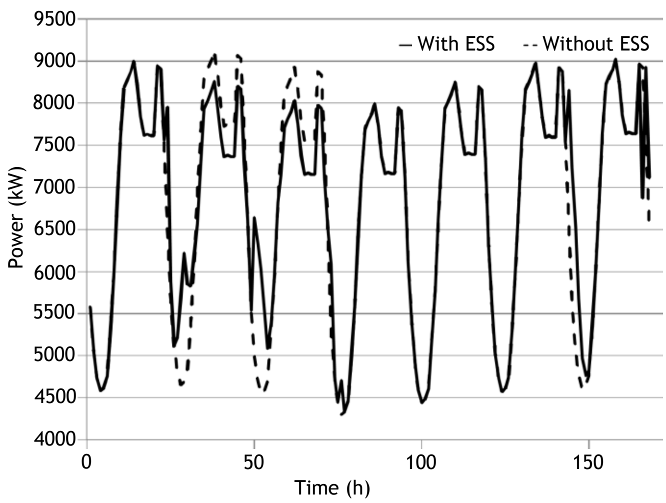

Figure 6.9. Load to be supplied by thermal and wind units.

Table 6.2. Unit scheduling of day 2 without incorporating ESS (MW).

n	Time (h)																						
	25	26	27	28	29	30	31	32	33	34	35	36	37	38	39	40	41	42	43	44	45	46	47	48
1	3.15	3.24	3.15	3.15	3.15	3.15	3.15	3.15	3.28	5.39	5.21	5.85	5.45	6.30	6.08	5.84	6.22	5.43	5.55	5.50	5.20	4.78	5.30	5.26
2	0	0	0	0	0	0	0	0	0	0.53	0.53	0.53	0.53	0.60	0.53	0.53	0.53	0.53	0.53	0.53	0.53	0.53	0.53	0
3	0	0	0	0	0	0	0	0	0	0	**0.48**	0.48	**0.48**	0.48	0.48	0.48	0.48	0	0	**0.48**	**0.48**	0	**0.48**	0
4	0	0	0	0	0	0	0	0	0	0	0	**0.60**	0	0.60	0.60	**0.60**	0	0	0	0	0	0	0	0
5	0	0	0	0	0	0	0	0	0	0	0	0	0	0	0	0	0	0	0	0	0	0	0	0
W^t	3.02	2.38	2.16	2.00	2.04	2.18	2.75	3.40	4.15	2.29	2.58	1.43	2.58	1.14	1.14	1.00	1.00	2.29	2.15	1.72	2.86	3.72	1.86	1.86

Table 6.3. Unit scheduling of day 2 incorporating ESS (MW).

n	Time (h)																						
	25	26	27	28	29	30	31	32	33	34	35	36	37	38	39	40	41	42	43	44	45	46	47	48
1	3.15	3.24	3.15	3.15	3.15	3.15	3.15	3.15	3.15	5.03	5.33	6.09	5.52	6.00	5.72	6.08	5.85	5.06	5.19	5. 62	5.31	4.42	5.42	5.26
2	0	0	0	0	0	0	0	0	0	0.53	0.53	0.53	0.53	0.53	0.53	0.53	0.53	0.53	0.53	0.53	0.53	0.53	0.53	0
3	0	0	0	0	0	0	0	0	0	0	**0**	0.48	**0**	0.48	0.48	0.48	0.48	0	0	**0**	**0**	0	**0**	0
4	0	0	0	0	0	0	0	0	0	0	0	**0**	0	0.60	0.60	**0**	0	0	0	0	0	0	0	0
5	0	0	0	0	0	0	0	0	0	0	0	0	0	0	0	0	0	0	0	0	0	0	0	0
W^t	3.23	2.38	2.57	3.04	3.57	3.20	3.18	3.54	3.91	2.29	2.58	1.43	2.58	1.14	1.14	1.00	1.00	2.29	2.15	1.72	2.86	3.72	1.86	1.86

Chapter 7

Conclusions

7.1. Main Conclusions

This section shows the main conclusions arising from this thesis, which are fourfold:

- A new hybrid evolutionary-adaptive methodology, called HEA, was proposed in this work for forecasting electricity market prices in the short-term. The HEA methodology results from the innovative joint characteristics of WT (bringing a filtering effect), EPSO (bringing evolutionary optimization) and ANFIS (bringing an adaptive architecture), considering also MI in the selection of the best input data. For a fair and clear comparison, identical test days/weeks used to test other methods were considered, but without exogenous variables. The application of the proposed HEA methodology was demonstrated to be accurate and effective, helping to reduce the uncertainty associated with market prices. The results for the Spanish and PJM markets showed the superiority of the HEA methodology, regarding both average MAPE and error variance criterions. Even if each day/week is analyzed per se the results are always better. The low computational burden was also confirmed, providing 168h electricity market prices forecast results in less than 40 seconds. Hence, it can be concluded that the proposed methodology is proficient, taking into account results previously reported in the literature, with the best trade-off between computation time and average MAPE. Furthermore, HEA methodology has been applied to forecast the behavior of wind power, tested for a short-term horizon (3h-ahead with 15-minute intervals) in the Portuguese system. For a fair and clear comparative study, identical test cases used by other methodologies were considered, also without exogenous variables. The application of the proposed HEA methodology was demonstrated to be accurate and effective, helping to reduce the uncertainty associated with wind power. The average MAPE value was only 3.75% for an average error variance of 0.0013 and a NRMSE of 2.66%. In addition, the low computational burden is evidenced in reality, providing wind power forecast results in less than 40 seconds per iteration. Hence, the proposed HEA methodology presents the best trade-off between computational time and accuracy, which is crucial for real-life and real-time applications.
- A novel methodology for solving an ED problem incorporating the uncertainty of wind power generation and generator reliability was presented. In this approach, the forecasting error of wind power generation is modeled as discretized beta PDF, which allows extreme conditions to be considered with their corresponding probabilities. Another important characteristic of the proposed methodology is that the power production of each unit at

the previous time instant is incorporated by means of simplified sampling of the discretized PDF of power generation at this time-step, which allows efficient treatment of the problem. Finally, failure events of each unit are incorporated through the calculation of joint PDF of power production and failure event, while ENS is probabilistically described through the convolution between the PDF of ENS related to wind power forecasting error and unit failure. The proposed methodology was illustrated through the analysis of two power systems of 5 and 10 units located in islands, and the results were compared with those obtained from MCS methodology. From this comparison it is possible to conclude that the proposed methodology can reasonably describe the PDF of wind power generation, thermal power generation, ENS, and generation cost when generator reliability is not taken into account.

- A novel methodology for solving the UC problem to be applied in those systems with a high integration of renewable energy sources was presented. The proposed methodology consists of the generation of some representative scenarios, which are selected considering the auto-correlated nature of wind power production, its hourly profile and its forecasting error. The probability of occurrence of each scenario is then estimated by solving the deterministic UC problem for each scenario previously generated. Finally, according to a determined probability level (α), those hours with a probability of occurrence equal to or higher than α are selected and the minimum up/down time repair is applied in order to obtain a feasible solution. The capabilities and performance of the proposed methodology were illustrated through the analysis of a case study applied in an insular power system, where the spinning reserve requirements were probabilistically verified.

- Finally, a new control strategy to be used in the weekly scheduling of insular power systems with ESS was presented. The methodology proposed incorporated the effects of the most relevant elements such as thermal generators, wind power generation, power converter, charge controller and VRB. The proposed methodology consisted of two major steps: in the first step, the UC problem is solved without taking into account the ESS, and from this procedure the total energy available to charge the ESS is estimated; in the second step, using the estimated energy available obtained in the first step, the ESS is incorporated into the UC problem. The effectiveness of the proposed methodology was illustrated by means of the scheduling of a 5-unit system located in an insular system during one week. In comparison with the case without an ESS, fuel savings of 2% (i.e., from 115,755.8 liters to 113,784.3 liters) could be reached from the integration of the ESS only in a single day of results, while the accommodation of wind power generation could be improved by 20% (from 79,340.9kWh to 99,960.7kWh), which was significant, for a CPU time of only four minutes.

7.2. Guidelines for Future Contributions

Some worthwhile perspectives exist for future development and research, namely:

- The study of new innovative techniques and their combination to forecast the electricity market prices and wind power forecasting with robustness and less average error, providing accurate results in the electrical industry, i.e., all electricity market players.
- The study of new integrating strategies combining more renewable integration, i.e., a combination of solar and wind power, or solar and hydro, wind and hydro, or the combination of them all, proposing new market strategies, and also the same strategy will enable greater storage capacity (combination of hydro and batteries storage) applied in larger systems.
- The study of new methodologies applying the forecasting of residual demand curves considering a dominant market player, risk control and stochastic programming problems in the short-term, showing the benefits reached with its application in comparison with already available methodologies.
- The application of new management strategies in the electricity industry that are able to reduce uncertainty, increase profits and increase the robustness and flexibility of the electrical framework.

7.3. Research Contributions Resulting from this Work

This section presents the various publications in peer-reviewed journals, book chapters and conference proceedings resulting from the research work carried out in this thesis.

7.3.1. Articles in Journals

[JP1] G.J. Osório, J.M. Lujano-Rojas, J.C.O. Matias, J.P.S. Catalão, “A fast method for the unit scheduling problem with significant renewable power generation”, *Energy Conversion and Management* (**ELSEVIER**), Vol. 94, pp. 178-189, April 2015. (**Impact Factor of 4.380, Q1 Quartile in Category ENERGY & FUELS of ISI Web of Knowledge**).

http://dx.doi.org/10.1016/j.enconman.2015.01.071

[JP2] G.J. Osório, J.M. Lujano-Rojas, J.C.O. Matias, J.P.S. Catalão, “A probabilistic approach to solve the economic dispatch problem with intermittent renewable energy sources”, *Energy* (**ELSEVIER**), Vol. 82, pp. 949-959, March 2015. (**Impact Factor of 4.844, Q1 Quartile in Category ENERGY & FUELS of ISI Web of Knowledge**).

http://dx.doi.org/10.1016/j.energy.2015.01.104

[JP3] G.J. Osório, J.C.O. Matias, J.P.S. Catalão, "Short-term wind power forecasting using adaptive neuro-fuzzy inference system combined with evolutionary particle swarm optimization, wavelet transform and mutual information", *Renewable Energy* (**ELSEVIER**), vol. 75, pp. 301-307, March 2015. (**Impact Factor of 3.476, Q1 Quartile in Category ENERGY & FUELS of ISI Web of Knowledge, already with 6 citation by other authors**).

http://dx.doi.org/10.1016/j.renene.2014.09.058

[JP4] G.J. Osório, J.M. Lujano-Rojas, J.C.O. Matias, J.P.S. Catalão, "A new scenario generation-based method to solve the unit commitment problem with high penetration of renewable energies", *International Journal of Electrical Power and Energy Systems* (**ELSEVIER**), vol. 64, pp. 1063-1072, January 2015 (**Impact Factor of 3.432, Q1 Quartile in Category ENGINEERING, ELECTRICAL & ELECTRONIC of ISI Web of Knowledge, with 1 citation by other authors**).

http://dx.doi.org/10.1016/j.ijepes.2014.09.010

[JP5] G.J. Osório, J.C.O. Matias, J.P.S. Catalão, "Electricity prices forecasting by a hybrid evolutionary-adaptive methodology", *Energy Conversion and Management* (**ELSEVIER**), vol. 80, pp. 363-373, April 2014 (**Impact Factor of 4.380, Q1 Quartile in Category ENERGY & FUELS of ISI Web of Knowledge, already with 5 citations by other authors**).

http://dx.doi.org/10.1016/j.enconman.2014.01.063

7.3.2. Book Chapters

[BC1] G.J. Osório, J.M. Lujano-Rojas, J.C.O. Matias, J.P.S. Catalão, "A heuristic approach for economic dispatch problem in insular power systems", in: Technological Innovation for Cloud-based Engineering Systems, Eds. L.M. Camarinha-Matos et al., DoCEIS 2015, **SPRINGER**, Heidelberg, Germany, April 2015.

7.3.3. Papers in Conference Proceedings

[PC1] G.J. Osório, J.M. Lujano-Rojas, M. Shafie-khah, J.C.O. Matias, J.P.S. Catalão, "Managing vanadium redox batteries towards the optimal scheduling of insular power systems", in: *Proceedings of the 2015* ***IEEE*** *Power & Energy Society General Meeting — PESGM 2015*, Denver, Colorado, USA, July 26-30, 2015 (accepted).

[PC2] G.J. Osório, J.M. Lujano-Rojas, J.C.O. Matias, J.P.S. Catalão, "Including forecasting error of renewable generation on the optimal load dispatch", in: *Proceedings of the* ***IEEE*** *Power Tech 2015 Conference*, Eindhoven, Netherlands, 29 June - 2 July, 2015 (accepted).

[PC3] G.J. Osório, J.M. Lujano-Rojas, J.C.O. Matias, J.P.S. Catalão, “Fast method to the unit scheduling of power systems with renewable power sources”, in: *Proceedings of the International Conference on Renewable Energies and Power Quality — ICREPQ’15*, La Coruña, Spain, 25-27 March, 2015 (accepted).

[PC4] G.J. Osório, J.M. Lujano-Rojas, J.C.O. Matias, J.P.S. Catalão, “Probability theory-based economic dispatch model for insular power systems”, in: *Proceedings of the 24th Australasian Universities Power Engineering Conference — AUPEC 2014 (technically co-sponsored by **IEEE**)*, Perth, Australia, USB flash drive, 28 September - 1 October, 2014.

[PC5] G.J. Osório, J.C.O. Matias, J.P.S. Catalão, “Hybrid evolutionary-adaptive approach to predict electricity prices and wind power in the short-term”, in: *Proceedings of the 18th Power Systems Computation Conference — PSCC 2014 (technically co-sponsored by **IEEE**)*, Wroclaw, Poland, USB flash drive, August 18-22, 2014.

[PC6] G.J. Osório, J.C.O. Matias, J.P.S. Catalão, “A review of short-term wind power forecasting approaches”, in: *Proceedings of the 2nd **IET** Renewable Power Generation Conference — RPG 2013*, Beijing, China, USB flash drive, 9-11 September, 2013.

[PC7] G.J. Osório, J.C.O. Matias, J.P.S. Catalão, “A review of short-term hydro scheduling tools”, in: *Proceedings of the 48th International Universities' Power Engineering Conference — UPEC 2013 (technically co-sponsored by **IEEE**)*, Dublin, Ireland, USB flash drive, 2-5 September, 2013.

[PC8] G.J. Osório, J.C.O. Matias, J.P.S. Catalão, “Intelligent and hybrid techniques to predict short-term electricity prices: a review”, in: Proceedings of the 17th International Conference on Intelligent System Applications to Power Systems — ISAP 2013 (technically co-sponsored by **IEEE**), Tokyo, Japan, USB flash drive, July 1-4, 2013.

References

[1] Santana J. J. E., Resende M. J., Reflectir Energia, Portugal: ETEP-LIVRIMPOR, 2006.

[2] Shahidehpour M., Yamin, H., Li Z., Market operations in electric power systems: forecasting, scheduling and risk, New York: Wiley, 2002.

[3] Ferreira, L. A. F. M., Anderson T., Imparato C. F., Miller T. E., Pang C. K., Svoboda A., Vojdani A. F., "Short-Term Resource Scheduling in Multi-Area Hydrothermal Power Systems," *Int. J. Electr. Power Energy Syst.*, vol. 11, pp. 200-212, 1989.

[4] Weron R., "Electricity price forecasting: A review of the state-of-the-art with a look into the future," *Int. J. Forecas.*, vol. 30, pp. 1030-1081, 2014.

[5] Sioshansi F. P., Evolution of global electricity markets: New paradigms, new challenges, nem approaches, 1 ed., USA: Academic Press, Elsevier, 2013.

[6] Peças-Lopes J. A., Hatziargyrio N., Mutale J., Djapic P., Jenkins N., "Integrating distributed generation into electric power systems: A review of drivers, challenges and opportunities," *Int. J. Electr. Power Syst. Res.*, vol. 77, pp. 1189-1203, 2007.

[7] "Mercado Ibérico de Electricidade (MIBEL)," [Online]. Available: http://www.mibel.com/index.php?lang=pt. [Accessed 16 09 2014].

[8] "Electricity Market Operator (OMEL)," [Online]. Available: http://www.omelholding.es/omel-holding/. [Accessed 16 09 2014].

[9] "Entidade Reguladora dos Serviços Energéticos (ERSE)," [Online]. Available: http://www.erse.pt/pt/Paginas/home.aspx. [Accessed 16 09 2014].

[10] "Framework Convention on Climate Changing," [Online]. Available: http://unfccc.int/meetings/lima_dec_2014/meeting/8141.php. [Accessed 15 09 2014].

[11] "Governo de Portugal," [Online]. Available: http://www.portugal.gov.pt/pt.aspx. [Accessed 17 09 2014].

[12] Gil H. A., Joos G., "Generalized estimation of average displaced emissions by wind generation," *IEEE Trans.Power Syst.*, vol. 22, pp. 1035-1043, 2007.

[13] Yang, M.; Nguyen, F.; De T'Serclaes, P.B., "Wind farm investment risks under uncertain CDM benefit in China," *Energy Policy*, vol. 38, pp. 1436-1447, 2010.

[14] "Our future energy," The Danish Government, Denmark, 2011.

[15] "European Comission Press Release Database," [Online]. Available: http://europa.eu/rapid/press-release_MEMO-14-434_en.htm. [Accessed 22 09 2014].

[16] "Roteiro das Energias Renováveis," [Online]. Available: http://europa.eu/legislation_summaries/energy/renewable_energy/l27065_pt.htm. [Accessed 22 09 2014].

[17] "Europe's Premier Wind Energy Event," [Online]. Available: http://www.ewea.org/annual2013/. [Accessed 24 09 2014].

[18] "Adapting renewable energy policies to dynamic market conditions," IRENA - International Renewable Energy Agency, Abu Dhabi, 2014.

[19] "Direcção Geral de Energia e Geologia (DGEG)," [Online]. Available: http://www.dgeg.pt/. [Accessed 26 09 2014].

[20] "Environmental impacts of wind-energy projects," National Academies Press, USA, 2007.

[21] Dica C., Dica, C. -I., Vasiliu D., Comanescu G. H., Ungureanu M., "Wind Power Short-Term Forecasting System," in *Proc. IEEE Power Tech. Conf.*, Bucharest, Romania, 2009.

[22] "Centro de Informação de Electricidade (REN)," [Online]. Available: http://www.centrodeinformacao.ren.pt/PT/Paginas/CIHomePage.aspx. [Accessed 01 10 2014].

[23] "Redes Energeticas Nacionais (REN)," [Online]. Available: http://www.ren.pt/. [Accessed 02 10 2014].

[24] "Sistema Eléctrico Português (EDP)," [Online]. Available: http://www.edp.pt/pt/aedp/sectordeenergia/sistemaelectricoportugues/Pages/SistElectNacional.aspx. [Accessed 02 10 2014].

[25] Erdinç O., Paterakis N., "Overview of Insular Power Systems: Challenges and Opportunities," in *Smart and Sustainable Power Systems: Operations, Planning, and Economics of Insular Electricity Grids*, Boca Raton, Florida, EUA, CRC Press, 2015, pp. 1-34.

[26] Chen F., Duic N., Alves, L. M., Carvalho M. G., "Renewislands-renewable energy solutions for islands," *Rene. Sust. Energy Rev.*, vol. 11, pp. 1888-1902, 2007.

[27] Bizuayehu A. W., Medina, P., Catalão J. P. S., Rodrigues, E. M. G., Contreras, J., "Analysis of electrical energy storage technologies' State-of-the-art and applications on islanded grid systems," in *IEEE PES T&D Conference and Exposition*, Chicago-USA, 2014.

[28] "United States of America insular areas energy assessment report," Pacific Power Association, Suva-Fiji, 2006.

[29] Conrad M. D., Esterly S., Bodell T., Jones T., "American Samoa: Energy strategies," The National Renewable Energy Laboratory (NREL), USA, 2013.

[30] Sanseverino E. R., Sanseverino R. R., Favuzza S., "Near zero energy islands in the meditteranean: supporting policies and local obstacles," *Energy Pol.,* vol. 66, pp. 592-602, 2014.

[31] Schallenberg-Rodríguez J., "Photovoltaic techno-economical potential on roofs in regions and islands: The case of the Canary Islands. Methodological review and methodology proposal," *Renew. Sust. Energy Rev.,* vol. 20, pp. 219-239, 2013.

[32] Fokaides P. A., Kylili A., "Grid parity in insular energy systems: The case of photovoltaics (PV) in Cyprus," *Energy Pol.,* vol. 65, pp. 223-228, 2014.

[33] Katsaprakakis D. A., Christakis D. G., Pavlopoylos K., Stamataki S., Dimitrelou I., Stefanakis I., Spanos P., "Introduction of a wind powered pumped storage system in the isolated insular power system of Karpathos-Kasos," *Appl. Energy,* vol. 97, pp. 38-48, 2012.

[34] Giatrakos G. P., Tsoutsos T. D., Zografaki N., "Sustainable power planning for the island of Crete," *Energy Pol.,* vol. 37, pp. 1222-1238, 2009.

[35] Wu Y., Han, G., Lee, C., "Planning 10 onshore wind farms with corresponding interconnection network and power system analysis for low-carbon-island development on Penghu Island, Taiwan," *Rene. Sust. Energy Rev.,* vol. 19, pp. 531-540, 2013.

[36] Cosentino V., Favuzza S., Graditi G., Ippolito M. G., Massaro F., Sanseverino E. R., Zizzo G., "Smart renewable generation for an islanded system. Technical and economic issues of future scenarios," *Energy,* vol. 39, pp. 196-204, 2012.

[37] Pina A., Baptista P., Silva C., Ferrão P., "Energy reduction potential from the shift to electric vehicles: The Flores island case study," *Energy Pol.,* vol. 67, pp. 37-47, 2014.

[38] Morales J. M., Conejo A. J., Madsen H., Pinson P., Zugno M., Integrating Renewables in Electricity Markets: Operational Problems, vol. 205, New York, USA: Springer, 2014.

[39] Castro R., Uma introdução às energias renováveis: eólica, fotovoltaica e mini-hídrica, Lisboa: IST Press, 2011.

[40] Conejo A. J., Carrión M., Morales J. M., Decision Making Under Uncertainty in Electricity Markets, New York, USA: Springer, 2010.

[41] Santos A., Santos V., Aprovação do Regulamento de Operação das Redes do Setor Elétrico, Regulamento n.º 557/2014, Entidade Reguladora dos Serviços Energéticos: Diário da República, 2ª série, n.º 245, 2014.

[42] Niknam T., Sharifinia S., Azizipanah-Abarghooee R., "A new enhanced batinspired algorithm for finding linear supply function equilibrium of GENCOs in the competitive electricity market," *Energy Convers. Manage.*, vol. 76, pp. 1015-1028, 2013.

[43] Li X. R., Yu C. W., Ren S. Y., Chiu C. H., Meng K., "Day-ahead electricity price forecasting based on panel cointegration and particle filter," *Electron. Power Syst. Res.*, vol. 95, pp. 66-76, 2013.

[44] González V., Contreras J., Bunn P. W., "Forecasting power prices using a hybrid fundamental-econometric model," *IEEE Trans. Power Syst.*, vol. 27, pp. 363-372, 2012.

[45] Dong Y., Wang J., Jiang H., Wu J., "Short-term electricity price forecast based on the improved hybrid model," *Energy Convers. Manage.*, vol. 52, p. 2987–2995., 2011.

[46] Pindoriya N. M., Singh S. N., Singh S. K., "An adaptive wavelet neural network-based energy price forecasting, in electricity market," *IEEE Trans. Power Syst.*, vol. 23, pp. 1423-1432, 2008.

[47] Amjady N., Vahidinasab V., "Security-constrained self-scheduling of generation companies in day-ahead electricity markets considering financial risk," *Energy Convers. Manage.*, vol. 65, pp. 164-172, 2013.

[48] Lin W. -M., Gow H. -J., Tsai M. -T., "Electricity price forecasting using enhanced probability neural network," *Energy Convers. Manage.*, vol. 51, pp. 2707–2714, 2010.

[49] Catalão J. P. S., Pousinho H. M. I., Mendes V. M. F., "Short-term electricity prices forecasting in a competitive market by a hybrid intelligent approach," *Energy Convers. Manage.*, vol. 52, pp. 1061–1065, 2011.

[50] Shayeghi H., Ghasemi A., "Day-ahead electricity prices forecasting by a modified CGSA technique and hybrid WT in LSSVM based scheme," *Energy Convers. Manage.*, vol. 74, pp. 482-491, 2013.

[51] Aggarwal S. K., Saini L. M., Kumar A., "Electricity price forecasting in deregulated markets: review and evaluation," *Int. J. Power Energy Syst.*, vol. 31, pp. 13–22, 2009.

[52] Catalão J. P. S., Pousinho H. M. I., Mendes V. M. F., "Hybrid wavelet-PSO-ANFIS approach for short-term electricity prices forecasting," *IEEE Trans. Power Syst.*, vol. 26, pp. 137-144, 2011.

[53] Marzband M., Sumper A., Domínguez-García J. L., Gumarra-Ferret R., "Experimental validation of a real time energy management system for microgrids in islanded mode using a local day-ahead electricity market and MINLP," *Energy Convers. Manage.*, vol. 76, p. 314–322, 2013.

[54] Shafie-khah M., Moghaddam M. P., Sheikh-El-Eslami M. K., "Price forecasting of day-ahead electricity markets using a hybrid forecast method," *Energy Convers. Manage.*, vol. 52, p. 2165–2169, 2011.

[55] Contreras J., Espínola R., Nogales F. J., Conejo A. J., "ARIMA models to predict nextday electricity prices," *IEEE Trans. Power Syst.*, vol. 18, pp. 1014-1020, 2003.

[56] Conejo A. J., Plazas M. A., Espínola R., Molina A. B., "Day-ahead electricity price forecasting using wavelet transform and ARIMA models," *IEEE Trans. Power Syst.,* vol. 20, pp. 1035-1042, 2005.

[57] Nogales F. J., Conejo A. J., "Electricity price forecasting through transfer function models," *J. Oper. Res.,* vol. 2006, pp. 350-356., 2006.

[58] Amjady N., "Day-ahead price forecasting of electricity markets by a new fuzzy neural network," *IEEE Trans. Power Syst.,* vol. 21, pp. 887-896., 2006.

[59] Amjady N., Hemmati H., "Day-ahead price forecasting of electricity markets by a hybrid intelligent system," *Euro. Trans. Electron. Power,* vol. 19, pp. 89-102., 2006.

[60] Catalão J. P. S., Mariano S. J. P. S., Mendes V. M. F., "Short-term electricity prices forecasting in a competitive market: A neural network approach," *Elec. Power Syst. Res.,* vol. 77, pp. 1297-1304, 2007.

[61] Mandal P., Senjyu T., Urasaki N., Funabashi T., Srivastava A. K., "A novel approach to forecast electricity price for PJM using neural network and similar days method," *IEEE Trans. Power Syst.,* vol. 22, pp. 2058–2065, 2007.

[62] Troncoso L., Riquelme-Santos J. M., Gómez-Expósito A., Martínez-Ramos J. L., Riquelme-Santos J. C., "Electricity market prices forecasting based on weighted nearest neighbors techniques," *IEEE Trans. Power Syst.,* vol. 22, pp. 1294-301, 2007.

[63] Amjady N., Keynia F., "Day ahead price forecasting of electricity markets by a mixed data model and hybrid forecast method," *Int. J. Elect, Power Energy Syst.,* vol. 30, pp. 533-546, 2008.

[64] Chen J., Deng S. -J., Huo X., "Electricity price curve modeling and forecasting by manifold learning," *IEEE Trans. Power Syst.,* vol. 23, pp. 877-888, 2008.

[65] Pino R., Parreno J., Gomez A., Priore P., "Forecasting next-day price of electricity in the Spanish energy market using artificial neural network," *Eng. Appl. Arti. Intel.,* vol. 21, pp. 53-62, 2008.

[66] Pindoriya N. M., Singh S. N., Singh S. K., "An adaptive wavelet neural network-based energy price forecasting in electricity markets," *IEEE Trans. Power Syst.,* vol. 23, pp. 1423-1432, 2008.

[67] Vahidinasab V., Jadid S., Kazemi A., "Day-ahead price forecasting in restrucutured power systems using artificial neural network," *Elect. Power. Syst. Res.,* vol. 78, pp. 1332-1342, 2008.

[68] Amjady N., Daraeepour A., "Design of input vector for day-ahead price forecasting of electricity markets," *Expert. Syst. Appl.,* vol. 2009, pp. 12281-12294, 2009.

[69] Amjady N., Keynia F., "Day-Ahead price forecasting of electricity markets by mutual information technique and cascaded neuro-evolutionary algorithm," *IEEE Trans. Power Syst.,* vol. 24, pp. 306-318, 2009.

[70] Amjady N., Keynia F., "Day-ahead price forecasting of electricity markets by a new feature selection algorithm and cascaded neural network technique," *Energy Conv. Manage.,* vol. 50, pp. 2976-2982, 2009.

[71] Amjady N., Daraeepour A., "Mixed price and load forecasting of electricity markets by a new iterative prediction method," *Elect. Power Syst. Rese.,* vol. 79, pp. 1329-1336, 2009.

[72] Meng K., Dong Z. Y., Wong K. P., "Self-adaptive radial basis function neural network for short-term electricty price forecasting," *IET Gene. Trans. Dist.,* vol. 3, pp. 325-335, 2009.

[73] Mandal P., Srivastava A. K., Park J. -W., "An effort to optimize similar days parameters for ANN-based electricity price forecasting," *IEEE Trans. Ind. Appl.,* vol. 45, pp. 1888-1896, 2009.

[74] Amjady N., Keynia F., "Application of a new hybrid neuro-evolutionary system for a day-ahead price forecasting of electricity markets," *App. Soft. Comp.,* vol. 10, pp. 784-792, 2010.

[75] Catalão J. P. S., Pousinho H. M. I., Mendes V. M. F., "Neural networks and wavelet transform for short-term electricity prices forecasting," *Eng. Intell. Syst. Electron. Eng. Commun.,* vol. 18, pp. 85–92, 2010.

[76] Areekul P., Senjyu T., Toyama H., Yona A., "A hybrid ARIMA and neural network model for short-term price forecasting in deregulated market," *IEEE Trans. Power Syst.,* vol. 25, pp. 524-530, 2010.

[77] Mandal P., Srivastava A. K., Park J. -W., "A new recursive neural network algorithm to forecast electricity price for PJM day-ahead market," *Int. J. Energy Rese.,* vol. 24, pp. 507-522, 2010.

[78] Lin W. -M., Gow H. -J., Tsai M. -T., "An enhanced radial basis function network for short-term electricity price forecasting," *Appl. Energy,* vol. 87, pp. 3226-3234, 2010.

[79] Wu L., Shahidehpour M., "A hybrid model for day-ahead price forecasting," *IEEE Trans. Power Syst.,* vol. 25, pp. 1519-1530, 2010.

[80] Amjady N., Daraeepour A., Keynia F., "Day-ahead electricity price forecasting by modified relief algorithm and hybrid neural network," *IET Gener. Transm. Distrib.,* vol. 4, pp. 432-444, 2010.

[81] Catalão J. P. S., Osório G. J., Pousinho H. M. I., "Application of an intelligent system based on EPSO and ANFIS to price forecasting," in *Proc. 16th Int. Conf. Int. Syst. Appl. Power Syst.- ISAP 2011*, Greece, 2011.

[82] Martinez-Alvarez F., Troncoso A., Riquelme J. C., Aguilar-Ruiz J. S., "Energy time series forecasting based on pattern sequence similarity," *IEEE Trans. Knowl. Data Eng.,* vol. 23, pp. 1230-1243, 2011.

[83] Chen X., Dong Z. Y., Meng K., Xu Y., Wong K. P., Ngan H. W., "Electricity price forecasting with extreme learning machine and bootstrapping," *IEEE. Trans. Power Syst.,* vol. 27, pp. 2055-2062, 2012.

[84] Keynia F., "A new feature selection algorithm and composite neural network for electricty price forecasting," *Eng. Appl. Arti. Intel.,* vol. 25, pp. 1687-1697, 2012.

[85] Mandal P., Haque A. U., Meng J., Martínez R., Srivastava A. K., "A hybrid intelligent algorithm for short-term energy price forecasting in the Ontario market," in *Proc. IEEE Power Energy Soci. Gene. Meet.*, 2012.

[86] Mingli L., Feng Z., "A proposed grey model for short-term electricity price forecasting in competitive power markets," *Int. J. Elect. Power Energy Syst.,* vol. 43, pp. 531-538, 2012.

[87] Pousinho H. M. I, Mendes V. M. F., Catalão J. P. S., "Short-term electricity prices forecasting in a competitive market by a hybrid PSO-ANFIS approach," *Int. J. Elect. Power Energy Syst.,* vol. 39, pp. 29-35, 2012.

[88] Li X. R., Yu C. W., Ren S. Y., Chiu C. H., Meng K., "Day-ahead electricity price forecasting based on panel cointegration and particle filter," *Elect. Power Syst. Rese.,* vol. 95, pp. 66-76, 2013.

[89] Zhang J., Tan Z., "Day-ahead electricity price forecasting using WT, CLSSVM and EGARCH model," *Electron. Power Energy Syst.,* vol. 45, pp. 362-368, 2013.

[90] Miranian A., Abdollahzade M., Hassani H., "Day-ahead electricity price analysis and forecasting by singular spectrum analysis," *IET Gener. Transm. Distrib.,* vol. 7, pp. 337-346, 2013.

[91] Mandal P., Haque A. U., Meng J., Srivastava A., Martinez R., "A novel hybrid approach using wavelet, firefly algorithm, and fuzzy ARTMAP for day-ahead electricity price forecasting," *IEEE Trans. Power Syst.,* vol. 28, pp. 1041-1051, 2013.

[92] Wu H. C., Chan S., Tsui K. M., Hou Y., "A new recursive dynamic factor analysis for point and interval forecast of electricity price," *IEEE Trans. Power Syst.,* vol. 28, pp. 2352-2365, 2013.

[93] Elattar E., Shebin E. -K., "Day-ahead price forecasting of electricity markets based on local informative vector machine," *IET Gener. Transm. Distrib.,* vol. 7, pp. 1063-1071, 2013.

[94] Wu Y. -K., Hong J. -S., "A literature review of wind forecasting technology in the world," in *Proc. IEEE Power Tech. Conf.*, Switzerland, 2007.

[95] Sideratos G., Hatziargyriou N. D., "Wind power forecasting focused on extreme power system events," *IEEE Trans. Sustain. Energy,* vol. 3, pp. 445-454, 2012.

[96] Botterud A., Zhi Z., Bessa R. J., Keko H., Sumaili J., Miranda V., "Wind power trading under uncertainty in LMP markets," *IEEE Trans. Power Syst.,* vol. 27, pp. 894-903, 2012.

[97] Wang X., Guo P., Huang X., "A review of wind power forecasting models," *Energy Proc.,* vol. 12, pp. 770-778, 2011.

[98] Costa A., Crespo A., Navarro J., Lizcano G., Madsen H., Feitosa E., "A review of the young history of wind power short-term prediction," *Renew. Sustain. Energy Rev.,* vol. 12, pp. 1725-1744, 2008.

[99] El-Fouly T. H. M., El-Saadany E. F., Salama M. M. A., "One day ahead prediction of wind speed and direction," *IEEE Trans. Energy Convers.,* vol. 23, pp. 191-201, 2008.

[100] WindAction, "The effects of integrating wind power on transmission system planning, reliability, and operations: Report on phase 2," New York, USA, 2005.

[101] Amjady N., Keynia F., Zareipour H., "Wind power prediction by a new forecast engine composed of modified hybrid neural network and enhanced particle swarm optimization," *IEEE Trans. Sustain. Energy,* vol. 2, pp. 265-276, 2011.

[102] Togelou A., Sideratos G., Hatziargyriou N., "Wind power forecasting in the absence of historical data," *IEEE Trans. Sustain. Energy,* vol. 3, pp. 416-421, 2012.

[103] Prasad R. D., Bansal R. C., Sauturaga M., "Some of the design and methodology considerations in wind resource assessment," *IET Renew. Power Gener.,* vol. 2009, pp. 53-64, 2009.

[104] Ma L., Luan S. Y., Jiang C. W., Liu H. L., Zhang Y., "A review on the forecasting of wind speed and generated power," *Renew. Sustain. Energy Rev.,* vol. 2009, pp. 915-920, 2009.

[105] Kariniotakis G., Pinson P., Siebert N., Giebel R., "The state of the art in short-term prediction of wind power from an offshore perspective," in *Proc. of 2004 Sea. Tech. Week*, France, 2004.

[106] Monteiro C., Bessa R., Miranda V., Botterud A., Wang J., Conzelmann G., "Wind Power Forecasting: State-of-the-Art 2009," Argonne National Laboratory, EUA, 2009.

[107] Kavassery R., Seetharaman K., "Day-ahead wind speed forecasting using f-ARIMA models," *Renew. Energy* , vol. 34, pp. 1388-1393, 2009.

[108] Nielsen T., Joensen A., Madsen H., Landberg L., Giebel G., "A new reference for wind power forecasting," *Wind Energy,* vol. 1, pp. 29-34, 1998.

[109] Catalão J. P. S., Pousinho H. M. I., Mendes V. M. F., "An artificial neural network approach for short-term wind power forecasting in Portugal," *Eng. Intell. Syst. Electr. Eng. Commun.,* vol. 17, pp. 5-11, 2009.

[110] Rosado I. J. -R., Jimenez L. A. -F., Monteiro C., Sousa J., Bessa R., "Comparison of two new short-term wind-power forecasting systems," *Renew. Energy,* vol. 34, pp. 1848-1854, 2009.

[111] Catalão J. P. S., Pousinho H. M. I., Mendes V. M. F., "Short-term wind power forecasting in Portugal by neural network and wavelet transform," *Renew. Energy,* vol. 34, pp. 1245-1251, 2011.

[112] Bhaskar K., Singh S., "AWNN-assisted wind power forecasting using feed-forward neural network," *IEEE Trans. Sustain. Energy ,* vol. 3, pp. 306-315, 2012.

[113] Pousinho H. M. I., Mendes V. M. F., Catalão J. P. S., "Application of adaptive neuro-fuzzy inference for wind power short-term forecasting," *IEEJ Trans. Elect. Electr. Eng.,* vol. 6, pp. 571-576, 2011.

[114] Sideratos G., Hatziargyriou N., "An advanced statistical method for wind power forecasting," *IEEE Trans. Power Syst.,* vol. 22, pp. 258-265, 2007.

[115] Jursa R., Rohrig K., "Short-term wind power forecasting using evolutionary algorithms for the automated specification of artificial intelligence models," *Int. J. Forecast,* vol. 24, pp. 694-709, 2008.

[116] Catalão J. P. S., Pousinho H. M. I., Mendes V. M. F., "Hybrid Wavelet-PSO-ANFIS approach for short-term wind power forecasting in Portugal," *IEEE Trans. Sustain. Energy,* vol. 2011, pp. 50-59, 2011.

[117] Bessa R. J., Miranda V., Gama J., "Entropy and correntropy against minimum square error in offline and online three-day ahead wind power forecasting," *IEEE Trans. Power Syst.,* vol. 24, pp. 1657-1666, 2009.

[118] Kusiak A., Zhang Z., "Short-horizon prediction of wind power: a data-driven approach," *IEEE Trans. Energy Conv.,* vol. 25, pp. 1112-11222, 2010.

[119] Amjady N., Keynia F., Zareipour H., "Short-term wind power forecasting using ridgelet neural network," *Elec. Power Syst. Res.,* vol. 81, pp. 2099-2107, 2011.

[120] Pousinho H. M. I., Mendes V. M. F., Catalão J. P. S., "A hybrid PSO-ANFIS approach for short-term wind power prediction in Portugal," *Ener. Conv. Manag.,* vol. 52, pp. 397-402, 2011.

[121] Catalão J. P. S., Osório G. J., Pousinho H. M. I., "Short-term wind power forecasting using a hybrid evolutionary intelligent approach," in *Proc. 16th Int. Conf. Int. Syst. Appl. to Power Syst.*, Greece, 2011.

[122] Khalid M., Savkin A. V., "A method for short-term wind power prediction with multiple observation points," *IEEE Trans. Power Syst.,* vol. 27, pp. 579-586, 2012.

[123] Venayagamoorthy G., Rohrig K., Erlich I., "Short-term wind power forecasting and intelligent predictive control based on data analytics," *IEEE Power Ener. Mag.,* vol. 10, pp. 71-78, 2012.

[124] Sideratos G. , Hatziargyriou N. D., "Probabilistic wind power forecasting using radial basis function neural network," *IEEE Trans. Pow. Syst.,* vol. 27, pp. 1788-1796, 2012.

[125] Liu Y., Shi J., Yang Y., Lee W. -J., "Shot-term wind-power prediction based on wavelet transform-support vector machine and statistic-characteristics analysis," *IEEE. Trans. Indus. Appl.,* vol. 48, pp. 1136-1141, 2012.

[126] Zhang Y., Wang J., Wang X., "Review on probabilistic forecasting of wind power generation," *Renew. Sust. Energy Rev.,* vol. 32, pp. 255-270, 2014.

[127] Haque A. U., Nehrir M. H., Mandal P., "A hybrid intelligent model for deterministic and quantile regression approach for probabilistic wind power forecasting," *IEEE Trans. Power Syst.,* vol. 29, pp. 1663-1672, 2014.

[128] Kou P., Liang D., Gao F., Gao L., "Probabilistic wind power forecasting with online model selection and warped gaussian process," *Energy Conv. Manage,* vol. 84, pp. 649-663, 2014.

[129] Papaefthymiou S. V., Papathanassiou S. A., "Optimum sizing of wind-pumped-storage hybrid power stations in island systems," *Renew. Energy,* vol. 64, pp. 187-196, 2014.

[130] Pye S., Usher W., Strachan N., "The uncertain but critical role of demand reduction in meeting long-term energy decarbonisation targets," *Energy Pol.,* vol. 73, pp. 575-586, 2014.

[131] Dietrich K., Latorre J. M., Olmos, L., Ramos A., "Demand response in an isolated system with high wind integration," *IEEE Trans. Power Syst.,* vol. 27, pp. 20-29, 2012.

[132] Wang J., Botterud A., Bessa R., Keko H., Carvalho L., Issicaba D., Sumaili J., Miranda, V., "Wind power forecasting uncertainty and unit commitment," *Applied Energy,* vol. 88, pp. 4014-4023, 2011.

[133] Tuohy A., Meibom P. , Denny E., O'Malley M., "Unit commitment for systems with significant wind penetration," *IEEE Trans. Power Syst.,* vol. 24, pp. 592-601, 2009.

[134] Aghaei J., Nikman T., Azizipanah-Abarghooee R., Arroyo J. M., "Scenario-based dynamic economic emission dispatch considering load and wind power uncertainties," *Electr. Power Energy Syst.,* vol. 47, pp. 351-367, 2013.

[135] Constantinescu E., Zavala V. M., Rocklin M., Lee S., Anitescu M., "A computational framework for uncertainty quantification and stochastic optimization in unit commitment with wind power generation," *IEEE Trans. Power Syst.,* vol. 26, pp. 431-441, 2011.

[136] Zhao C., Guan Y., "Unified stochastic and robust unit commitment," *IEEE. Trans. Power Syst.,* vol. 28, pp. 3353-3361, 2013.

[137] Ruiz P. A., Philbrick C. R., Cheung K. W., Sauer P. W., "Uncertainty management in the unit commitment problem," *IEEE Trans. Power Syst.,* vol. 24, pp. 642-651, 2009.

[138] Liu X., Xu W., "Economic load dispatch constrained by wind power availability: a here-and-now approach," *IEEE Trans. Sust. Energy,* vol. 1, pp. 2-9, 2010.

[139] Liu X., "Economic load dispatch constrained by wind power availability: a wait-and-see approach," *IEEE Trans. Smart Grid,* vol. 1, pp. 347-355, 2010.

[140] Liu X., Xu W., "Minimum emission dispatch constrained by stochastic wind power availability and cost," *IEEE. Trans. Power Syst.,* vol. 25, pp. 1705-1713, 2010.

[141] Hargreaves J. J., Hobbs B. F., "Commitment and dispatch with uncertain wind generation by dynamic programming," *IEEE Trans. Sust. Energy,* vol. 3, pp. 724-734, 2012.

[142] Roy S., "Inclusion of short duration wind variations in economic load dispatch," *IEEE Trans. Sust. Energy,* vol. 3, pp. 365-273, 2012.

[143] Azizipanah-Abarghooee R., Niknam T., Roosta A., Malekpour A. R., Zare M., "Probabilistic multiobjective wind-thermal economic emission dispatch based on point estimated method," *Energy,* vol. 37, pp. 322-335, 2012.

[144] Luh P. B., Yu Y., Zhang B., Litvinov E., Zheng T., Zhao F., Zhao J., Wang C., "Grid integration of intermittent wind generation: A Markovian approach," *IEEE Trans. Smart Grid,* vol. 5, pp. 732-741, 2014.

[145] Zachariadis T., Poullikkas A., "The costs of power outages: A case study from Cyprus," *Energy Policy,* vol. 51, pp. 630-641, 2012.

[146] Wu L., Shahidehpour M., Li T., "Cost of reliability analysis based on stochastic unit commitment," *IEEE Trans. Power Syst.,* vol. 23, pp. 1364-1374, 2008.

[147] Chang G. W., Chuang C. -S., Lu T. -K., Wu C. -C., "Frequency-regulating reserve constrained unit commitment for an isolated power system," *IEEE Trans. Power Syst.,* vol. 28, pp. 578-586, 2013.

[148] Sahin C., Shahidehpour M., Erkmen I., "Allocation of hourly reserve versus demand response for security-constrained scheduling of stochastic wind energy," *IEEE Trans. Sust. Energy,* vol. 4, pp. 219-228, 2013.

[149] Hesamzadeh M. R., Galland O., Biggar D. R., "Short-run economic dispatch with mathematical modelling of the adjustment cost," *Electr. Power Energy Syst.,* vol. 58, pp. 9-18, 2014.

[150] Bahmani-Firouzi B., Farjah E., Azizipanah-Abarghooee R., "An efficient scenario-based and fuzzy self-adaptive learning particle swarm optimization approach for dynamic economic emission dispatch considering load and wind power uncertainties," *Energy,* vol. 50, pp. 232-244, 2013.

[151] Ding X., Lee W. -J., Jianxue W., Liu L., "Studies on stochastic unit commitment formulation with flexible generating units," *Electr. Power Syst. Rese.,* vol. 80, pp. 130-141, 2010.

[152] Wang Q., Guan Y., Wang J., "A chance-constrained two-stage stochastic program for unit commitment with uncertain wind power output," *IEEE Trans. Power Syst.,* vol. 27, pp. 206-215, 2012.

[153] Hetzer J., Yu D. C., Bhattarai K., "An economic dispatch model incorporating wind power," *IEEE Trans. Energy Conv.,* vol. 23, pp. 603-611, 2008.

[154] De Giorgi M. G., Ficarella A., Tarantino M., "Error analysis of short term wind power prediction models," *Appl. Energy,* vol. 88, pp. 1298-1311, 2011.

[155] Bludszuweit H., Domínguez-Navarro J. A., Llombart A., "Statistical analysis of wind power forecast error," *IEEE Trans. Power Syst.,* vol. 23, pp. 983-991, 2008.

[156] Tewari S., Geyer C. J., Mohan C. J., "A statistical model for wind power forecast error and its application to the estimation of penalties in liberalized markets," *IEEE Trans. Power Syst.,* vol. 26, pp. 2031-2039, 2011.

[157] Zhang Z. -S., Sun Y. -Z., Gao D. W., Lin J., Cheng L., "A versatile probability distribution model for wind power forecast errors and its application in economic dispatch," *IEEE Trans. Power Syst.,* vol. 29, pp. 3114-3125, 2013.

[158] Zhang N., Kang C., Xia Q., Liang J., "Modeling conditional forecast error for wind power in generation scheduling," *IEEE Trans. Power Syst.,* vol. 29, pp. 1316-1324, 2014.

[159] Bruninx K., Delarue E., "A statistical description of the error on wind power forecasts for probabilistic reserve sizing," . *IEEE Trans. Sust. Energy,* vol. 5, pp. 995-1002, 2014.

[160] Blechinger P., Seguin R., Cader C., Bertheau P., Breyer C. H., "Assessment of the global potential for renewable energy storage systems on small islands," *Energy Proce.,* vol. 46, pp. 294-300, 2014.

[161] Papaefthymiou S. V., Papathanassiou S. A., "Optimum sizing of wind-pumped-storage hybrid power stations in island systems," *Rene. Energy,* vol. 64, pp. 187-196, 2014.

[162] Senjyu T., Miyagi T., Yousuf S. A., Urasaki N., Funabashi T., "A technique for unit commitment with energy storage system," *Int. J. Elect. Power Energy Syst.,* vol. 29, pp. 91-98, 2007.

[163] Mohammadi S., Mohammadi A., "Stochastic scenario-based model and investigating size of battery energy storage and thermal energy storage for micro-grid," *Int. J. Elect. Power Energy Syst.,* vol. 61, pp. 531-546, 2014.

[164] Chen S. X., Gooi H. B., Wang M. Q., "Sizing of energy storage for microgrids," *IEEE Trans. Smart Grid,* vol. 3, pp. 142-151, 2012.

[165] Daneshi H., Srivastava A. K., "Security-constrained unit commitment with wind generation and compressed air energy storage," *IET Gene. Trans. Dist.,* vol. 6, pp. 167-175, 2012.

[166] Nazari M. E., Ardehali M. M., Jafari S., "Pumped-storage unit commitment with considerations for energy demand, economics, and environmental constraints," *Energy,* vol. 35, pp. 4092-4101, 2010.

[167] Ming Z., Kun Z., Liang W., "Study on unit commitment problem considering wind power and pumped hydro energy storage," *Int. J. Elect. Power Energy Syst.,* vol. 63, pp. 91-96, 2014.

[168] Jiang R., Wang J., Guan Y., "Robust unit commitment with wind power and pumped storage hydro," *IEEE Trans. Power Syst.,* vol. 27, pp. 800-810, 2012.

[169] Khodayar M. E., Shahidehpour M., Lei W., "Enhancing the dispatchability of variable wind generation by coordination with pumped-storage hydro units in stochastic power systems," *IEEE Trans. Power Syst.,* vol. 28, pp. 2808-2818, 2013.

[170] Suazo-Martinez C., Pereira-Bonvallet E., Palma-Behnke R., Xiao-Ping Z., "Impacts of energy storage on short term operation planning under centralized spot markets," *IEEE Trans. Smart Grid,* vol. 5, pp. 1110-1118, 2014.

[171] Yu Z., Zhao Y. D., Feng J. L., Ke M., Jing Q., Kit P. W., "Optimal allocation of energy storage system for risk mitigation of DISCOs with high renewable penetrations," *IEEE Trans. Power Syst.,* vol. 29, pp. 212-220, 2014.

[172] Pozo D., Contreras J., Sauma E. E., "Unit commitment with ideal and generic energy storage units," *IEEE Trans. Power Syst.,* vol. PP, pp. 1-11, 2014.

[173] Rodrigues E. M. G., Godina R., Bizuayehu A. W., Contreras J., Catalão J. P. S., "Energy storage systems supporting increased penetration of renewables in islanded systems," *Energy,* vol. 75, pp. 265-280, 2014.

[174] "International Renewable Energy Agency (IRENA)," [Online]. Available: http://www.irena.org. [Accessed 02 10 2014].

[175] Domenica N. D., Mitra G., Valente P., Birbilis G., "Stochastic programming and scenario generation within a simulation framework: an information systems perspective," *Deci. Supp. Systm.,* vol. 42, pp. 2197-2218, 2007.

[176] Amjady N., Keynia F., "Electricity market price spike analysis by a hybrid data model and feature selection technique," *Electr. Power Syst. Res.,* vol. 80, pp. 318-327, 2010.

[177] Cai R., Hao Z., Yang X., Wen W., "An efficient gene selection algorithm based on mutual information," *Neurocomputing,* vol. 72, pp. 991-999, 2009.

[178] Eynard J., Grieu S., Polit M., "Wavelet-based multi-resolution analysis and artificial neural networks, for forecasting temperature and thermal power consumption," *Eng. App. Art. Intell.,* vol. 24, pp. 501-516, 2011.

[179] Amjady N., Keynia F., "Short-term loads forecasting of power systems by combining wavelet transform and neuro-evolutionary algorithm," *Energy,* vol. 34, pp. 46-57, 2009.

[180] Conejo A. J., Contreras J., Espínola R., Plazas M. A., "Forecasting electricity prices for a day-ahead pool-based electric energy market," *Int. J. Forecast.,* vol. 21, pp. 435-462, 2005.

[181] Noori R., Abdoli M. A., Farokhnia A., Abbasi M., "Results uncertainty of solid waste generation forecasting by hybrid of wavelet transform-ANFIS and wavelet transform-neural network," *Exp. Syst. Appl.,* vol. 36, pp. 9991-9999, 2009.

[182] Chen Y., Luh P. B., Guan C., Zhao, Y. Michel L., Coolbeth M. A., Friedland P. B., Rourke S. J., "Short-term load forecasting: similar days-based wavelet neural network," *IEEE Trans. Power Syst.,* vol. 25, pp. 322-330, 2010.

[183] Heo J. S., Lee K. Y., Garduno-Ramirez R., "Multiobjective control of power plants using particle swarm optimization techniques," *IEEE Trans. Energy Conv.,* vol. 21, pp. 552-561, 2006.

[184] Miranda V., Oo N. W., "New experiments with EPSO-Evolutionary particle swarm optimization," in *Proc. IEEE Swarm Intel. Sympo.*, Indiana, USA, 2006.

[185] Chen M., Wu C., Fleming P., "An evolutionary particle swarm algorithm for multi-objective optimization," in *Proc. 7th World Congr. Intel. Contr. Auto.- WCICA2008*, Chongqing, China, 2008.

[186] Abdelhalim M. B., Salama A. E., Habib S.E.D., "Hardware software partitioning using particle swarm optimization technique," in *Proc. 6th Int. workshop on system-on-chip for real-time appl.*, Cairo, Egypt, 2007.

[187] Miranda V., Carvalho L. M., Rosa M. A., Silva A. M. L., Singh C., "Improving power system reliability calculation efficiency with EPSO variants," *IEEE Trans. Power Syst.*, vol. 24, pp. 1772-1779, 2009.

[188] Miranda V., "Evolutionary Algorithms with Particle Swarm Movements," in *Proc. 13th Int. Conf. Intel. Syst. Appl. Power Syst.*, Arlington VA, USA, 2005.

[189] Yun Z., Quan Z., Caixin S., Shaolan L., Yuming L., Yang S., "RBF neural network and ANFIS-based short-term load forecasting approach in real-time price environment," *IEEE Trans. Power Syst.*, vol. 23, pp. 853-858, 2008.

[190] Roy S. S., "Design of adaptive neuro-fuzzy inference system for prediciting surface roughness in turning operation," *J. Scient. Indust. Rese.*, vol. 64, pp. 653-659, 2005.

[191] Jang J. -S. R., "ANFIS: Adaptive-network-based fuzzy inference system," *IEEE Trans. Syst. Man. Cybern.*, vol. 23, pp. 665-685, 1993.

[192] Giebel G., Sørensen P., Holttinen H., "Forecast error of aggregated wind power," TradeWind Consortium Report, 2007.

[193] Emst B., Schreier U., Berster F., Pease J. H., "Large-scale wind and solar integration in Germany," U. S. Department of Energy, Pacific Northwest National Laboratory, 2010.

[194] Amjady N., Keynia F., "A new prediction strategy for price spike forecasting of day-ahead electricity markets," *Appl. Soft Comput.*, vol. 11, pp. 4246-4256, 2011.

[195] Anbazhagan S., Kumarappan N., "Day-ahead deregulated electricity market price forecasting using recurrent neural network," *IEEE Syst. J.*, vol. 7, pp. 866-872, 2013.

[196] Garcia C. -M., Rodriguez J., Sanchez M., "Mixed models for short run forecasting of electricity prices – application for the Spanish market," *IEEE Trans. Power Syst.*, vol. 22, pp. 544-552, 2007.

[197] "Pennsylvania-New Jersey-Maryland (PJM) electricity markets," [Online]. Available: http://www.pjm.com. [Accessed 04 11 2013].

[198] Catalão J. P. S., Pousinho H. M. I., Mendes V. M. F., "Hybrid intelligent approach for short-term wind power forecasting in Portugal," *IET Renew. Power Gener.*, vol. 5, pp. 251-257, 2011.

[199] Punzo A., Zini A., "Discrete approximations of continuous and mixed measures on a compact interval," *Statis. Papers*, vol. 53, pp. 563-575, 2012.

[200] Zhu J., Optimization of power system operation, Wiley-IEEE Press, 2009.

[201] Karaki S. H., Chedid R. B., Ramadan R., "Probabilistic performance assessment of wind energy conversion systems," *IEEE Trans. Energy Conv.*, vol. 14, pp. 217-224, 1999.

[202] Billinton R., Allan R. N., Reliability evaluation of power systems, New York and London: Plenum Press, 2th ed., 1996.

[203] Shah S. D., Cocker III D. R., Johnson K. C., Lee J. M., Soriano B. L., Miller J. W., "Emissions of regulated pollutants from in-use diesel back-up generators," *Atmos. Environ.*, vol. 40, pp. 4199-4209, 2006.

[204] Ji B., Yuan X., Chen Z., Tian H., "Improved gravitational search algorithm for unit commitment considering uncertainty of wind power," *Energy*, vol. 67, pp. 52-62, 2014.

[205] Ma X. -Y., Sun Y. -Z., Fang H. -L., "Scenario generation of wind power based on statistical uncertainty and variability," *IEEE Trans. Sustain. Energy*, vol. 4, pp. 894-904, 2013.

[206] Lambert T., Gilman P., Lilienthal P., Micropower system modeling with HOMER, in: Integration of alternative sources of energy, John Wiley & Sons, 2006, pp. 379-418.

[207] Rosenblatt M., "Remarks on a multivariate transformation," *Ann. Math. Statist.*, vol. 4, pp. 470-472, 1952.

[208] Li Y., Wu H., "A clustering method based on k-means algorithm," *Phys. Procedia,* vol. 25, pp. 1104-1109, 2012.

[209] Carrión M., Arroyo J. M., "A computationally efficient mixed-integer linear formulation for the thermal unit commitment problem," *IEEE Trans Power Syst.,* vol. 21, pp. 1371-1378, 2006.

[210] Delarue E., Cattysse D., D'haeseleer W., "Enhanced priority list unit commitment method for power systems with a high share of renewables," *Electr. Power Syst. Res.,* vol. 105, pp. 115-123, 2013.

[211] Senjyu T., Miyagi T., Saber A. Y., Urasaki N., Funabashi T., "Emerging solution of large-scale unit commitment problem by stochastic priority list," *Electr. Power Syst. Res.,* vol. 76, pp. 283-292, 2006.

[212] Senjyu T., Miyagi T., Yousuf S. A., Urasaki N., Funabashi T., "A technique for the unit commitment with energy storage system.," *Int. J. Electr. Power Energy Syst.,* vol. 29, pp. 91-98, 2007.

[213] Dieu V. N., Ongsakul W., "Ramp rate constrained unit commitment by improved priority list and augmented Lagrange Hopfield network," *Electr. Power Syst. Res.,* vol. 78, pp. 291-301, 2008.

[214] Chandram K., Subrahmanyam N., Sydulu M., "Unit commitment by improved pre-prepared power demand table and Muller method," *Int. J. Electr. Power Energy,* vol. 33, pp. 106-114, 2011.

[215] Dieu V. N., Ongsakul W., "Augmented Lagrange Hopfield network based Lagrangian relaxation for unit commitment," *Int. J. Electr. Power Energy Syst.,* vol. 33, pp. 522-530, 2011.

[216] Pires V. F., Romero-Cadaval E., Vinnikov D., Roasto I., Martins J. F., "Power converter interfaces for electrochemical energy sotrage systems - A review,' *Energy Conv. Mana.,* vol. 86, pp. 453-475, 2014.

[217] Rampinelli G. A., Krenzinger A., Romero F. C., "Mathematical models for efficiency of inverters used in grid connected photovoltaic systems," *Renew. Sust. Energy Rev.,* vol. 34, pp. 578-587, 2014.

[218] Lujano-Rojas J. M., Monteiro C., Dufo-López R., Bernal-Agustín J. L., "Optimum load management strategy for wind/diesel/battery hybrid power systems," *Renew. Energy,* vol. 44, pp. 288-295, 2012.

[219] Qiu X., Nguyen T. A., Guggenberger J. D., Crow M. L., Elmore A. C., "A field validated model of a vanadium redox flow battery for microgrids," *IEEE Trans. Smart Grid,* vol. 5, pp. 1592-1601, 2014.

[220] Turker B., Klein S. A., Hammer E. -M., Lenz B., Komsiyska L., "Modeling a vanadium redox flow battery system for large scale applications," *Energy Conv. Mana.,* vol. 66, pp. 26-32, 2013.

[221] Schreiber M., Harrer M., Whitehead A., Bucsich H., Dragschitz M., Seifert E., Tymciw P., "Practical and commercial issues in the design and manufacture of vanadium flow batteries," *J. Power Sources,* vol. 206, pp. 483-489, 2012.

[222] Copetti J. B., Lorenzo E., Chenlo F., "A general battery model for PV system simulation," *Progr. Photo.: Rese. Appl.,* vol. 1, pp. 283-292, 1993.

[223] Duic N., Carvalho M. G., "Increasing renewable energy sources in island energy supply: Case study Porto Santo," *Renew. Sust. Energy Rev.,* vol. 8, pp. 383-399, 2014.

[224] Katsaprakakis D. A., Christakis D. G., "Seawater pumped storage systems and offshore wind parks in islands with low onshore wind potential. A fundamental case study," *Energy,* vol. 66, pp. 470-486, 2014.